

FINAL REPORT

**FINE-SCALE SPATIAL AND TEMPORAL VARIABILITY OF PARTICLE NUMBER
CONCENTRATIONS WITHIN COMMUNITIES AND IN THE VICINITY OF FREEWAY
SOUND WALLS**

Principal Investigator:
Dr. Constantinos Sioutas

Prepared for:
The California Air Resources Board
and
The California Environmental Protection Agency

Prepared by:
University of Southern California
3620 S. Vermont Avenue
Los Angeles CA, 90089

April 26, 2011

Disclaimer

The statements and conclusions in this Report are those of the contractor and not necessarily those of the California Air Resources Board. The mention of commercial products, their source, or their use in connection with material reported herein is not to be construed as actual or implied endorsement of such products.

Acknowledgments

We would like to acknowledge the following people for their contribution and assistance to the study.

California Air Resources Board:

Leon Dolislager, Lei Guo, Jorn Herner, Kathleen Kozawa, Steve Mara

USC and Southern California Particle Center

Ehsan Arhami, Mari Cruz Minguillón, Katharine Moore, Neelakshi Hudda, Zhi Ning, Winnie Kam, Nancy Daher, Andrea Polidori, Payam Pakbin, Michael Geller

South Coast Air Quality Management District

Phil Fine

Ports of Long Beach and Los Angeles

The West Long Beach/Wilmington/San Pedro Community

The Berns Company

Dale Seymour

John Cross

Jesse Marquez

Balthasar Alvarez

Superior Electrical Advertising

This Report was submitted in fulfillment of ARB contract number 05-317 by The University of Southern California under the partial sponsorship of the California Air Resources Board. Work was completed as of April 26, 2011.

TABLE OF CONTENTS

Disclaimer	ii
Acknowledgments	iii
LIST OF FIGURES	vi
LIST OF TABLES	ix
ABSTRACT	x
EXECUTIVE SUMMARY	xi
BACKGROUND	xi
METHODS	xi
RESULTS	xii
CONCLUSIONS	xii
1. INTRODUCTION	1
1.1. BACKGROUND	1
1.2. STUDY STATEMENT OF SIGNIFICANCE	3
1.3. SPECIFIC OBJECTIVES	3
2. MATERIALS AND METHODS	5
2.1. STUDY DESIGN	5
2.1.1. MONITORING COMPONENTS	5
2.1.2. SOURCE REGION STUDY	6
2.1.3. RECEPTOR REGION STUDY	8
2.1.4. SOUND WALL STUDY	11
2.2. INSTRUMENTATION AND QUALITY ASSURANCE	13
2.2.1. SOURCE AREA STUDY	13
2.2.2. RECEPTOR AREA STUDY	16
2.2.3. SOUNDWALL STUDY	18
2.3. ANALYTICAL METHODS	20
2.3.1. SOURCE AREA AND RECEPTOR AREA STUDY	20
2.3.2. SOUNDWALL STUDY	21
3. RESULTS	22
3.1. SOURCE AREA STUDY	22
3.1.1. METEOROLOGY	22
3.1.2. ULTRAFINE PARTICLE CONCENTRATIONS	26
3.2. RECEPTOR AREA STUDY	35
3.2.1. METEOROLOGY	35

3.2.2	ULTRAFINE PARTICLES.....	38
3.3.	SOUNDWALL STUDY	51
4.	DISCUSSION.....	55
4.1.	SOURCE AREA STUDY	55
4.2.	RECEPTOR AREA STUDY	60
4.3.	COMPARISON WITH CHILDREN’S HEALTH STUDY AND IMPLICATIONS ..	62
5.	SUMMARY AND CONCLUSIONS	64
5.1	SOURCE AREA STUDY	64
5.2.	RECEPTOR AREA STUDY	65
5.3.	SOUNDWALL STUDY	66
6.	RECOMMENDATIONS.....	67
7.	REFERENCES.....	68
8.	LIST OF INVENTIONS REPORTED AND COPYRIGHTED MATERIALS PRODUCED	73
9.	GLOSSARY OF TERMS, ABBREVIATIONS, AND SYMBOLS	74
APPENDIX A:	RELATED PUBLICATIONS.....	75
A1.1	Intra-community spatial variation of size-fractionated PM mass, OC, EC and trace elements in Long Beach, CA.....	76
A1.2	Seasonal and spatial variations of sources of fine and quasi-ultrafine particulate matter in neighborhoods near the Los Angeles-Long Beach Harbor.....	77
A1.3	Redox Activity and Chemical Speciation of Size Fractioned PM in the Communities of the Los Angeles - Long Beach Harbor.....	79
A1.4	Size -segregated Inorganic and Organic Components of PM In the Communities of the Long Angeles Harbor Across Southern Los Angeles Basin, California.....	81
A1.6	Intra-community Spatial Variability of Particulate Matter Size Distributions ..	83
A1.7	Intra-community spatial variation of size-fractionated organic compounds in Long Beach, CA.....	85
APPENDIX B:	RELEVANT DETAILS ON CPC 3022A USED.....	87
B1	Known recalibration of CPCs used in the study	87
B2	Operation Schedule of CPCs at Sites	88
B3	Adjustment Factors for CPCs at Sites in Phase-II and concentrations	89

LIST OF FIGURES

Figure 1: Locations of monitoring sites for Source Area (Phase I shown in blue inset), Receptor Area (Phase II shown in brown background) and Soundwall (shown in green inset) components of particle number study.....	5
Figure 2: Locations of UFP monitoring sites in the Harbor Communities.	6
Figure 3: Location of the PNC sampling sites in the Los Angeles air basin during the receptor area study (Phase II).....	9
Figure 4: Location of the sampling sites: (a) I-710 without roadside barrier; (b) I-5 without roadside barrier; (c) I-710 with roadside barrier; (d) I-5 with roadside barrier. ...	12
Figure 5: Intercomparison of CPC performance via side-by-side testing, December 2006 - February 2007. One-minute data were used for this comparison.	14
Figure 6: Intercomparison of CPC performance via side-by-side testing, December 2007. One-minute data were used for comparison.	15
Figure 7: Intercomparison of CPC performance via side-by-side testing, December 2009. One-minute data were used for comparison.	16
Figure 8: All hours wind rose for site W1 during September 2007. The mean wind speed was 1.2 ms^{-1} and calm winds occurred 10% of the hours.....	24
Figure 9: All hours wind rose for site SP1 during September 2007. The mean wind speed was 3.2 ms^{-1} and calm winds occurred 5% of the hours.....	24
Figure 10: All hours wind rose for site LB8 during September 2007. The mean wind speed was 1.1 ms^{-1} and calm winds occurred 23% of the hours.....	25
Figure 11: All hours wind rose for site LB1 during September 2007. The mean wind speed was 2.0 ms^{-1} and calm winds occurred 8% of the hours.....	25
Figure 12: All hours wind rose for site LA1 during September 2007. The mean wind speed was 1.1 ms^{-1} and calm winds occurred 17% of the hours.....	26
Figure 13: Hourly average particle number concentrations shown for alternate months (standard error of the mean shown) for three sites: (a) LA1, (b) LB9, and (c) W2.....	27
Figure 14: San Pedro/Wilmington site cluster and LA1 site — hourly average particle number concentrations shown by alternate months: (a) March, (b) May, (c) July, (d) September, and (e) November.....	29
Figure 15: West Long Beach site cluster and LA1 site — hourly average particle number concentrations shown by alternate months: (a) March, (b) May, (c) July, (d) September, and (e) November.	30

Figure 16: Harbor background sites comparison - hourly mean particle number concentration data at sites SP1 and LB1 are shown for selected alternate months (Note: The “August– SP1” plot excludes August 5–13 data, which are included in the “August plume–SP1” plot)..... 32

Figure 17: Day-of-the-week diurnal concentration profiles calculated from all available monthly mean data for site LB2..... 33

Figure 18 : Day-of-the-week PNCs at site LA1 during the study (the standard error of each mean is shown). 34

Figure 19: Day-of-the-week PNCs at site LB9 during the study (the standard error of each mean is shown). 35

Figure 20: Hourly average particle number concentration at USC plotted for hours of the day in Pacific Standard Time (PST). The relative standard error for the hourly averages reported above was less than 2%. The inset is a plot of vector averaged wind direction (WD) with the bubble area weighed to wind speed plotted for hours of the day in PST. 40

Figure 21: Average size distribution of particles during six time periods of the day at USC during September 2009. 41

Figure 22: Average size distribution of particles during six time periods of the day at USC during December 2009. 42

Figure 23: Hourly average particle number concentration at UPL for hours of the day in Pacific Standard Time (PST). The relative standard error for the hourly averages reported above was less than 2%. The inset is a plot of vector averaged wind direction (WD) with the bubble area weighed to wind speed plotted for hours of the day in PST.43

Figure 24: Average size distribution of particles during six time periods (PST) of the day at UPL during September 2009..... 44

Figure 25: Average Size Distribution of Particles during six time periods (PST) of the day at UPL during December 2009. 45

Figure 26: Hourly average particle number concentration at AGO for hours of the day in Pacific Standard Time (PST). The relative standard error for the hourly averages reported above was less than 3%. The inset is a plot of vector averaged wind direction (WD) with the bubble area weighed to wind speed plotted for hours of the day in PST.46

Figure 27: Average size distribution of particles during six time periods (PST) of the day at AGO during September 2009..... 47

Figure 28: Average size distribution of particles during six time periods (PST) of the day at AGO during December 2009. 47

Figure 29: Mean hourly PNC and coefficients of divergence for various sites in the Los Angeles basin during December 2008. 50

Figure 30: Mean hourly PNCs and coefficients of divergence for various sites in the Los Angeles basin during August 2009..... 50

Figure 31: Particle size distributions measured at various distances downwind of freeway using FMPS (6-523nm) and in the immediate proximity of freeway using SMPS (10-225nm) shown as subplot: (a) I-710 without roadside barrier; (b) I-5 without roadside barrier; (c) I-710 with roadside barrier; (d) I-5 with roadside barrier..... 52

Figure 32: Normalized concentrations of BC and gaseous pollutants at various distances downwind of the freeway: (a) I-710 no noise barrier (b) I-5 no noise barrier; (c) I-710 with noise barrier; and (d) I-5 with noise barrier. 53

Figure 33: Coefficients of Divergence (CODs, (a)) and the correlation coefficient (r, (b)) calculated for the entire study based upon all hourly mean particle number concentration data and using all site pairs in Phase I study. In both (a) and (b), the 1st quartile, median, and 3rd quartile are represented by the box. The whisker/cross symbols represent the 10%/5% and 90%/95% values. 56

Figure 34: Site LA1 – COD (top) and correlation coefficients (bottom) calculated for PNCs across all site pairs for the entire Phase I study. 57

Figure 35: Coefficients of Divergence (CODs, (a)) and correlation coefficient (r, (b)) calculated from all PNC data for only the LB5-LB8 site pair. In both (a) and (b), the 1st quartile, median, and 3rd quartile are represented by the box. The whisker/cross symbols represent the 10%/5% and 90%/95% values. 58

Figure 36: Median coefficients of divergence (CODs) and correlation coefficient (r) calculated for PNCs at the LB2–LB3 site pair (March–May data). 59

Figure 37: Diurnal variation in the coefficients of divergence for PNCs in the receptor area (Phase II) study during the summer months of May-August, 2009..... 60

Figure 38: Diurnal variations in coefficients of divergence for PNCs in the receptor area (Phase II) study during the winter months of December 2008 - February 2009. 61

Figure 39: Coefficients of Divergence for different size (mobility diameter) of particles during Sep.-Dec. 2009 at select sites: USC, UPL & AGO. 62

Figure 40: Monthly mean particle number concentrations by month and selected sites including data from the 2002–2003 Children’s Health Study in California (named locations, data from Singh et al., 2006). 63

Figure 41: Comparison of PNC at select sites measured during 2008/09 with Singh et al. (2006) measured during 2002/03. 63

LIST OF TABLES

Table 1: Site information including the site designation (identification) code, geographic co-ordinates, site and equipment elevations, sampling period and data recovery with the condensation particle counter.	8
Table 2: Information on potential PM sources near Phase II (receptor area) sites.	10
Table 3: Site information including the identification code, geographic co-ordinates, site and equipment elevations, sampling period and CPC data recovery ^a	10
Table 4: Monitoring instruments deployed in stationary sampling station and the mobile platform.	19
Table 5: Temperature and Relative Humidity—monthly mean for select sites	23
Table 6: Prevailing wind direction and speed at sampling sites during Phase II (receptor area study).	37
Table 7: Temperature (^o C) and relative humidity (%) at sites during sampling period for Phase II (receptor area study).	38
Table 8: NO ₂ , BC, and CO concentration decay curves with distance from freeway section without a sound wall barrier.	53
Table 9: COD and correlation coefficient for PNC data collected in the source area study (Phase I) and presented by study site.	55

ABSTRACT

A network of monitoring sites were established to assess ultrafine particle (UFP; diameter $<0.1\mu\text{m}$) concentrations and their variability. The study was conducted in two phases at two very diverse spatial scales. A cluster of 13 sites was studied in Phase I, distributed over a few miles in communities located in the port area of San Pedro and Long Beach, to understand intra-community variability. In Phase II, a cluster of five sites covering over 50 miles was set up in the eastern Los Angeles basin to assess inter-community variability. Additionally, a site common to both phases was situated in downtown Los Angeles to provide a reference point with typical urban background particle number concentrations (PNC).

Meaningful variability in particle number concentrations was observed over the limited geographical area from San Pedro to Long Beach. The PNC variability across this source area appears to be driven by proximity to heavily trafficked roadways. The PNC at the sites in eastern Los Angeles exhibited lesser divergence in comparison to the source area even though they were spread over a larger area. However, the greatest variability was associated with impacts of local emissions and certain meteorological conditions. The measurements made in this study help to characterize the variability but it is suggested, due to the dynamic and transient nature of ultrafine particles, that UFPs be studied/measured more closely.

EXECUTIVE SUMMARY

BACKGROUND

Numerous adverse health outcomes are associated with atmospheric particulate matter (PM). Consequently, ambient air quality standards (based on particle mass) have been established to protect public health. Due to their small size, ultrafine particles (UFP) contribute very little to the overall PM mass but comprise the vast majority of the number of airborne particles in the atmosphere. As one of many sources contributing to urban air pollution, the combustion of fossil fuels in motor vehicles is a major source of particles in urban atmospheres. Recent studies in the Los Angeles basin have demonstrated that gradients in ultrafine number concentrations with increasing distance from busy freeways can be steep or shallow, depending on the time of day and meteorological conditions. Thus, although high particle number concentrations (PNCs) tend to be a local phenomenon, they can impact a larger community. In addition to primary, or direct, ultrafine particle emissions, secondary (photochemical and physical) formation from gases in the atmosphere contributes to the number of ultrafine particles and a broader regional influence. Given the toxicity of ultrafine particles (Oberdörster, 2001) and the very limited correlation between ambient particle numbers and mass, measurements of ambient PNCs have become increasingly important for assessing public exposure. Due to their short atmospheric lifetimes and strong dependence on local sources, ultrafine particle numbers can vary significantly on short spatial and temporal scales. Thus, measurements of ambient PNCs at a single monitoring station might not be indicative of the actual human exposure in the surrounding community. In order to address this problem and to more accurately estimate human exposure to UFPs and the subsequent health impacts, particle number measurements on finer spatial scales are needed.

METHODS

In order to meet this need for fine-scale UFP monitoring, a series of intensive monitoring campaigns were carried out in Southern California over a three-year project period. Two communities of interest were examined in this project. The first community was located in the San Pedro/Wilmington/Long Beach, CA area, which includes a complex mix of industrial (e.g., refineries, power plants) and transportation sources (e.g., marine vessels, diesel trucks, port activities) influencing UFP concentrations. The second community was located approximately 50 miles inland in the City of Riverside. The air pollution in Riverside is characterized by local emissions mixing with air masses transported from the upwind urban areas near downtown Los Angeles and the coast. Thus, Riverside represents a very different particle pollution situation as a —receptor” site than the upwind —source” site in Wilmington/Long Beach. Additionally, pollutant dispersion downwind of freeway sound walls was also studied. The standard equipment at most sites included a temperature-controlled, insulated, all-weather enclosure, a condensation particle counter (CPC), a weather station (temperature, relative humidity, wind speed and wind direction), and a laptop computer. Fifteen identical butanol-based CPCs were obtained for this study and have a nominal 50% detection efficiency

diameter of 7 nm, increasing to approximately 100% for particles larger than 20 nm. All fifteen CPCs were returned to the manufacturer for factory re-calibration prior to the start of the study.

RESULTS

Significant intra-community variability in total particle number concentrations was observed near the San Pedro Harbor/Wilmington/Long Beach area. PNC correlations between most site pairs were weak. Considerable differences in concentration were observed between sites in close proximity to each other due to multiple factors including proximity to sources, source strength, and traffic patterns. Diurnal patterns varied between sites but a pattern consistent with the high fractions of heavy duty diesel vehicles (HDDV) associated with goods movement to and from the ports was observed at several of the sites. The intra-community variability observed in this phase was on the order of the inter-community variability observed during the Children's Health Study conducted earlier in Los Angeles (Sardar et al., 2004). Moderate inter-community variability in total particle number concentrations was observed across the sites of the eastern Los Angeles basin implying that PNCs at these sites were homogeneous-to-moderately heterogeneous. Although, there were differences in the spatial variability through different seasons, the temporal patterns were consistent and exhibited least variability during the hours when local sources were not dominant. Comparable PNCs can be observed overnight during stable stratification conditions at sites separated by several tens of kilometers. The variability in size distributions (indicative of the aerosol source, composition, and age) was higher than that of total particle number concentrations. Overall the spatial variability in PNCs in the Riverside area was lower than the values reported in the earlier "source" area study. Additionally, the sound wall study found that, with the presence of roadside barrier, the dispersion dynamics of particulate and gaseous pollutants change dramatically. A deficit zone is formed in close vicinity downwind of the barrier (observed at 15 m in this present study) resulting in a concentration deficit zone in the lee of the barrier, where the particle number concentrations are 45-50% of those measured at similar downwind distances of freeways without a roadside barrier.

CONCLUSIONS

Our observations in an emissions source region (Phase I) substantiate concerns about the applicability of centrally-located PM_{2.5} mass concentration measurements for estimating exposure to UFPs (Wilson and Zawar-Reza, 2006; Wilson et al., 2005; Pinto et al., 2004). Even though our receptor region (Phase II) results suggest that PNCs are only moderately heterogeneous in the downwind areas of the Los Angeles basin, the multitude of local and highly variable emission sources associated with an urban area still raised concerns related to population exposure assessment based on monitoring data from a central location. Moreover, despite the moderate heterogeneity in total PNC at the inter-community level of receptor sites in the LAB, particle size distributions may vary significantly, resulting in differences in the overall inhaled dose of PM mass. Coordination efforts should be made to characterize the seasonal nature of the variability in both number concentrations and size distributions because meteorological factors can influence both even when PM sources are similar.

FINE-SCALE SPATIAL AND TEMPORAL VARIABILITY OF PARTICLE NUMBER CONCENTRATIONS WITHIN COMMUNITIES AND IN THE VICINITY OF FREEWAY SOUND WALLS

1. INTRODUCTION

1.1. BACKGROUND

Recent research has demonstrated that numerous adverse health outcomes are associated with atmospheric particulate matter (PM). Epidemiological studies have shown significant relationships between ambient PM and respiratory and cardiovascular related mortality and morbidity (Adler et al., 1994, Dockery et al., 1993). The observed effects are even more significant in susceptible populations, such as the elderly, with pre-existing respiratory and cardiovascular diseases (Oberdörster, 2001). Although current federal, state, and local regulatory efforts are focused on reduction of ambient levels of particulate mass for PM₁₀ and PM_{2.5}, recent studies have demonstrated that ultrafine particles (less than ~100 nanometers in diameter) are comparatively more toxic than larger particles with identical chemical composition and mass (Oberdörster et al. 1996 and Donaldson et al. 1998).

Due to their small size, ultrafine particles contribute very little to the overall PM mass, but comprise a significant majority of the number of airborne particles in the atmosphere (Oberdörster, 2001, Morawska et al., 1998). Many studies have suggested that particle number, rather than particle mass, may be more responsible for the observed health effects. Studies on rodents show that inflammatory response is more prominent when ultrafine particles are administered compared to larger particles (Oberdörster, 2001), suggesting either a particle number or surface area effect. In vitro toxicological studies have also shown that ultrafine particles have higher oxidative stress potential and can penetrate and destroy mitochondria within epithelial cells (Li et al., 2003). Penttinen et al. (2001) found that daily mean number concentration and peak expiratory flow (PEF) are negatively associated and that the effect is most prominent with particles in the ultrafine range. Another study by Peters et al. (1997) also found associations between number concentrations of ultrafine PM and lowered PEF among asthmatic adults.

As one of many sources contributing to urban air pollution in general, the combustion of fossil fuel in motor vehicles is the major emission source of ultrafine particle numbers to urban atmospheres (Shi et al., 1999; Cyrus et al., 2003). Recent studies have demonstrated that ultrafine number concentrations drop dramatically with increasing distance from busy freeways in the Los Angeles basin, confirming that vehicular pollution is the major source of ultrafine particles near and on the freeways, and that high particle number counts can be a very local phenomenon (on scales of 100-500 meters; Zhu et al., 2002a,b). Other combustion sources, such as food cooking and

wood burning, can also be sources of ultrafine particles to the atmosphere (Kleeman et al., 1999).

In addition to primary, or direct, ultrafine particle emissions, secondary formation in the atmosphere is also responsible for a portion of the ultrafine particles in the atmosphere. Kulmala et al. (2004) reviewed the observations of particle formation by secondary processes and showed that such particle formation events are more distinct in summer in the Los Angeles basin. Particle formation rates depend strongly on the intensity of solar radiation, but the exact mechanism by which the process occurs is not fully understood (Zhang and Wexler, 2002). Once formed, particles are transformed by coagulation and condensation in the atmosphere as they are advected downwind. This cross-basin transport, as well as photochemical particle formation in the atmosphere, can lead to increased particle number observations downwind of urban areas (Kim et al., 2002; Fine et al., 2004).

Given the toxicity of ultrafine particles noted above, and because there is little or no correlation between ambient particle numbers and mass (Sardar et al., 2004), measurements of ambient particle number concentrations have become important and are increasingly being made. However, measurements of ambient ultrafine particle number concentrations at a single central monitoring station might not be indicative of actual human exposure in the communities surrounding a single monitoring site. Due to their short atmospheric lifetimes and strong dependence on very local sources, ultrafine particle numbers vary significantly on very short spatial and temporal scales. In order to address this problem and to more accurately estimate human exposure and the subsequent health impacts of UFPs, more intensive particle number measurements on finer spatial scales is needed.

Previous studies measuring particle number concentrations in the atmosphere have either focused on one or two near-roadway sampling sites or several sampling sites separated by large distances (Shi et al., 1999; Sardar et al, 2004; Singh et al, 2004). For instance, a previous jointly funded ARB/SCAQMD study measured particle number concentrations in each of the Children's Health Study (CHS) communities at a single central monitoring station (Sardar et al., 2004). Results showed predictable daily and seasonal patterns with generally low correlation with other co-pollutants, such as PM mass and carbon monoxide (CO). However, other studies show that UFP concentrations vary dramatically within 100 meters of roadways (Zhu et al., 2002 a, b) and point out the need for more spatially resolved UFP monitoring within impacted communities.

The Zhu et al., studies sampled near freeways without sound walls adjacent to the roadway shoulders. But the effects of freeway characteristics, such as the existence of sound walls and the elevation of the roadway, also need to be assessed. However, there have been limited studies to date that have examined or demonstrated this scenario. It is possible that the degree of protection, or lack thereof, will vary with pollutant, or with the elevation of the freeway relative to the downwind neighborhood. Detailed studies are needed to assess the effects of such freeway characteristics and

determine whether sound walls can be used as a method to protect the public from freeway related pollutants.

1.2. STUDY STATEMENT OF SIGNIFICANCE

Although current federal, state, and local regulatory efforts are focused on reduction of ambient levels of particulate mass for PM₁₀ and PM_{2.5}, recent studies have demonstrated that UFP (less than ~100 nanometers in diameter) are more toxic. Other studies have shown that individual particles are capable of penetrating cellular membranes and causing cell damage, suggesting that particle number, rather than particle mass, might be more responsible for the potential health effects. Because UFPs make up the majority of ambient particle numbers but only a small fraction of ambient PM mass, and given that there is little or no correlation between ambient particle numbers and mass, measurements of ambient particle number concentrations have become increasingly important. However, measurements of ambient ultrafine particle number concentrations (PNCs) at a single central monitoring station might not be indicative of actual human exposure in the surrounding communities. Due to their short atmospheric lifetimes and strong dependence on very local sources, UFP numbers vary significantly on very short spatial and temporal scales. In order to address this problem and to more accurately estimate human exposure and the subsequent health impacts of UFPs, more intensive particle number measurements on finer spatial scales are needed.

The predominant sources of UFPs in urban areas are vehicular emissions and secondary production in the atmosphere from photochemical reactions of gaseous precursors and from physical processes (e.g., condensation, evaporation, agglomeration). A previous jointly-funded ARB/SCAQMD study measured UFP number concentrations in each of the Children's Health Study (CHS) communities at a single central monitoring station in each community. Results showed very predictable daily and seasonal patterns. But other studies show that UFP number concentrations vary dramatically within 100 meters of roadways, pointing out the need for more spatially resolved UFP monitoring within impacted communities. The effects of freeway characteristics such as the existence of sound walls and the elevation of the roadway also need to be assessed. Better information on the local-scale variability and sources of UFPs will improve our understanding of human exposure to and the health impacts of this unregulated pollutant. Such information perhaps would lead to UFP standards and more effective control measures that will reduce the public health risk.

1.3. SPECIFIC OBJECTIVES

This 3-year study sought to accomplish several specific objectives:

1. To determine the fine-scale spatial variability of ambient particle number (PN) concentrations within communities.

2. To demonstrate the feasibility of identifying specific ultrafine particle sources within a community using highly time-resolved and spatially-resolved measurements of PN.
3. To determine regional vs. local contributions to particle number concentrations.
4. To examine how the variability of particle number concentrations within communities are affected by season and location of the communities (source vs. receptor areas).
5. To determine the effects of freeway sound walls on particle size distribution and particle number, CO, NO₂ and BC concentrations in adjacent neighborhoods.

2. MATERIALS AND METHODS

2.1. STUDY DESIGN

2.1.1. MONITORING COMPONENTS

This particle number study was designed to address the study objectives in three components or phases:

- 1) A source area study (associated with the Harbor Communities Monitoring Study) in 2007, Phase I
- 2) A receptor area study (Riverside) in 2008/2009, Phase II and,
- 3) A sound wall study (I-5 and I-710) in 2009, Phase III.

A map showing the South Coast Air Basin and the approximate locations of the sites involved in the various study components is shown in Figure 1.



Figure 1: Locations of monitoring sites for Source Area (Phase I shown in blue inset), Receptor Area (Phase II shown in brown background) and Soundwall (shown in green inset) components of particle number study.

2.1.2. SOURCE REGION STUDY

This component of the project was designed to collect data and analyze the results from a dense network of monitoring sites to characterize intra-community variability in UFP number concentrations in a Los Angeles community with extensive and varied emission sources.

This study was conducted at 14 sites in southern Los Angeles County from February 12, 2007 through December 11, 2007 in coordination with the other investigators participating in the Harbor Communities Monitoring Study (HCMS). The relative locations of the monitoring sites to each other are shown in Figure 2. Previous work (Arhami et al., 2009; Minguillon et al., 2008) identified motor vehicles as the dominant source of UFPs in the Los Angeles area. Principal roadways, including major interstate freeways and heavily travelled surface streets, are shown in Figure 2 and criss-cross the study area. Sites in the vicinity of the Ports—described in detail below—were chosen in urban industrial and mixed industrial/residential areas by taking into consideration meteorology and the strength and location of probable nearby sources while also maintaining the study goal of monitoring in a limited area.

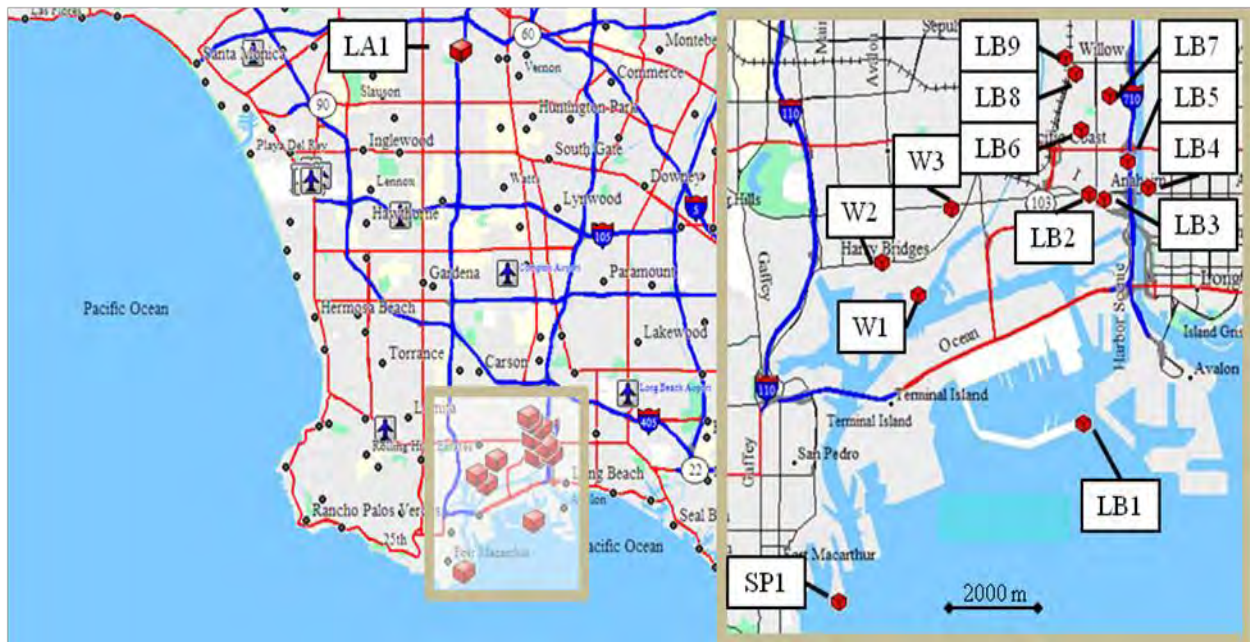


Figure 2: Locations of UFP monitoring sites in the Harbor Communities.

With the possible exception of the two —“background” sites on San Pedro Bay itself (SP1 and LB1), the mix of probable sources at any given study site was reasonably representative of multiple locations within the Harbor Communities. However, it is important to recognize that distinguishing between residential and commercial sites as a meaningful framework to interpret the data presented here is of limited utility as the majority of the sites are located near busy roadways (e.g., mobile sources). Characterizing PNC variability within this limited spatial area heavily impacted by activities associated with the movement of goods through the busiest port complex in the USA was the goal of this study.

A brief description of the five UFP monitoring sites in the western cluster of the HCMS is as follows and some relevant monitoring information is summarized in Table 1.

1. LA1 - downtown Los Angeles (on the campus of USC) provided a regional context to the observations being made in the vicinity of the Ports.
2. Site SP1 is located at a generally vacant berth (Berth 47) on southern edge of the Port of Los Angeles (PoLA). With air flow typically from the south, SP1 is a harbor background site, largely representative of air quality in the air coming into the southern portion of the Harbor Communities.
3. Site W1 is located in an industrial area north of the Port of Los Angeles, but not near heavily traveled roadways.
4. Site W2 is at the intersection of Harry Bridges Boulevard and Fries Avenue - major arterial roadway with significant HDDV traffic.
5. Site W3 is located in a mixed residential/commercial area affected by traffic and rail lines.

The eight UFP monitoring sites in the West Long Beach cluster are primarily located within a rectangle bounded by the Terminal Island Freeway (SR-103) to the west, Willow Avenue to the north, the I-710 on the east, and Anaheim Street to the south.

1. Site LB1 is located in the Port of Long Beach (PoLB) and is a companion harbor background site to SP1 located in the Port of Los Angeles (PoLA).
2. Sites LB2 and LB3 are located in a commercial area.
3. Site LB4 is an industrial area 10 m north of Anaheim Street, adjacent to the Los Angeles River, 400 m east of the I-710 (25% HDDV fraction).
4. Site LB5 is on a frontage road west of the I-710.
5. Site LB6 is 200 m north and 50 m east of the intersection of the Pacific Coast Highway and Santa Fe Streets.
6. Sites LB7 and LB8 are in primarily residential neighborhoods near the commercial strip on Santa Fe Avenue.
7. Site LB9 is located approximately 20 m to the north of the termination of the Terminal Island Freeway (SR-103) at Willow Street.

Table 1: Site information including the site designation (identification) code, geographic coordinates, site and equipment elevations, sampling period and data recovery with the condensation particle counter.

Site designation [†]	Latitude	Longitude	Site elevation (m)	Inlet elevation (m) [*]	Anemometer elevation (m) [*]	Sampling period	Data recovery (%)
LA1	34° 1' 9" N	118° 16' 39" W	61	4.6	9.1	2/15–12/15/2007	97%
SP1	33° 42' 54" N	118° 16' 28" W	1	3.0	3.4	6/1–12/12/2007	91%
W1	33° 45' 57" N	118° 15' 22" W	3	13.7**	14.0**	2/22–12/11/2007	95%
W2	33° 46' 16" N	118° 15' 52" W	4	3.2	3.4	4/27–12/12/2007	87%
W3	33° 46' 48" N	118° 14' 55" W	4	4.6	3.4	2/24–12/12/2007	92%
LB1	33° 44' 40" N	118° 13' 5" W	5	3.0	3.4	3/12–12/12/2007	87%
LB2	33° 46' 57" N	118° 13' 0.7" W	2	5.6	6.9	2/16–12/11/2007	84%
LB3	33° 46' 54" N	118° 12' 49" W	2	3.0	3.4	3/7–5/30/2007, 11/21–12/11/2007	98%, 45%
LB4	33° 47' 0.9" N	118° 12' 13" W	4	3.4	3.4	8/2–12/11/2007	99%
LB5	33° 47' 16" N	118° 12' 29" W	4	5.6	5.9	2/14–12/11/2007	88%
LB6	33° 47' 35" N	118° 13' 7" W	4	3.4	5.2	2/13–11/12/2007	88%
LB7	33° 47' 55" N	118° 12' 44" W	5	5.9	6.9	2/23–12/11/2007	91%
LB8	33° 48' 9" N	118° 13' 12" W	6	4.6	5.2	3/7–12/11/2007	86%
LB9	33° 48' 18" N	118° 13' 21" W	6	2.7	3.4	3/13–12/11/2007	88%

[†]The site codes include a city identifier and number. The sites are numbered roughly from S – N (LA = Los Angeles, SP = San Pedro, W = Wilmington, and LB = Long Beach).

^{*}height relative to ground.

^{**}roof elevation estimated to be 10.7 m.

2.1.3. RECEPTOR REGION STUDY

In large urban areas like the Los Angeles air basin (LAB), both primary (direct) emissions, secondarily-formed aerosols from emissions of gaseous pollutants, and also aged aerosols transported from locations upwind (some potentially distant) contribute to the observed PM concentrations at any given location. These PM processes, especially when coupled with local factors like the meteorology at a monitoring site and its exposure to local emission sources, can produce distinct diurnal patterns that vary over spatial scales at which inter-community variability can be assessed. It has been suggested (Turner et al., 2008) that secondary aerosol formation during regional transport can be a homogenizing factor on spatial variability. However, in 2002 and 2003, investigators in the USC Children's Health Study (Sardar et al., 2004; Singh et al., 2006) made measurements at several locations in the LAB and found that, although some sites may exhibit similar diurnal patterns, PNC can still vary considerably, and have only a modest correlation among even proximate sites. Lianou et al. (2007) found that the spatial variation in PNC might far exceed that in particulate mass concentrations. Fine et al. (2004) have also shown that sites in the receptor areas of LAB can have different particle size distribution patterns as well as different diurnal patterns in PNC.

Thus, in order to better quantify the risk that ultrafine PM poses to human health, it is necessary to characterize its spatial variability better, both in terms of particle numbers and size distribution compared to PM mass, if the potentially different population exposure to UFP is to be assessed well.

This study was conducted at five sites in eastern Los Angeles air basin and another site in downtown Los Angeles during November 2008 - December 2009. Site Information is

provided in Table 2 and the actual locations of these sites are shown in Figure 3. Highways and major arterials, common sources of ultrafine particles, are identified in Figure 3. The distances to freeways are also tabulated on the following page. The sites in the receptor area were within 50 kilometers of each other in the E-W direction and 20 kilometers in the N-S direction. Sampling sites were located in areas where there were no known major local contributors to UFP, except for light traffic (e.g., residential neighborhoods).

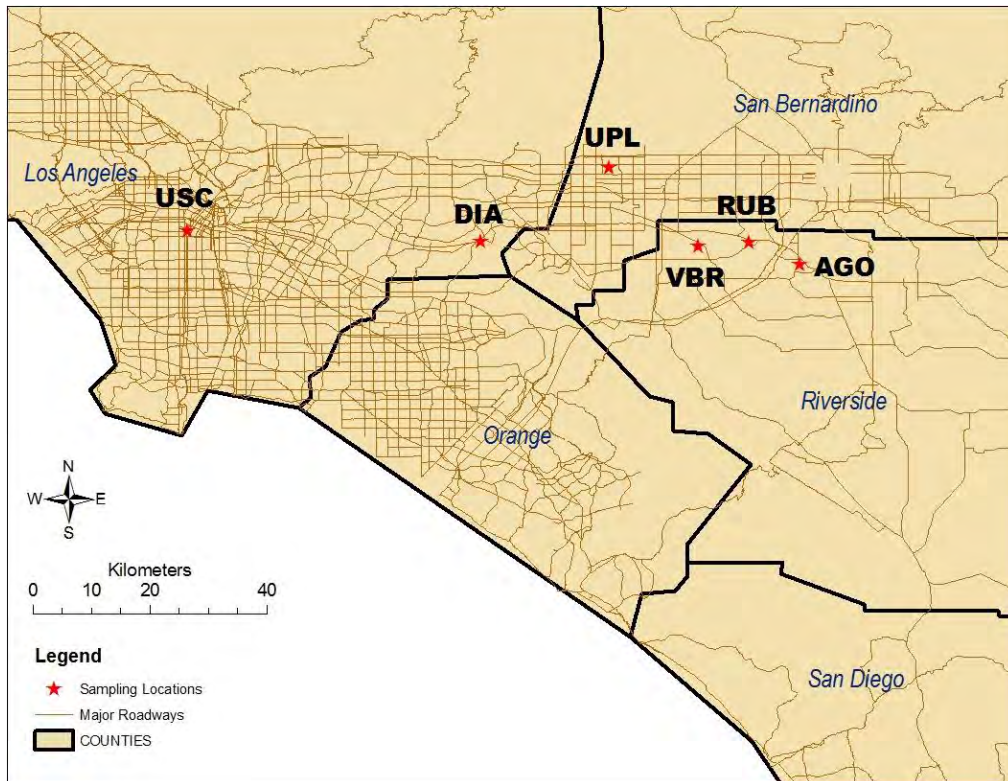


Figure 3: Location of the PNC sampling sites in the Los Angeles air basin during the receptor area study (Phase II).

A brief description of the sites in the receptor area study and some relevant information are summarized in Table 2.

Table 2: Information on potential PM sources near Phase II (receptor area) sites.

Site ID	Site Information
USC	USC Particle Instrumentation Unit - Located in a parking lot next to a freeway dominated by gasoline-powered vehicles; urban background site
DIA	Diamond Bar - Located in a parking lot on a hill over 100 m above the neighboring freeway CA 60, sub-urban regional site
UPL	Upland - Located in the foothills of the San Gabriel Mountains with limited local PM sources; regional site in terms of northern extent of LAB
VBR	VanBuren - Located in a residential neighborhood in a rural area; rural regional site
RUB	Rubidoux - Located behind an office building near a low-trafficked street and within 0.15 miles of freeway I-10, sub-urban regional site
AGO	UCR Agricultural Office - Located in an agricultural research facility near a university, freeways nearby (I-10), furthest inland site of study, regional downwind receptor site

Table 3: Site information including the identification code, geographic co-ordinates, site and equipment elevations, sampling period and CPC data recovery^a.

Site ID	Latitude	Longitude	Site elev ASL (m)	Inlet height (m)	Distance from nearest freeway (m), [average vehicle count/day]	Sampling period	Data recovery (%)
USC	34° 1' 9" N	118° 16' 39" W	61	4.6	150 [112,000]	11/17/2008 - 12/21/2009	91%
DIA	34° 0' 1" N	117° 49' 54" W	223	2	200 [99,000]	2/25/2009 - 12/21/2009	96%
UPL	34° 6' 14"N	117° 37' 45" W	386	1.85	2000 [96,000]	11/17/2008 - 12/21/2009	90%
VBR	33°59' 45"N	117° 29' 31" W	220	1.9	3000 [85,000]	11/17/2008 - 4/30/2009	95%
RUB	33°59' 58"N	117° 24' 58" W	248	2	200 [72,000]	11/17/2008 - 12/21/2009	93%
AGO	33°57' 41"N	117° 20' 0" W	323	2.1	750 [81,000]	11/17/2008 - 12/21/2009	98%
SBR	34° 6' 24"N	117° 16' 27" W	317	1.8	2000 [65,000]	5/18-6/30, 7/15-7/30, 9/4- 12/17/2009	87%

^a The SMPs were operated at sites USC, UPL and AGO from 9/4/2009 - 12/21/2009 at greater than 90% data recovery.

2.1.4. SOUND WALL STUDY

An intensive summer sampling campaign was conducted during June-July, 2009, to investigate the impact of roadside noise barriers on the dispersion profile of particles and co-pollutants emitted on freeways. Two highly trafficked freeways in greater Los Angeles area (I-710 and I-5) were selected, with two sampling sites (one with roadside noise barrier and the other without) located along a span of each freeway. At each of the four sites, a stationary sampling station was set up in the immediate proximity of the freeways to characterize the freeway emissions, while a mobile monitoring platform was deployed downwind of the traffic emissions to collect ambient data at varying distances from these freeways. Figure 4 (a, b, c and d) shows the locations of the four sampling sites and the routes of the mobile platform downwind of the selected freeways.

The non-noise barrier site on I-710 (Figure 4a) was located in Downey. No major roadway in the upwind direction of the stationary sampling station was located within 1 km. The inlet of the sampling instruments was extended to 2 m from the freeway edge. The location of the station and the route of the mobile platform are also highlighted in Figure 4a. The I-710 noise barrier site (Figure 4c) was located 2 km north of the non-noise barrier site in a residential neighborhood in Bell Gardens, CA, with no major roadways upwind, other than the freeway, for more than 1 km from the stationary sampling station. The station was set up on the freeway curbside and the inlet reached over the noise barrier to within 2 m of the freeway edge. The barrier was 3.7 m in height as measured above the adjacent surface road next to the noise barrier and extended more than few hundred meters from the site in both north and south bound sections along the freeway. The mobile platform route downwind of the freeway is also identified in the Figure 4c.

The non-noise barrier site on I-5 (Figure 4b) was located in the stretch of the freeway near La Mirada. There are no other major roadways upwind of the sampling site other than the freeway and the vicinity of the sampling site is mainly comprised of office buildings without industrial sources nearby. The stationary sampling location was set next to the freeway curb with the inlet reaching within 0.5 m of the freeway edge. The noise barrier site on I-5 (Figure 4d) was located in a residential neighborhood, with the barrier extending for hundreds of meters along the freeway north of the sampling location, and about 100 meters south. The height of the noise barrier at the site was 5.2 m as measured above the adjacent surface road next to the noise barrier. The inlet of the stationary sampling station was extended over the barrier and was located about 4 m from the edge of the freeway.

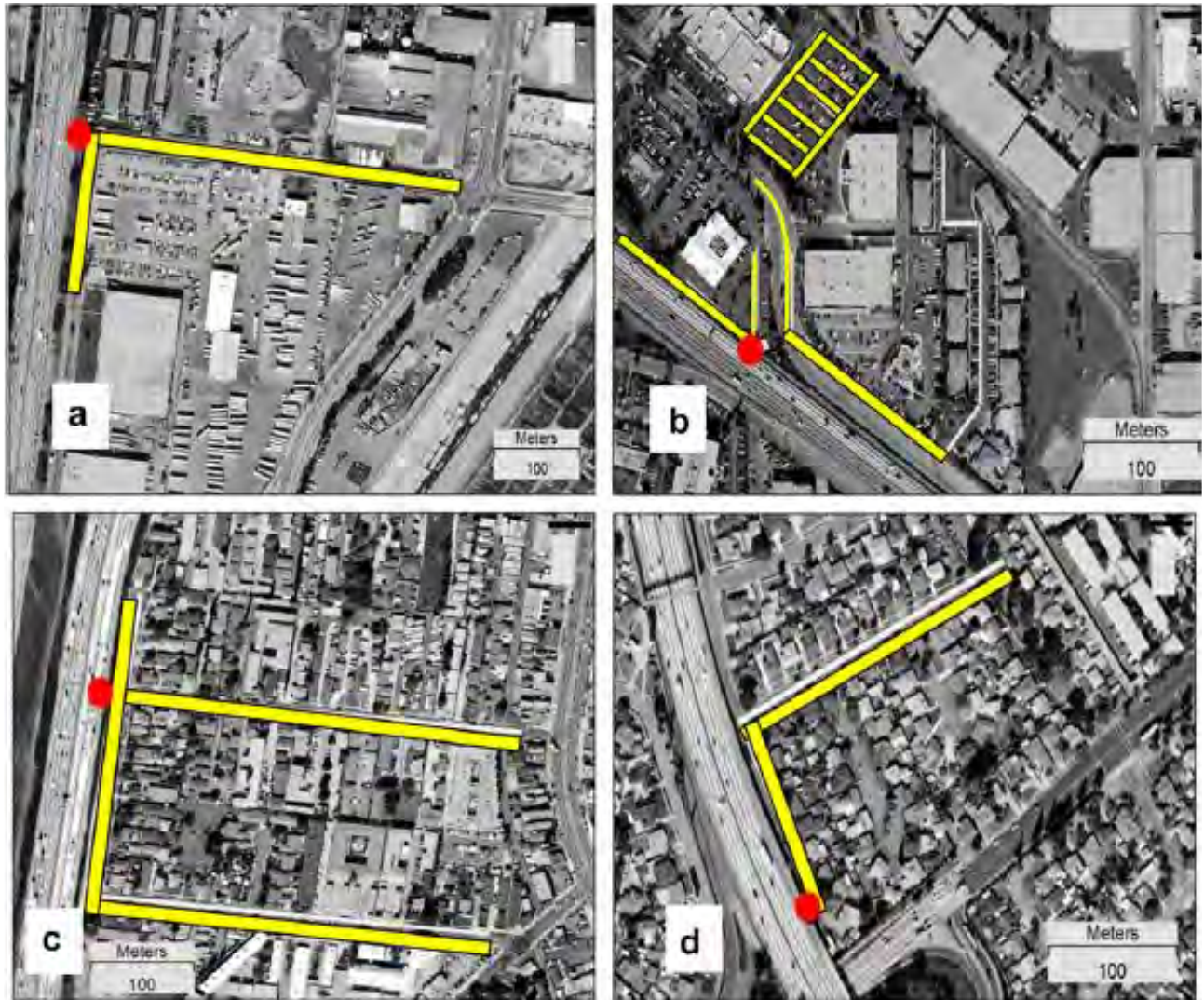


Figure 4: Location of the sampling sites: (a) I-710 without roadside barrier; (b) I-5 without roadside barrier; (c) I-710 with roadside barrier; (d) I-5 with roadside barrier.

2.2. INSTRUMENTATION AND QUALITY ASSURANCE

The instrumentation and quality assurance is discussed for each phase of the monitoring campaign below.

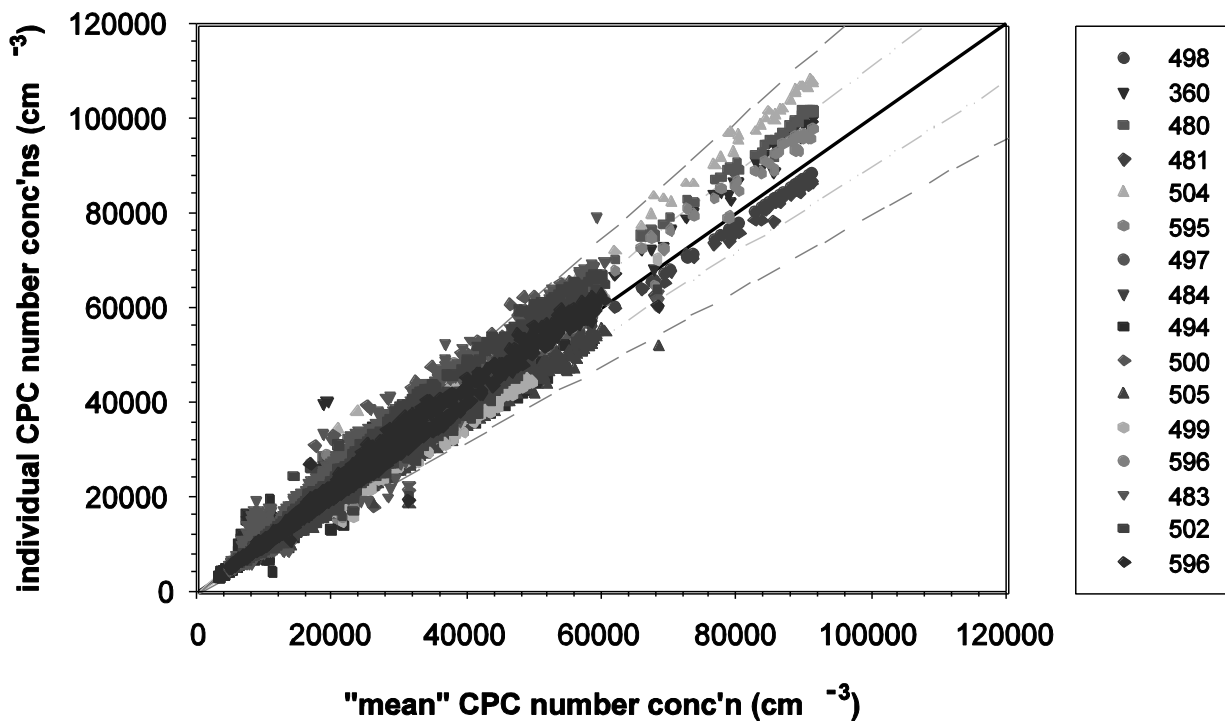
2.2.1. SOURCE AREA STUDY

The standard equipment package installed at most sites included a temperature-controlled, insulated, all-weather enclosure, condensation particle counter (CPC), weather station, and laptop computer. Fifteen identical butanol-based CPCs (Model 3022A, TSI, Inc., Shoreview, MN) were obtained for this study and have a nominal 50% detection efficiency diameter of 7 nm increasing to approximately 100% for particles *larger than* 20 nm. All fifteen CPCs were returned to the manufacturer for factory re-calibration prior to the start of the study. As much as possible, a single CPC was used to perform measurements at each site. The CPC measurements were controlled and the total number concentration recorded using Aerosol Instrument Manager software (v7.3, TSI, Inc., Shoreview, MN). The sampling inlet for each CPC was typically 2 m in length and 0.63 cm in diameter. At selected sites, inlets up to 3.25 m in length were used to locate the sampling point above local obstructions. The sampling stream was not conditioned prior to measurement and the sampling flow rate was 1.5 liters min⁻¹ (lpm). Davis Vantage Pro2 or Pro2 Plus weather stations (Davis Instruments, Hayward, California) were installed at each site except LA1 where data were collected by an existing meteorological station. Wind speed, direction, temperature and relative humidity was collected at each site and analyzed.

Both the CPC and weather station data were logged continuously at one-minute intervals using Pacific Standard Time (PST). The standard operating protocol required weekly visits to download data, check equipment performance, and perform maintenance (instrument operation could not be checked remotely).

The low and high flow rates of each CPC were measured and the flowrates adjusted if they exceeded 0.3±0.03 lpm and 1.5 ± 0.2 lpm, respectively. (It is noted that high flow rate was used when CPCs were operated by themselves and the low flow rate when used with the scanning mobility particle sizer (SMPS) setup.) During the summer (when fog and high relative humidity are common), the routine CPC maintenance procedure was revised to include repeated drain/refill cycles of the butanol reservoir to remove condensed water.

In addition to factory calibration prior to the start of field sampling, side-by-side operation of the CPCs was conducted by measuring ambient concentrations at site LA1. One-minute data were collected over several days for sets of 4–6 CPCs. The average slope of an individual CPC against the mean of concentrations reported by all CPCs is 1.04 ± 0.08 (mean ± standard deviation, range 0.93–1.21) with very high correlation (r^2 range was 0.9–1.0).



1:1 line (solid), ±10%, ±20% (dashed lines)

Figure 5: Intercomparison of CPC performance via side-by-side testing, December 2006 - February 2007. One-minute data were used for this comparison.

Variations in performance between the CPCs could not be readily explained by measured differences in the low or high CPC flow rates or the re-calibration data supplied by the manufacturer. The side-by-side tests were also repeated at the end of the sampling campaign (Figure 6). There is more scatter in the post-HCMS data, but the average slopes changed little (0.98 ± 0.16 , range 0.72–1.26) and the correlation remains high (r^2 is 0.98 ± 0.3). The ratio of post- to pre-study slope of each instrument was $0.94 \pm 14\%$ (75–121% range).

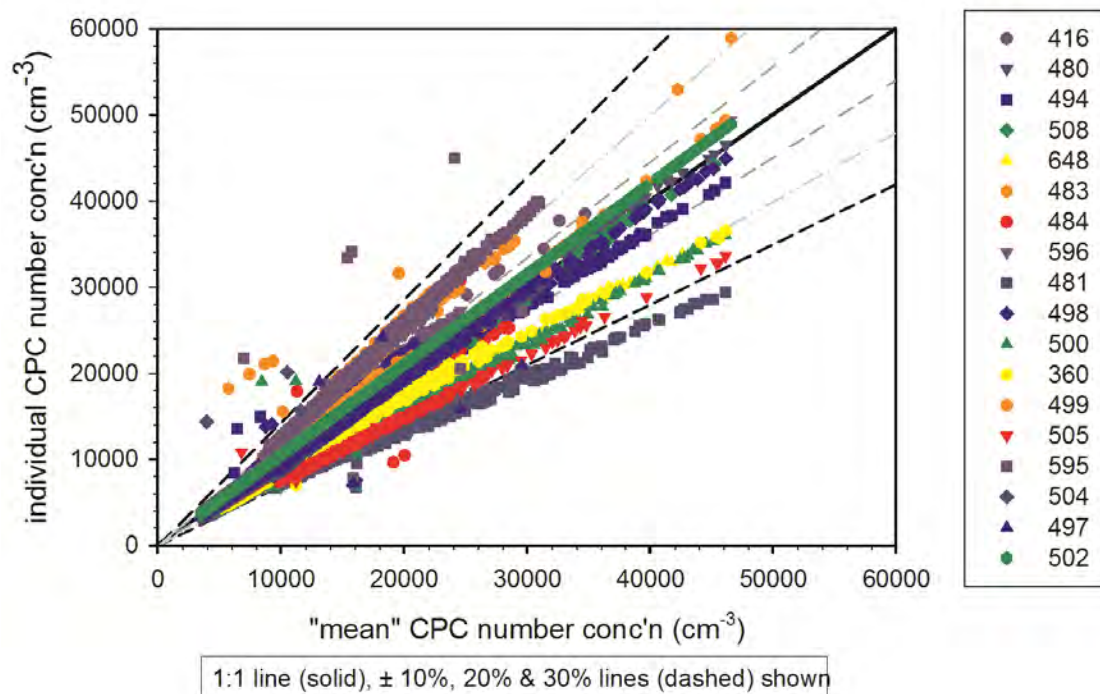


Figure 6: Intercomparison of CPC performance via side-by-side testing, December 2007. One-minute data were used for comparison.

Given the relative consistency in these results, no corrections to account for variations in individual CPC performance were made to the mean data reported here. Observations using the longest inlet (3.2 m) were 3% less than those using a standard inlet, consistent with theoretical predictions using the Gormeley-Kennedy equations and particle size distribution data (Krudysz et al., 2009). No corrections for inlet length were made. Further, theoretical calculations suggest inertial losses in the inlets and sampling lines for larger particles (e.g., 1 μm in diameter) are negligible and were also ignored. It should be further noted from a parallel study (Krudysz et al., 2009), that the particles susceptible to these losses formed an insignificant fraction of the particle number concentration.

All one-minute weather and CPC data were reviewed and screened for irregularities using a procedure similar to that reported elsewhere (Puustinen et al., 2007) with comparable data removal rates. In this report, only hourly averages are reported. Overall, data are available for approximately 90% of the sampling periods at each site. For most months and sites, data availability exceeded 90%, but water condensation in the butanol reservoir during June and July (75% data availability overall, 65% minimum value) reduced the campaign's average.

2.2.2. RECEPTOR AREA STUDY

Total particle number concentrations were measured at all sites using Condensation Particle Counters (CPC, Model 3022A, TSI, Inc., Shoreview, MN). A Scanning Mobility Particle Sizer (SMPS, Model 3936, TSI, Inc., Shoreview, MN) was used at select sites to measure the particle size distributions. The CPC used can measure with about 100% efficiency particles above 20 nm and has 50% detection efficiency for a diameter of 7 nm. The upper size limit for detection is 3 μm . The CPC recorded data at one-minute intervals. The sampling rate was maintained at 1.5 ± 0.2 liters per minute and the air stream was not conditioned prior to sampling. The SMPS system consists of a long Differential Mobility Analyzer (DMA; Model 3081, TSI, Inc., Shoreview, MN) and CPC 3022A (operating at 0.3 ± 0.03 liters per minute, sheath air was not pre-conditioned), set to 5 minute scans covering the size range 14-736 nm. TSI software Aerosol Instrumentation Manager was used to collect data from both the CPC and the SMPS. Weekly site visits were made to ensure proper equipment operation and perform maintenance. Flow rates were checked weekly and maintained within the ranges specified above. All inlets used to sample ambient aerosols were copper tubes of 1 cm diameter.

Similar to the Source Area Study, the CPCs were run simultaneously at LA1 to evaluate performance. The data are shown in Figure 7 below.

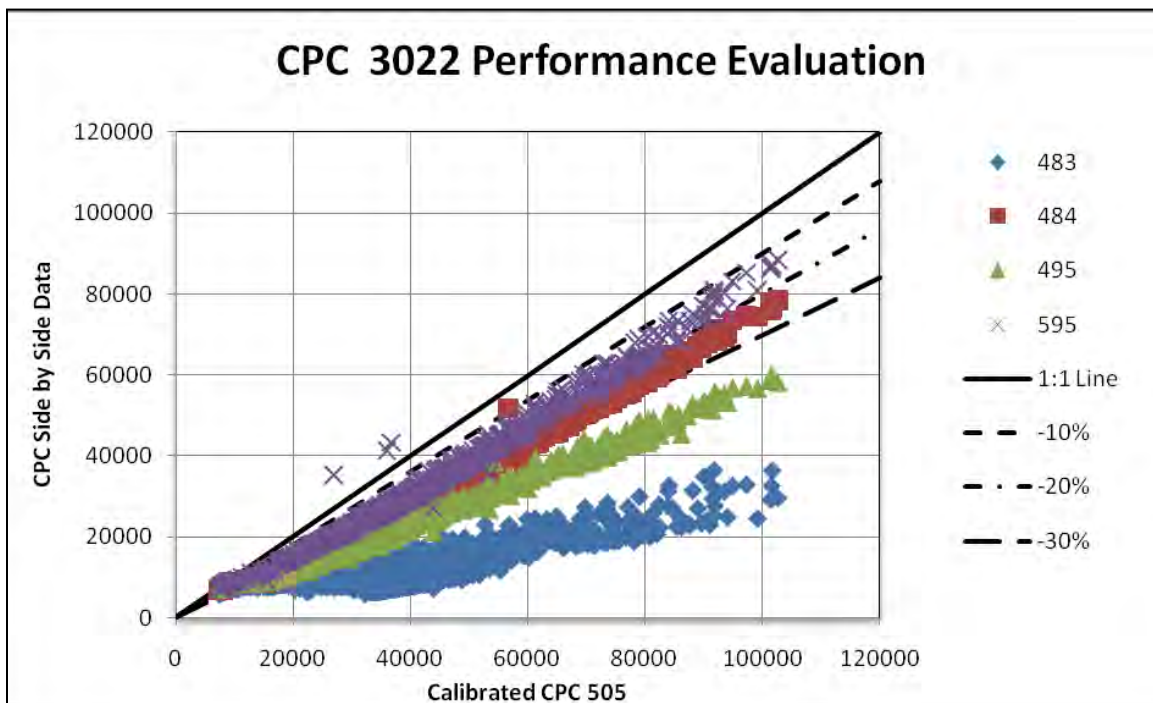


Figure 7: Intercomparison of CPC performance via side-by-side testing, December 2009. One-minute data were used for comparison.

At the end of the study, the CPCs were set up to run side-by-side for over 48 hours. Analysis of the data indicated that the average slope of a CPC against the mean concentration of all CPCs was 0.98 ± 0.16 and the range was 0.72-1.26. CPC concentrations were compared to the corresponding concentration measured by a factory-calibrated CPC (#505). The correlation coefficient (r) between all the CPCs was in the range 0.86-0.99, even though two CPC reported an average slope less than 0.7 against a factory-calibrated CPC. We elected to compare CPCs with a unit calibrated by the factory instead of the mean of the CPC values because the CPCs had been operating in field continuously for over two years, and several units used in earlier studies by our group had shown performance deterioration with prolonged field use. The data were corrected (assuming a linear deterioration in performance over the span of operating period) to compensate for the inconsistency between the CPCs. Details of CPC calibration, adjustment factors used and corrected data are reported in Appendix B of the report. No corrections were made for diffusion losses, due to different inlet lengths, because our earlier characterization showed that they are insignificant (Moore et al., 2009).

Meteorological data, i.e., temperature, relative humidity, wind speed and direction among other parameters were collected using Vantage Pro 2 Weather Stations (Davis Instruments, Hayward, CA). The meteorological station was placed above the enclosure and the wind vane sampled at a height of 5 m above the ground surface. The USC meteorological data were compared with similar data collected at neighboring AQMD stations with more standardized meteorological equipment. Only for wind speed and direction were slight differences observed. This was likely because of the lower height of the USC equipment compared to the typical height of 10 m for most AQMD meteorological measurements. Even then, the diurnal patterns of these parameters were consistent with those reported by AQMD.

All particle monitoring equipment were placed in an air-conditioned enclosure, but there were instances in summer when temperatures exceeded the optimum operation temperature for the equipment ($\sim 35^{\circ}\text{C}$) and the data for such instances were screened from the analysis. At times during summer, water condensation was observed in the CPC. For such events, the CPC reservoirs were drained and the CPC data were excluded from analysis.

Given the high temporal resolution of the data (i.e., 1-minute particle number concentration, 5-minute size distribution scans, wind speed, wind direction, temperature, relative humidity, and other parameters collected up to a year at 7 sites) it was not practical to provide detailed description and interpretation of all data. Therefore, in this report we present data as hourly averages and for consistency, the hourly averages are reported in local time for the entire year. All collected data were thoroughly reviewed for irregularities, similar to the work of Puustinen et al., (2007). Data were not included in averages if the counts reported were below 1000 particles/cm³ or exceeded 10^6 particles/cm³, which were associated with electronic errors in CPC. The data recovery rates are reported in Table 3. The lowest data recovery was reported for June 2009, when we experienced excessive water

condensation inside the CPC butanol reservoirs. Data from site VBR are not reported after April 2009, as the measured concentrations were unreliable due to a CPC malfunction. Prior to the commencement of the sampling campaign, CPCs were operated side-by-side at USC for a 24-hour period to ascertain consistency. The statistical methods used for analysis in the present study are discussed in our earlier work (Moore et al., 2009 and Krudysz et al., 2009).

2.2.3. SOUNDWALL STUDY

Two sets of sampling instruments were deployed simultaneously, one at the stationary sampling station and the other in the mobile platform. A list of the instruments at both sampling stations, including their data resolution, is shown in Table 4. The stationary station set up included a Scanning Mobility Particle Sizer (Model 3080, TSI) configured to measure the particle size distribution in the size range of 10 to 225nm.

Concentrations of black carbon (BC) and two gaseous pollutants (carbon monoxide (CO) and nitrogen dioxide (NO₂)) were also measured at the station in the immediate proximity of freeway. A video camera was set up on top of the sampling station to record the traffic on the freeway and a sonic anemometer was set up at a height of 4 m above the freeway road surface at all four sampling sites to collect wind speed and direction data. For the noise barrier sites, the sampling inlet was placed upwind of the barrier within 2 meters of the freeway edge.

The mobile platform was a 1998 electric Toyota RAV4 SUV equipped with various onboard monitoring instruments. The same vehicle has been used in many previous studies (Westerdahl et al., 2005; Fruin et al., 2008; Kozawa et al., 2008) in Southern California. The sampling inlet consisted of a 6-inch diameter galvanized steel duct, located 1.5 m above the roadway in the rear passenger space of the vehicle. The particle size distribution data (6-523 nm) were collected using a Fast Mobility Particle Sizer (Model 3091, TSI). Black carbon and co-pollutants (CO, NO₂) concentrations were measured simultaneously to calculate their downwind concentration ratios. A GPS unit was used to record the exact location of the mobile platform and the geo-coded data were used to derive its downwind distance from the freeway. The mobile platform was also equipped with an on-board camera to distinguish times when the mobile platform measurements were impacted by a passing vehicle.

Quality assurance measures, including flow and zero checks of all instruments as well as calibration of gaseous pollutant monitoring instruments, were carried out before and after the sampling campaign. The side-by-side tests of the stationary and mobile platform measurements showed that the CO, NO₂ and BC data pairs were within 5% of each other. All the instruments at both the stationary station and the mobile platform ran on synchronized time. The two instrument sets were run side-by-side overnight at the beginning and end of each sampling period for all four sampling sites to assess the systematic uncertainty due to the difference of monitoring instruments and to inspect the time lag (a consequence of different flow rates, inlet lengths, and instrument response time) between the actual sampling and the reported time.

Table 4: Monitoring instruments deployed in stationary sampling station and the mobile platform.

Measurement	Stationary sampling station	Mobile platform
Geodata	GPS (Garmin GPSmap 76CSx)	GPS (Garmin GPSmap 76CSx)
Particle size distribution	SMPS: TSI model 3080 (long DMA) w/TSI model 3022A (CPC) @ 5 min intervals (10 – 225 nm range)	FMPS: TSI model 3091 @ 20 sec intervals (6 – 523 nm range)
Black Carbon	Aethalometer: Anderson model 14 (dual channel) @ 1 min intervals	Aethalometer: Magee Scientific @ 1 min intervals
CO	QTrak – TSI model 7565 @ 1 min intervals	Teledyne API model 300E @ 20 s intervals
NO₂	Teledyne-API model 200A @ 1 min intervals	Teledyne-API Model 200E @ 20 s intervals
Meteorological data	3-D sonic anemometer (RS Young model 81000) @ 1 min intervals	2-D sonic anemometer (RS Young) @ 1 sec intervals

2.3. ANALYTICAL METHODS

The analytical methods for each monitoring phase are discussed below.

2.3.1. SOURCE AREA AND RECEPTOR AREA STUDY

The correlation coefficient (r) is a standard method used to evaluate the (linear) relationship between paired data points. The coefficient can vary from 0 (no correlation, independent data points) to ± 1 indicating perfect positive or negative correlation. In this study, the correlation coefficient is calculated between specific site pairs using hourly mean number concentration values (these are plotted for each month in Figures 33, 34, 35 & 36). This analysis helps to determine what fraction of the number concentrations at any particular site can be explained by the concentrations simultaneously measured at the other site. One limitation of this method, however, is that perfect correlation can be observed between two sites where the concentrations vary by a consistent factor. In other words high correlations between paired sites would only imply uniform temporal variation (Lianou et al., 2007). Therefore, calculating r alone with matched hours would not necessarily provide sufficient information to characterize the similarity between two sites.

A more useful method to characterize the spatial variability between site pairs is the coefficients of divergence (COD). The COD is defined as:

$$\text{COD}_{jk} = \sqrt{\frac{1}{n} \sum_{i=1}^n \left(\frac{x_{ij} - x_{ik}}{x_{ij} + x_{ik}} \right)^2}$$

where x_{ij} is the i^{th} concentration measured at site j for a given sampling period, j and k are two monitoring sites being compared, and n is the number of observations (Krudysz et al., 2009). In this case, the sampling period is one hour and “ n ” is the number of valid samples in a month (<720). By inspection, the COD for a given site pair will vary from 0 (where concentrations are identical at both sites) to 1 (where concentrations are very different). The COD therefore specifically addresses the limitation to the correlation coefficient described above where concentrations at two sites can exhibit similar temporal variation but have very different concentrations. A low COD value (e.g., 0 – 0.1) indicates a high level of homogeneity in concentrations between site pairs, and a high COD, the opposite. COD values larger than 0.2 indicate heterogeneous concentrations (Wilson et al., 2005).

CODs have been used to quantify the variability in PM_{2.5} and PM₁₀ mass concentrations between specific site pairs in several studies—for example in the Los Angeles region where CODs varied from 0.07–0.48 (Pinto et al., 2004). Most maximum values reported in California and at other locations in the United States and the world were on the order about 0.2 and less (Pinto et al., 2004; Kim et al., 2005; Wilson et al., 2006). Overall, these results imply a fair amount of spatial homogeneity between the concentrations measured.

However, while CODs of PM_{2.5} mass concentration may be relatively low, recent studies of PM_{2.5} individual chemical components in the Los Angeles-area yield widely varying CODs indicating homogenous (Wongphatarakul et al., 1998) to very heterogeneous spatial distributions (Krudysz et al., 2008). Heterogeneous distributions were also observed for trace elements in St. Louis (Kim et al., 2005). Similarly, concurrent observations of PM mass and number concentrations in four European cities using paired residential and city center sites yielded homogeneous CODs for the mass measurements (PM_{2.5} and PM₁₀, 0.02–0.10 COD range), but heterogeneous values for particle number concentrations (0.07–0.53 range) (Lianou et al., 2007). In order to evaluate intra-community variability in total particle number concentrations, both the correlation coefficient and the COD for each individual site pair must be calculated.

2.3.2. SOUNDWALL STUDY

All data from the stationary sampling station were downloaded and exported using proprietary software and data from the mobile platform were exported to a custom database for all instruments. Data used for data analysis were chosen from the sampling time periods when the measured wind direction was ± 45 degrees from perpendicular to the freeway, placing the sampling locations of the mobile platform downwind of the selected roadway region. Time periods that were influenced by nearby emissions (i.e., a truck passing by the mobile platform) were excluded from the data analysis. GPS tracking data were exported and converted to determine the mobile platform's perpendicular distance downwind of the freeway. The particle size distribution and other pollutant concentration data at various downwind distances were segregated into several distance ranges, and the distance values presented in the X-axis of the figures hereafter represent the midpoint of each distance range. The concentration ratios of NO₂, CO, and BC at different downwind distances of the freeway were determined by normalizing the downwind data from mobile platform with their corresponding data collected at the stationary sampling station. The CO data from the stationary station on the I-5 freeway were not available due to a malfunctioning instrument, therefore absolute concentrations are presented. The particle size distribution data were further segregated into several size groups to derive their respective number and mass concentrations at various distances. The particle mass concentrations were determined by their corresponding particle volume concentrations using an assumed particle density of 1.2 g/cm³ (Geller et al., 2006).

3. RESULTS

3.1. SOURCE AREA STUDY

3.1.1. METEOROLOGY

In general, meteorological conditions during the study exhibited limited diurnal and seasonal variability. Table 5 shows the mean temperature and relative humidity at three selected sites — LA1 (the regional site, 32 km inland), LB1 (in the San Pedro Harbor), and LB8 (5 km inland from the Harbor). Temperature tends to peak mid-day, declining overnight and into the early morning, and relative humidity (RH) follows the opposite pattern. At LB1, cooler mean temperatures are observed in March (14.3°C) warming to 20.7°C in August before cooling again in November (16.9°C). The RH (70–85% range) is relatively stable and high, and variability in both the temperature and RH is muted due to the presence of San Pedro Bay. Moving inland to LB8, the same seasonal pattern in temperature is observed, although it is about 2°C warmer on average and the RH is correspondingly slightly reduced (65–74% range). At LA1, mean temperatures are about another 1°C warmer than at LB8 and the mean RH is also lower (51–64% range). At sites located further inland, the moderating influence of the marine air is reduced, variability increases and some urban heat island effect is also observed.

The conditions at LB1 and LB8 bound the observations made at the other sites in the Harbor Communities. Wind speed and direction can significantly affect observations of ultrafine particle number concentrations. A general discussion of the wind patterns observed at the study sites during the field measurement campaign is included here. More specific information is provided as necessary in the presentation of the UFP number concentration results that follow. At the regional site LA1, wind was most often from the SW (28%), WSW (15%), and S (12%) and typically light (predominantly $< 2.0 \text{ ms}^{-1}$). Calm winds (16%) were observed overnight with wind speed increasing into the afternoon. Given this pattern, LA1 was usually downwind from the I-110, particularly during daylight hours. As the study progressed from March into the spring and summer, peak wind speeds increased slightly (mean wind speed in March about 1 ms^{-1} and about 1.6 ms^{-1} in July) and fewer calms were observed overnight. These observations are very consistent with previous measurements reported for this site (Moore et al., 2007).

Occasionally during the fall, this consistent pattern was disrupted by Santa Ana wind conditions in the Los Angeles basin (dry persistent offshore winds driven by synoptic high pressure systems over the southwestern United States). During these periods (e.g., October 19–26), SE and SSE components in the wind rose are observed, particularly from 8 pm through noon. In the afternoon, the SW component is again evident. Measured wind speeds at LA1 remain light and variable throughout the Santa Ana conditions.

Similar to the observations at LA1, wind patterns at the study sites near the Harbor tended to be relatively stable throughout the study period. Overall wind speeds tended

to increase into the late summer. Calms were observed overnight, with fewer occurring in the spring/summer months. Mean and peak wind speeds were often higher closer to the Harbor where there are fewer obstructions to the flow. Mean monthly wind speeds overall, however, remained relatively light (not more than a few ms^{-1}), although this may in part reflect the relatively low installation height of the study anemometers. Some sites (e.g., W1, W2, LB4, LB5) exhibited a predominantly onshore/offshore (e.g., S/N) flow pattern with the offshore flow strongest in the early morning followed by the onshore return flow in the afternoon. Many of the farther inland sites in Long Beach exhibit the same general pattern (e.g., LB2, LB3, LB6, LB7, LB8, LB9) but include the development of a strong WNW or NW wind (reflecting onshore flow from the Pacific Ocean rather than onshore flow from San Pedro Bay) in the early afternoon that persists into at least the early evening. Santa Ana wind conditions generally produced somewhat lighter winds overall and a significant overnight N component.

Table 5: Temperature and Relative Humidity—monthly mean for select sites

Month	LAI		LBI		LBS	
	T (°C)	RH (%)	T (°C)	RH (%)	T (°C)	RH (%)
March	16.7 ± 4.4	51 ± 25	14.3 ± 1.2	78 ± 6	15.5 ± 3.0	70 ± 12
April	16.2 ± 3.2	61 ± 19	14.3 ± 0.9	79 ± 4	15.9 ± 2.6	70 ± 11
May	17.7 ± 4.0	59 ± 19	15.5 ± 1.0	78 ± 4	17.3 ± 2.7	68 ± 10
June	19.6 ± 3.5	64 ± 14	17.2 ± 1.1	84 ± 3	19.0 ± 2.6	74 ± 10
July	22.6 ± 3.3	62 ± 14	19.6 ± 1.0	85 ± 3	22.0 ± 2.7	73 ± 10
August	23.5 ± 3.9	58 ± 15	20.7 ± 1.4	82 ± 6	22.9 ± 3.0	70 ± 11
September	21.7 ± 4.7	56 ± 16	18.8 ± 1.3	80 ± 5	21.0 ± 3.1	69 ± 12
October	20.3 ± 4.7	50 ± 23	18.1 ± 1.6	73 ± 6	18.9 ± 4.0	65 ± 14
November	16.9 ± 4.0	58 ± 26	15.6 ± 1.1	78 ± 3	15.9 ± 2.8	73 ± 10

^aBased upon hourly mean data.

^bMean ± standard deviation.

Illustrative wind roses are shown as follows for September 2007.

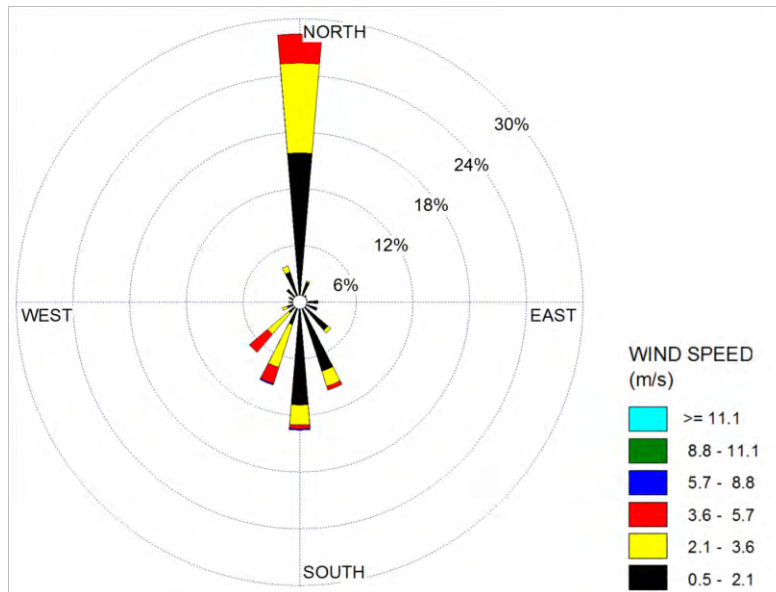


Figure 8: All hours wind rose for site W1 during September 2007. The mean wind speed was 1.2 ms^{-1} and calm winds occurred 10% of the hours.

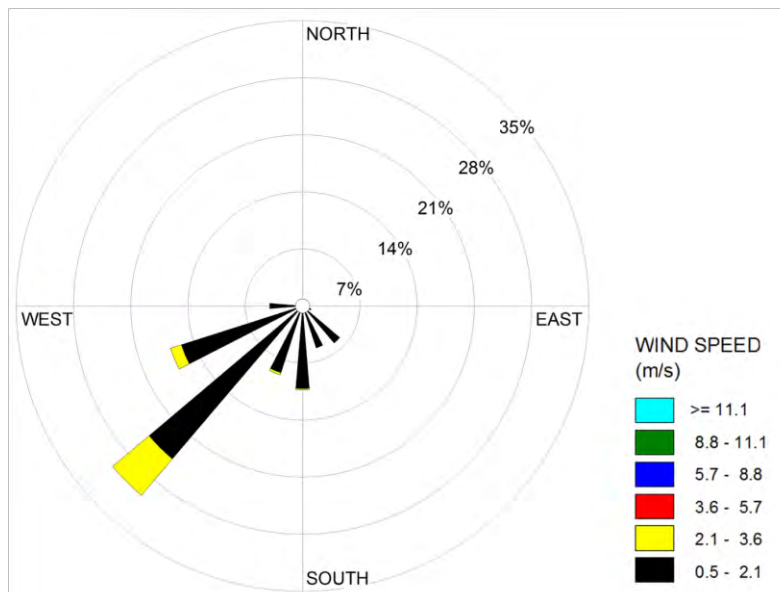


Figure 9: All hours wind rose for site SP1 during September 2007. The mean wind speed was 3.2 ms^{-1} and calm winds occurred 5% of the hours.

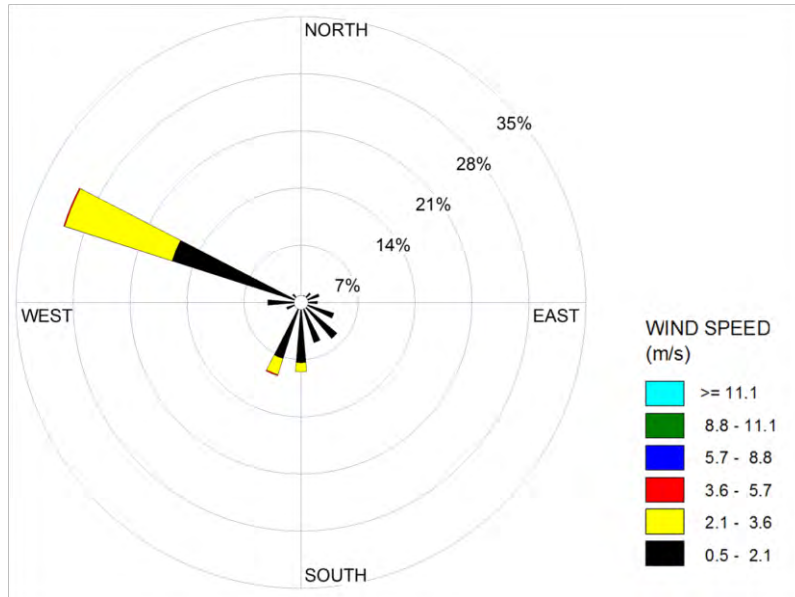


Figure 10: All hours wind rose for site LB8 during September 2007. The mean wind speed was 1.1 ms^{-1} and calm winds occurred 23% of the hours.

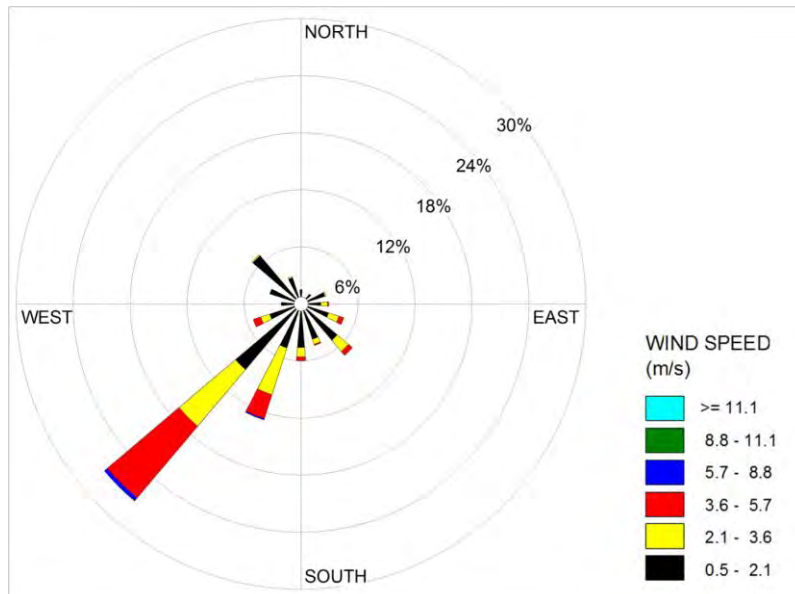


Figure 11: All hours wind rose for site LB1 during September 2007. The mean wind speed was 2.0 ms^{-1} and calm winds occurred 8% of the hours.

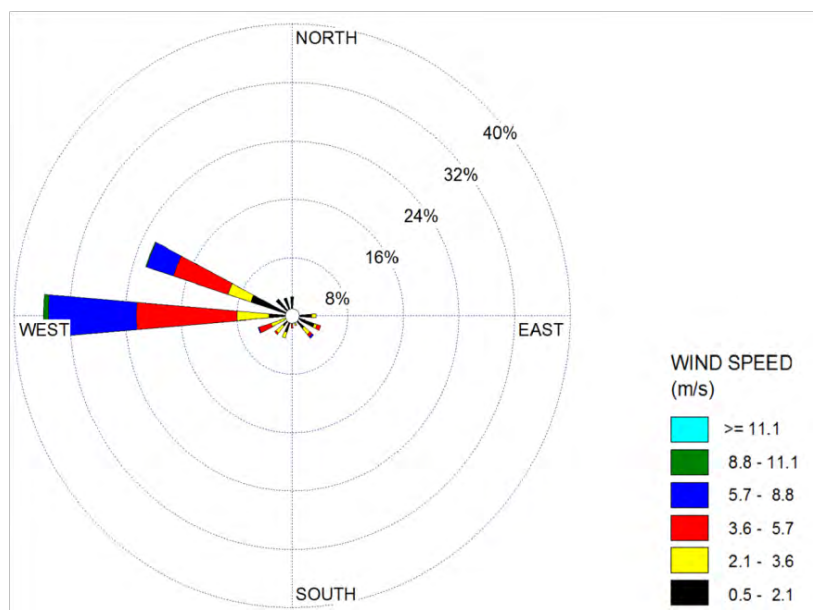


Figure 12: All hours wind rose for site LA1 during September 2007. The mean wind speed was 1.1 ms^{-1} and calm winds occurred 17% of the hours.

3.1.2. ULTRAFINE PARTICLE CONCENTRATIONS

The hourly average UFP concentration data are presented for selected sites to highlight the differences/similarities between emission sources and observations at these sites. Comprehensive hourly mean data for each site (shown for alternate months) are presented below in Figure 13. Alternate months only are shown to improve the clarity of the figures. A few examples are presented where specific impacts on total particle number concentrations are identified (e.g., weekday vs. weekend concentrations), followed by the monthly mean 24-hr concentrations and selected correlation coefficient and COD results calculated across all site pairs. While not shown in each figure for clarity, the standard error of the mean for each hour at most of the sites was about 10%. The two exceptions are the harbor background sites (i.e., SP1, LB1) where the standard error was about 10–30%, primarily due to lower mean concentrations. Geometric mean concentrations are not provided, but, where calculated, were typically 80–90% of the arithmetic mean.

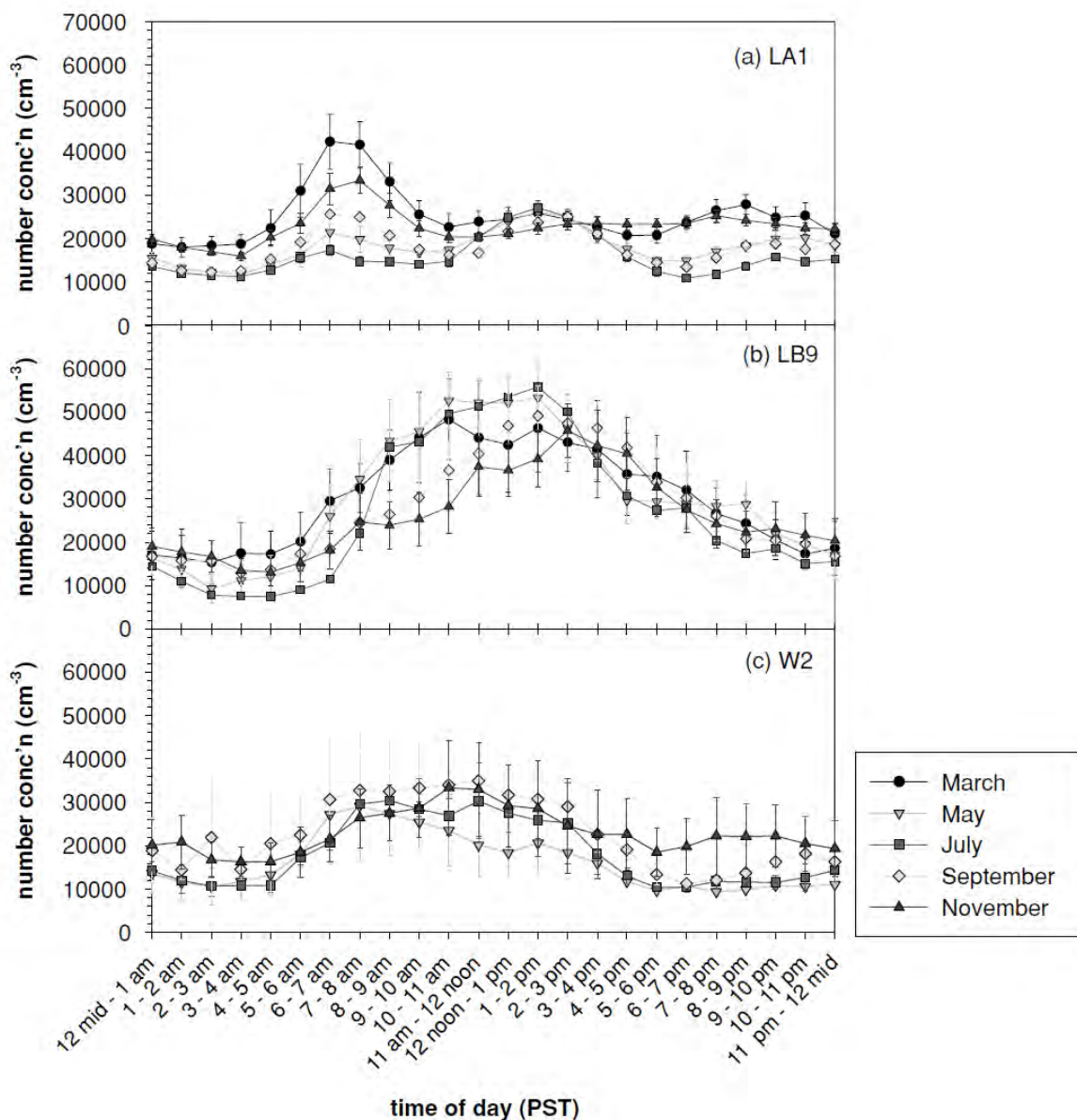


Figure 13: Hourly average particle number concentrations shown for alternate months (standard error of the mean shown) for three sites: (a) LA1, (b) LB9, and (c) W2.

At site LA1, PNC data, considered to be typical of the Los Angeles urban background, were observed (Figure 13a). In the early spring and late fall months, a distinct early commute peak from light duty gasoline vehicles (LDGV) between 5–10 am is evident. As overnight temperatures and the mixing height increase into the late spring and summer, this peak almost vanishes (e.g., July), but a later peak in the early afternoon (12 noon–4 pm) slightly increases, despite the mixing height change. We interpret this peak to represent secondary production of particles, which is consistent with earlier summertime observations of changes in physical properties and chemical composition in the UFP reported for the same site (Moore et al., 2007; Ning et al., 2007). The

evening peak in the data is consistent with secondary condensation of low vapor pressure compounds into the particle-phase, growing sub-7 nm particles into the range observable by the CPC, and a decreasing mixing height; both of these features have been observed previously in Los Angeles (Kuhn et al., 2005; Biswas et al., 2007). At several sites in the study area, however, the influence of HDDV traffic and the routine goods movement patterns are starkly evident and very different from the LA1 observations. At site LB9, only limited early morning commute peaks and no distinct secondary afternoon or evening peaks are observed (Figure 13b). Instead, particle number concentrations start to climb around 5 am, reach a plateau at 40,000–50,000 cm^{-3} from 10 am–4 pm and then start a slow decline into the evening. Peak concentrations decline somewhat in the summer months and the concentration gradient in the morning is less steep due to higher mixing heights and warmer overnight temperatures consistent with their impacts on site LA1 (discussed above). Limited measurements at a nearby intersection indicate up to 600–700 HDDVs per hour pass by during the day en route to the adjacent Intermodal Container Transfer Facility (ICTF) (Houston et al., 2008), and traffic can become considerably backed up, particularly in the afternoon. Therefore, this UFP concentration pattern is representative of HDDVs and goods movement from the Ports. A similar pattern was also observed at site W2 (Figure 13c) where concentrations are somewhat lower and limited data suggest this site experiences comparatively lighter HDDV traffic compared to the ICTF (Port of Los Angeles, 2004; Houston et al., 2008).

In both community clusters, the LA1 data are included for regional context. In March, site W3—near the Alameda and Anaheim intersection—shows a similar early morning peak as LA1 (Figure 14a). While the available traffic data are old, this would be consistent with the relatively large fraction of Light Duty Gasoline Vehicles (LDGV) at this intersection compared to other locations (e.g., W2) in the Harbor Communities (Port of Los Angeles, 2004). Site W2 shows relatively constant concentrations throughout, as it is immediately adjacent to traffic sources. Concentrations at both sites are not appreciably different from those observed at LA1. As the sampling campaign progressed (Figures 14b–14d), sites W2 and SP1 came on-line, respectively showing impacts from the HDDV traffic (discussed previously) as well as the lower harbor background concentrations. Total particle number concentrations at site W3 in the mixed residential/industrial area remain comparable to or larger than site LA1, downwind of the I-110, although site W3 is much further away from freeways. The morning commute peak returns to site W3 as the fall progresses. Even site W1—at least a 1000 m from high traffic roadways—shows concentrations comparable to LA1 with observations roughly double those observed at the harbor background sites. Given W1's location across the channel from the Ports, this suggests that Port-related activities are primarily responsible for the change in concentrations.

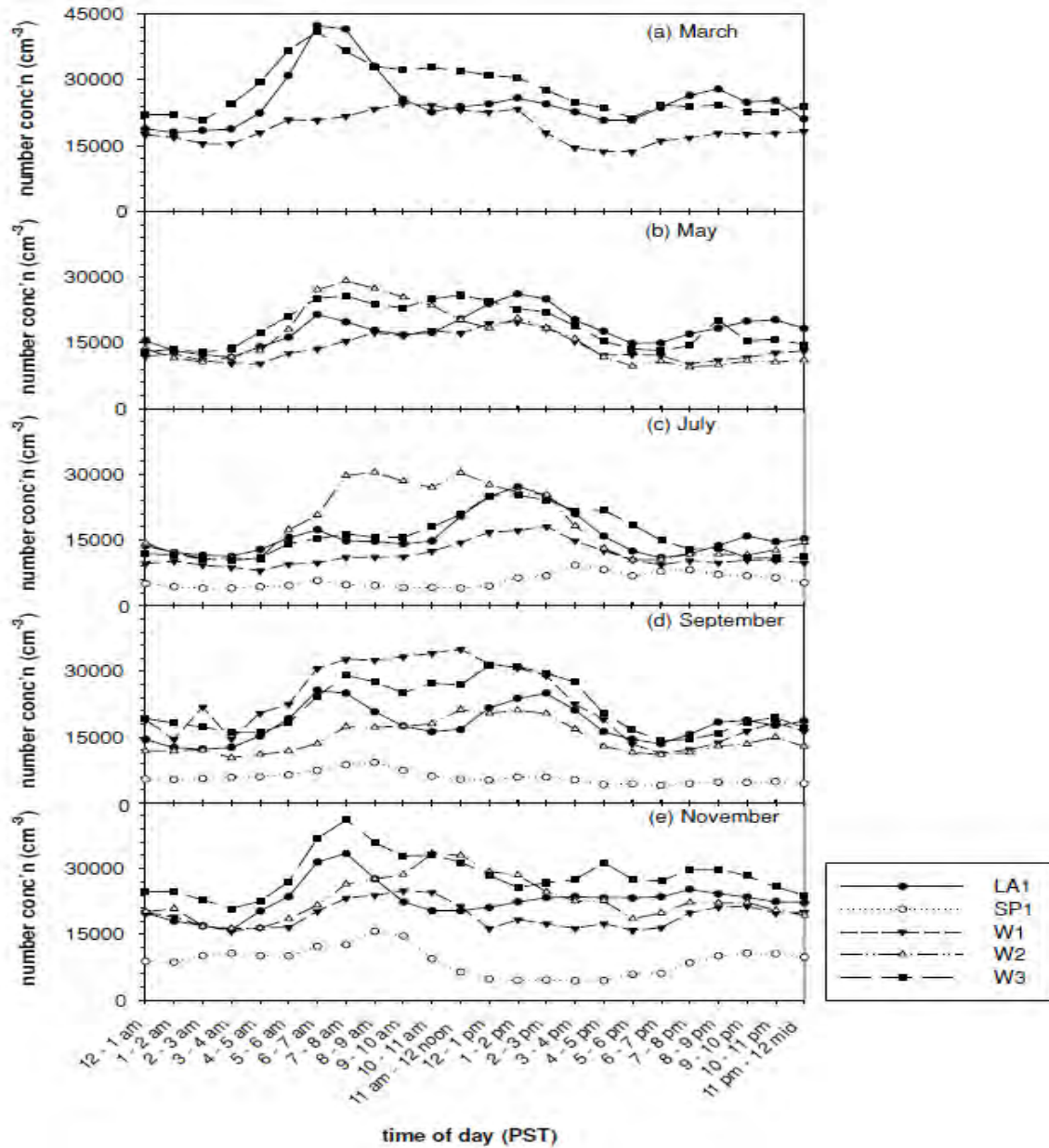


Figure 14: San Pedro/Wilmington site cluster and LA1 site — hourly average particle number concentrations shown by alternate months: (a) March, (b) May, (c) July, (d) September, and (e) November.

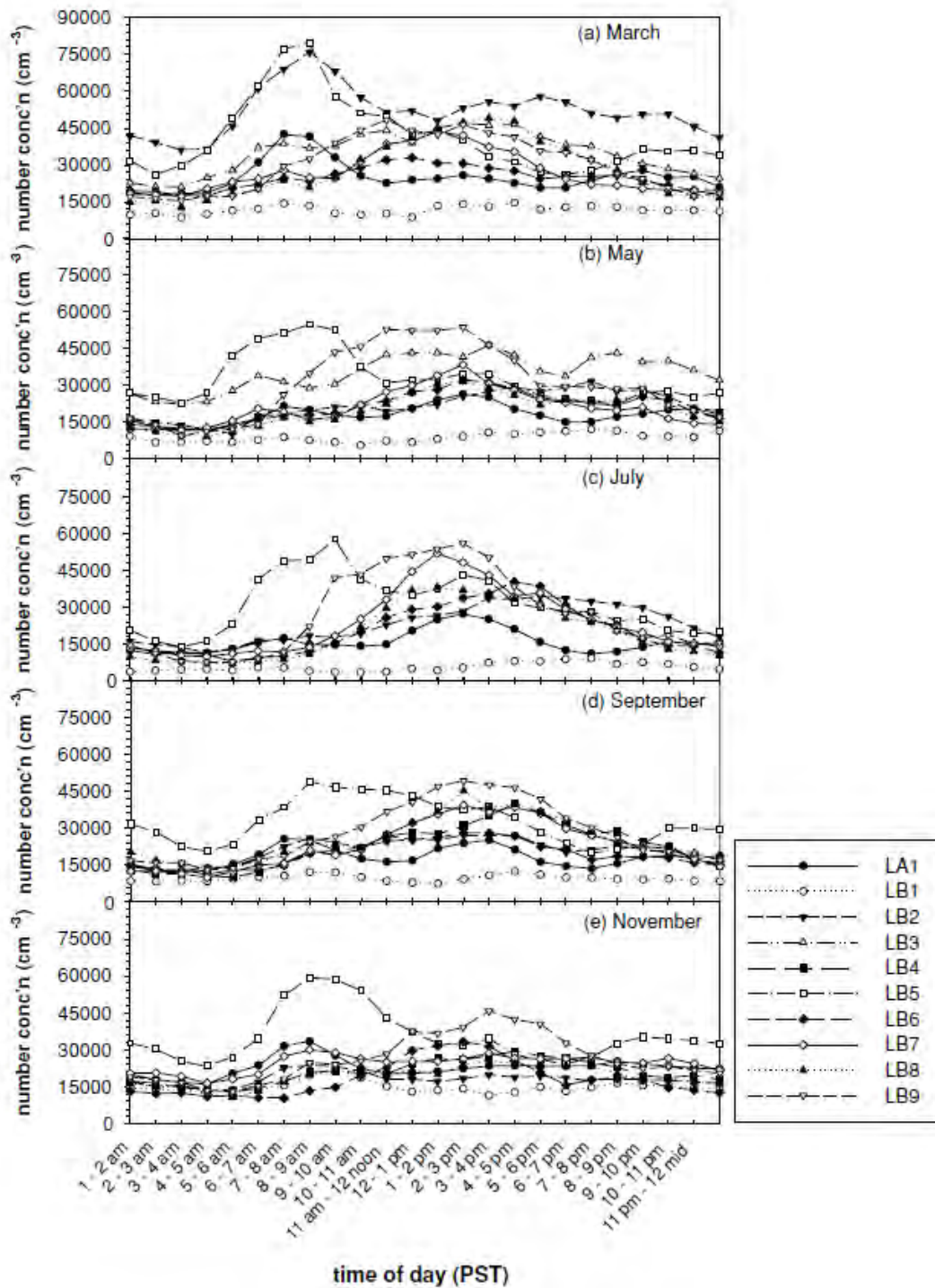


Figure 15: West Long Beach site cluster and LA1 site — hourly average particle number concentrations shown by alternate months: (a) March, (b) May, (c) July, (d) September, and (e) November.

In both community clusters, the LA1 data are included for regional context. In March, site W3—near the Alameda and Anaheim intersection—shows a similar early morning peak as LA1 (Figure 14a). While the available traffic data are old, this would be consistent with the relatively large fraction of Light Duty Gasoline Vehicles (LDGV) at this intersection compared to other locations (e.g., W2) in the Harbor Communities (Port of Los Angeles, 2004). Site W2 shows relatively constant concentrations throughout, as it is immediately adjacent to traffic sources. Concentrations at both sites are not appreciably different from those observed at LA1. As the sampling campaign progressed (Figures 14b–14d), sites W2 and SP1 came on-line, respectively showing impacts from the HDDV traffic (discussed previously) as well as the lower harbor background concentrations. Total particle number concentrations at site W3 in the mixed residential/industrial area remain comparable to or larger than site LA1, downwind of the I-110, although site W3 is much further away from freeways. The morning commute peak returns to site W3 as the fall progresses. Even site W1—at least a 1000 m from high traffic roadways—shows concentrations comparable to LA1 with observations roughly double those observed at the harbor background sites. Given W1’s location across the channel from the Ports, this suggests that Port-related activities are primarily responsible for the change in concentrations.

In the West Long Beach cluster (Figure 15a–e), total particle number concentrations at many of the sites are higher than at LA1, particularly in the afternoon. While this is expected at site LB5, immediately adjacent to the I-710, this is also true at LB2 due to the high LDGV and HDDV traffic volume (Houston et al., 2008; Port of Los Angeles 2004) and at the other sites with the exceptions of the harbor background site, LB1, and LB6 where particle number concentrations are comparable. Of particular note is the persistent HDDV signal at LB9 during the day, which is also apparent at many other sites. The prevailing westerly winds that affect the West Long Beach cluster in the afternoon may well be responsible. While the morning commute signal remains evident at LB5 throughout the study period, it is stronger in the early spring and fall as observed at LA1. As the fall progresses, concentrations at LB1 increase while concentrations at other sites tend to decrease, such that the PNCs at LB1 are no longer distinctly lower than observed at the other sites. The two harbor background sites—SP1 and LB1—generally yielded the lowest total particle number concentrations of the study sites as they were mostly upwind of the nearby UFP sources (Figure 16 includes monthly data not shown in Figures 14–15). Concentrations were generally comparable between the two, although in the fall, LB1 concentrations (as discussed above) became consistently higher than SP1’s. Overall PNCs increased during the cooler months but consistent diurnal patterns were infrequently observed. There was one distinct period, however, during early August when SP1 was strongly impacted each afternoon by a ship’s plume. The bulk carrier Xiamen Sea was docked at Berth 47 while undergoing engine repairs intermittently during the summer (June–August). The ship’s buoyant plume—even if present and upwind of the sampling site—was above our sampling site and no evidence for significant plume impacts from this source were observed prior to August 5. On August 5–13, highly elevated UFP concentration plumes were measured every afternoon, with hourly concentrations occasionally exceeding $140,000 \text{ cm}^{-3}$. Concurrent

site operator notes indicate that the plume was from the ship. These observations suggest the potential for near-field impacts from strong sources such as ship plumes.

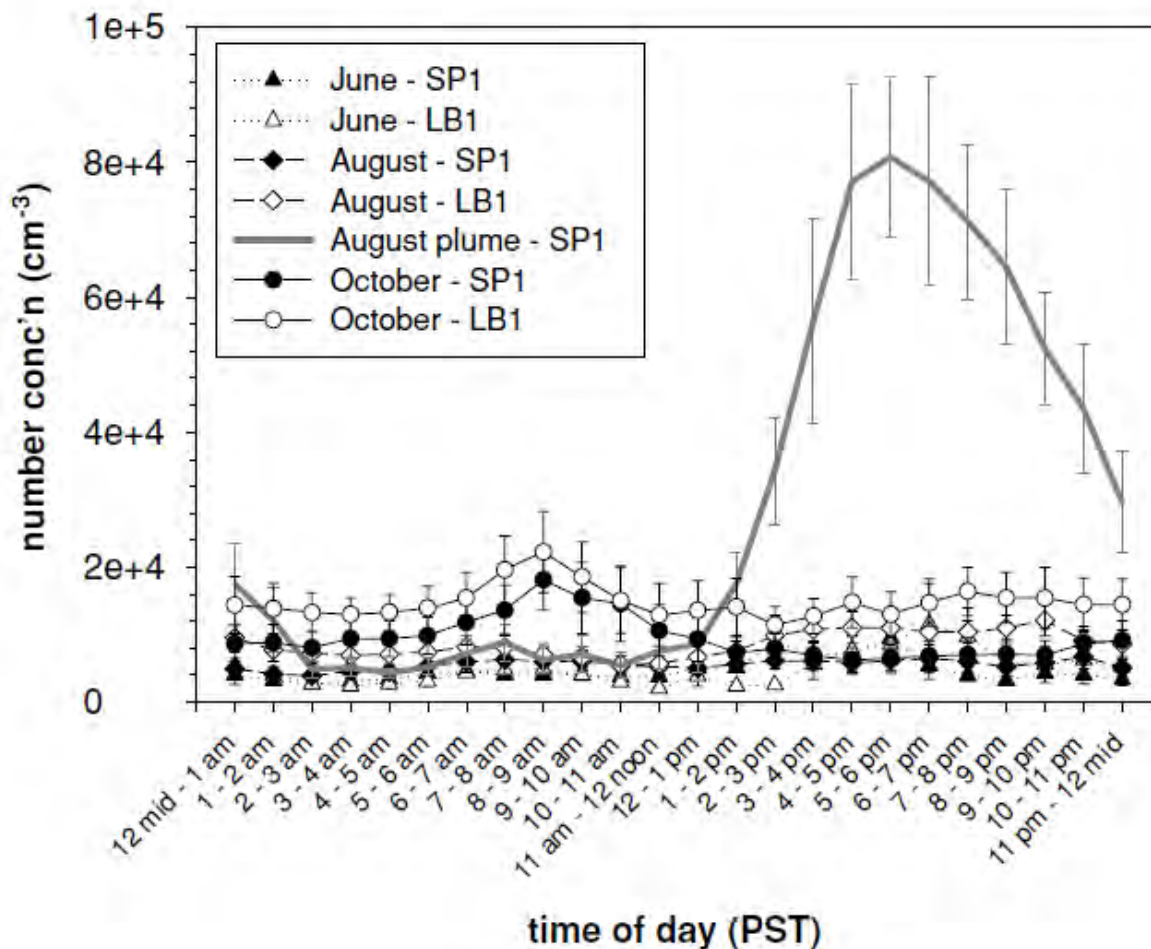


Figure 16: Harbor background sites comparison - hourly mean particle number concentration data at sites SP1 and LB1 are shown for selected alternate months (Note: The –August– SP1” plot excludes August 5–13 data, which are included in the –August plume–SP1” plot).

Day-of-the-week differences in PM mass concentrations have been routinely observed where motor vehicle traffic is the dominant source of PM (e.g., Motabelli et al., 2003; Aalto et al., 2005). We observed similar differences in the number concentration at selected sites representative of the overall study (Figures 17-19).

PNCs on Saturday follow a similar pattern to the mean weekday concentrations, but are somewhat lower in overall amount while Sunday’s concentrations are lower yet. There is a larger relative reduction in total particle number concentration during the weekend at the sites near the Ports (70% and 60% on Saturday and Sunday, respectively) than there is at LA1 near downtown Los Angeles (90 to 80%). This again indicates the importance of commercial traffic in the Port area. The amount of change depends very

strongly on the measurement location, including the proximity to industry, roads and traffic. In the last few years, the Ports have begun to implement a program (“Pier Pass”) to shift container movement via truck to off-peak hours (evenings and weekends). As more HDDV activity is shifted, these time-of-day and day-of-the-week patterns may well change.

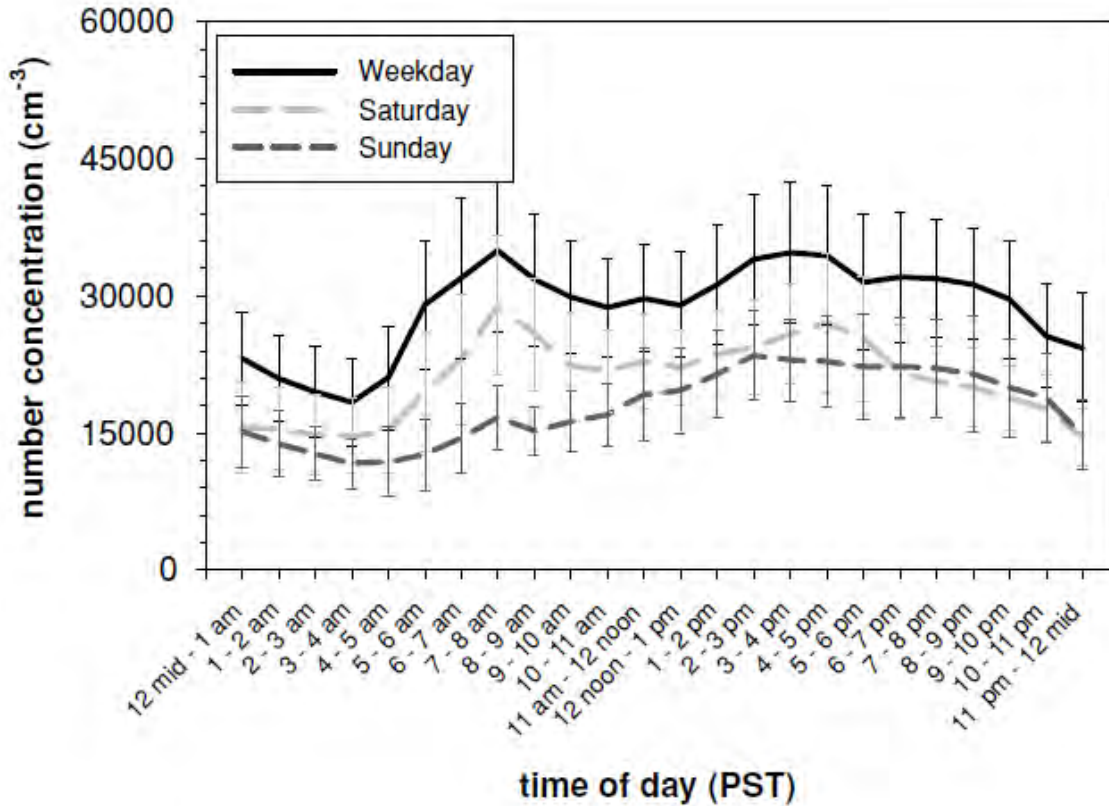


Figure 17: Day-of-the-week diurnal concentration profiles calculated from all available monthly mean data for site LB2.

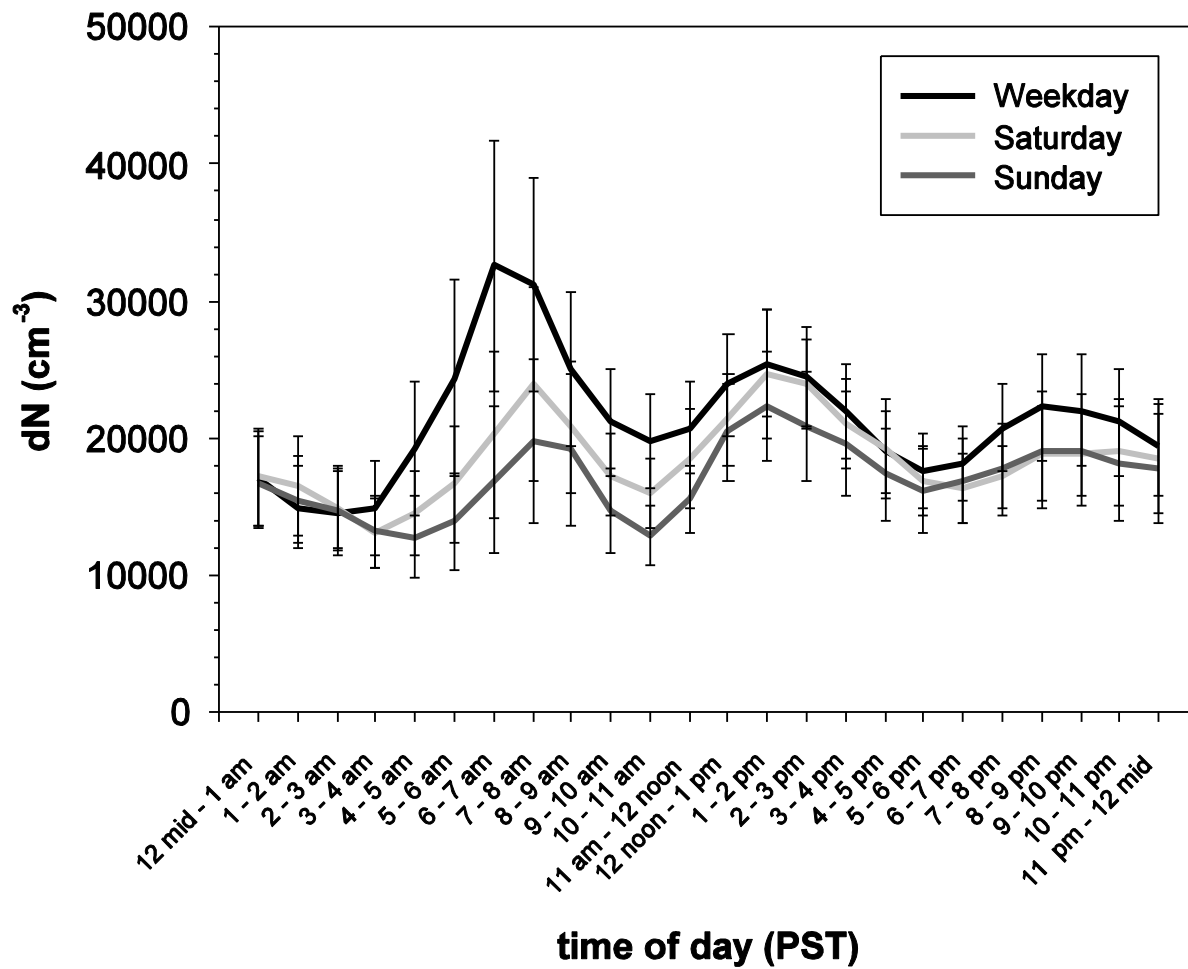


Figure 18 : Day-of-the-week PNCs at site LA1 during the study (the standard error of each mean is shown).

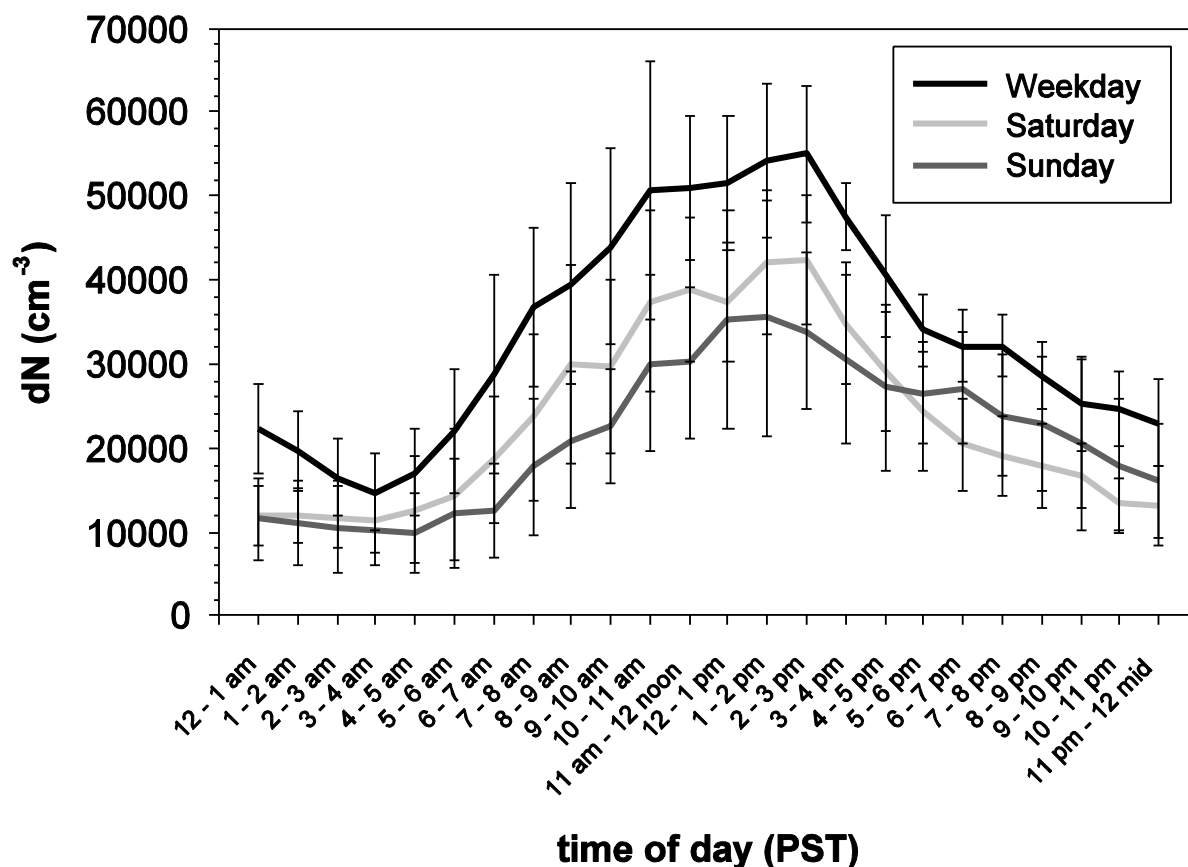


Figure 19: Day-of-the-week PNCs at site LB9 during the study (the standard error of each mean is shown).

3.2. RECEPTOR AREA STUDY

3.2.1 METEOROLOGY

Meteorological conditions can influence ultrafine particle concentrations significantly, but the Los Angeles area exhibits relatively limited diurnal and seasonal variation, as was the case during the study period. The mesoscale meteorology of the area that is most relevant in context of this study is the interaction of coastal winds with the San Gabriel Mountains. The pollution generated in west LA during the morning is transported over the course of several hours of aging toward the eastern portion of the Los Angeles Basin and up the southern flanks of the San Gabriel Mountains. The strong subsidence inversion layer, frequently present over the area in the winter and almost always in the summer, limits the vertical dispersion and the westerly sea breeze, which develops during the day, transports this pollution further inland. This is also evident from the inset plots in Figures 20 (a), 21 (a), 22(a), which show vector average wind directions during three months (January, May and September) of 2009. Across the sites, winds were observed from the west during afternoons, at relatively higher speeds than most hours

of the day. As the mixing layer stabilizes during evenings, the trapped pollutants can linger overnight and then be re-entrained to the surface during early morning hours in east LA (Lu et al., 1995). The particle number concentrations and the size distributions will be discussed in this context. Tables 6 and 7 present an overview of select data for the stable meteorological conditions at the sampling sites. Air temperatures do not vary much across sites and the seasonal trend across sites is quite similar, with slightly lower temperatures observed at sites further inland during winter. January was warmer than February, and September across sites was at least as warm as, or warmer than, August, which is quite typical of the area. The relative humidity at all sites was consistent during sampling period, except during Santa Ana conditions that brought dry winds from the desert, due to a synoptic high-pressure system, which is also common this time of the year in southwest United States. The predominant wind direction at the sites, except for winter months (Dec-Feb), was from the west, with stronger winds from the west recorded during afternoons, and nighttime stagnation being the predominant wind speed characteristics in the basin.

Table 6: Prevailing wind direction and speed at sampling sites during Phase II (receptor area study).

Predominant Wind Direction and Wind Speed by month													
Month	Nov	Dec	Jan	Feb	Mar	Apr	May	Jun	Jul	Aug	Sep	Oct	Nov
AGO	2008		2009										
WD (deg)	SW	E	E	E	W	W	W	W	W	W	W	W	E
WS (m/s)	0.70	0.89	1.21	0.93	1.21	1.31	1.17	1.23	1.13	1.04	0.96	1.37	0.93
SD (m/s)	0.70	0.81	1.35	0.82	1.22	1.21	1.10	1.16	1.21	1.13	1.23	1.55	1.04
DIA			2009										
WD (deg)			S	S	SW	S	W	W	W	S	W	S	
WS (m/s)			0.62	0.47	0.53	0.50	0.41	0.40	0.38	0.31	0.39	0.35	
SD (m/s)			0.81	0.48	0.48	0.40	0.30	0.33	0.36	0.32	0.56	0.55	
RUB	2008		2009										
WD (deg)	NW	N	N	N	W	W	W	W	W	W	W	W	NW
WS (m/s)	0.53	0.96	2.38	0.78	0.97	0.84	0.84	0.71	0.70	0.62	0.62	1.00	1.28
SD (m/s)	0.75	1.49	2.66	0.98	1.20	0.63	0.56	0.57	0.60	0.54	0.67	1.48	0.37
SBR	2008		2009										
WD (deg)	NE	NE	NE	SE	SW	W	W	W	W	W	W	W	NE
WS (m/s)	0.47	0.56	0.94	0.63	1.09	1.38	1.50	1.47	1.40	1.26	1.08	1.12	0.66
SD (m/s)	0.64	0.78	1.29	0.80	1.22	1.45	1.22	1.14	1.27	1.24	1.21	1.33	0.89
UPL	2008		2009										
WD (deg)	W	N	N	W	SW	SW	W	W	W	W	W	W	W
WS (m/s)	0.39	0.48	0.52	0.56	0.86	1.14	1.15	1.19	1.11	1.01	0.90	0.80	0.65
SD (m/s)	0.37	0.46	0.47	0.53	0.69	0.94	0.92	0.89	1.05	0.93	0.87	0.70	0.51
VBR	2008		2009										
WD (deg)	W	W	N	W	SW	W	SW	W	W	SW	W	W	W
WS (m/s)	0.45	0.64	2.04	0.67	0.92	1.01	1.03	1.09	1.01	0.92	0.88	1.02	0.43
SD (m/s)	0.81	1.18	2.27	0.92	1.08	1.03	0.89	0.92	1.00	0.90	1.02	1.19	0.56
USC	2008		2009										
WD (deg)			NE	NE	W	W	W	W	W	W	W	NE	NE
WS (m/s)			2.23	2.41	2.44	2.71	2.50	2.53	2.66	2.74	2.45	2.58	2.34
SD (m/s)			0.86	0.97	1.04	1.16	0.96	1.04	1.05	1.12	1.02	1.05	0.77

Table 7: Temperature (°C) and relative humidity (%) at sites during sampling period for Phase II (receptor area study).

Sites	AGO		DIA		RUB		SBR	
Months	RH	Temp	RH	Temp	RH	Temp	RH	Temp
Dec' 08	64 ± 22	11.3 ± 5.0			62 ± 23	12.1 ± 5.6	59 ± 20	12 ± 6.1
Jan '09	44 ± 23	15.4 ± 5.0			42 ± 26	16.2 ± 6.1	47 ± 23	14.5 ± 6.6
Feb '09	63 ± 23	12.1 ± 5.3	67 ± 22	67.3 ± 21.7	64 ± 24	12.8 ± 5.7	62 ± 20	12.1 ± 5.9
Mar '09	58 ± 21	14.0 ± 5.2	64 ± 19	63.5 ± 19.4	58 ± 21	15.1 ± 5.7	55 ± 18	14.8 ± 5.7
April '09	55 ± 21	16.0 ± 6.3	58 ± 21	58.2 ± 21.0	54 ± 20	17.2 ± 6.6	53 ± 19	16.7 ± 6.5
May '09	65 ± 17	19.9 ± 5.3	69 ± 15	68.7 ± 14.8	62 ± 18	21.4 ± 5.8	58 ± 16	21.5 ± 5.5
June '09	66 ± 16	19.7 ± 5.1	69 ± 14	69.0 ± 13.8	65 ± 16	20.8 ± 5.2	60 ± 15	21.0 ± 5.3
July '09	52 ± 18	25.9 ± 6.0	58 ± 18	58.4 ± 18.4	52 ± 19	28 ± 6.4	47 ± 16	27.7 ± 5.9
Aug '09	53 ± 22	24.9 ± 6.4	55 ± 22	55.2 ± 21.7	52 ± 21	26.2 ± 6.9	49 ± 18	26.3 ± 6.4
Sep '09	47 ± 22	26 ± 6.6	53 ± 22	52.8 ± 21.7	52 ± 21	26.2 ± 7.0	47 ± 18	26.5 ± 6.7
Oct '09	52 ± 23	18.8 ± 5.8	56 ± 24	55.8 ± 23.9	52 ± 24	19.7 ± 6.4	49 ± 20	19.3 ± 6.5
Nov '09	47 ± 24	16.6 ± 5.5	51 ± 25	51.3 ± 24.8	49 ± 25	17.1 ± 6.3	48 ± 21	16.2 ± 6.8
Dec '09	67 ± 18	12.6 ± 2.9	69 ± 16	68.4 ± 16.4	67 ± 18	13.6 ± 3.8	65 ± 16	12.8 ± 4.0
Sites	UPL		VBR		USC			
Months	RH	Temp	RH	Temp	RH	Temp		
Dec' 08	67 ± 21	10.7 ± 5.4	62 ± 26	12.7 ± 5.8				
Jan '09	52 ± 25	14.2 ± 5.9	44.3 ± 29	16.3 ± 6.7	73 ± 15	14.0 ± 3.4		
Feb '09	64 ± 24	11.9 ± 5.6	68 ± 25	12.1 ± 5.7	83 ± 8	12.2 ± 1.8		
Mar '09	67 ± 18	13.3 ± 5.3	64 ± 22	14.0 ± 5.4	72 ± 19	13.6 ± 3.1		
April '09	59 ± 22	16.0 ± 6.6	59 ± 21	16.0 ± 6.3	68 ± 14	14.6 ± 4.0		
May '09	68 ± 17	19.4 ± 5.4	68 ± 17	19.9 ± 5.1	78 ± 7.7	17.5 ± 1.7		
June '09	67 ± 16	20.2 ± 4.8	66 ± 17	21.0 ± 5.1	76 ± 7.4	17.7 ± 1.1		
July '09	60 ± 20	24.2 ± 5.5	61 ± 19	24.7 ± 6.1	69 ± 11	22.7 ± 3.4		
Aug '09	61 ± 20	23.4 ± 5.7	59 ± 22	24.2 ± 6.4	64 ± 18	22.4 ± 4.4		
Sep '09	56 ± 22	24.3 ± 6.4	57 ± 23	24.8 ± 6.8	66 ± 17	23.1 ± 4.2		
Oct '09	57 ± 23	18.2 ± 5.9	57 ± 25	18.5 ± 6.0	60 ± 21	19.1 ± 3.9		
Nov '09	54 ± 23	15.7 ± 5.9	55 ± 27	16.2 ± 6.4	52 ± 22	16.7 ± 4.3		
Dec '09	72 ± 19	12 ± 3.6			58 ± 20	13.8 ± 3.8		

3.2.2 ULTRAFINE PARTICLES

In this section, particle number concentrations (PNC) for different sites are discussed as diurnal (hourly averaged) data for selected months. Alternate months of the year were chosen (unless another particular month was more relevant) to maintain clarity in graphs and to illustrate the similarities/differences across the diurnal, seasonal and spatial trends observed at these sites. The relative standard error was less than 5%. The hourly average data presented are arithmetic means. Further, the CODs are discussed in context of the spatial variability.

3.2.2.1 Diurnal and Seasonal Variations across Sites

Figure 20 shows the PNC hourly averages across the odd months of the year at USC. This site is regarded as a typical urban background site in Los Angeles. In the cooler months of late spring and late fall, a characteristic early morning peak, associated with mostly light-duty gasoline vehicle morning commute, is observed from 5-10 am. Advancing into summer months, this peak is not as robust and eventually disappears, as higher temperatures during the early mornings increase mixing heights, thus enhancing dispersion, and also lead to possible volatilization of semi-volatile organics bound to PM from traffic emissions (Biswas et al., 2007, Ning et al., 2007). However, another peak emerges, which has its crest in the late morning or early afternoon, and in July is associated with the highest diurnal values for PNC. This peak has been identified with secondary particle formation, and is consistent with the work of Moore et al. (2009), Moore et al. (2007), Ning et al. (2007) and Verma et al. (2009). The presence of this peak implies that secondary photochemical formation can contribute to PNC in some months as significantly as primary emissions from local sources. During the cooler months of the year, another peak is observed in the evenings and early night, possibly related to particle formation by condensation of semi-volatile vapors emitted by traffic during preceding hours. A shallower mixing layer in this season and time period also leads to these elevated concentrations and its effect is most pronounced in peak winter months (Dec-Feb) when night time concentrations can reach about $30,000/\text{cm}^3$. Biswas et al. (2007) previously reported a similar data pattern. The observations at USC suggest that PNC can vary significantly at a site across seasons (morning commute peak in winters $\sim 40,000/\text{cm}^3$ and in summers $\sim 15,000/\text{cm}^3$) even though they may be associated with very consistent local emission sources, with the differences primarily due to different meteorological conditions. Thus, when considering exposure to UFP, especially using a number-based metric, meteorological conditions and secondary sources can have as much consequence as direct emissions from local sources.

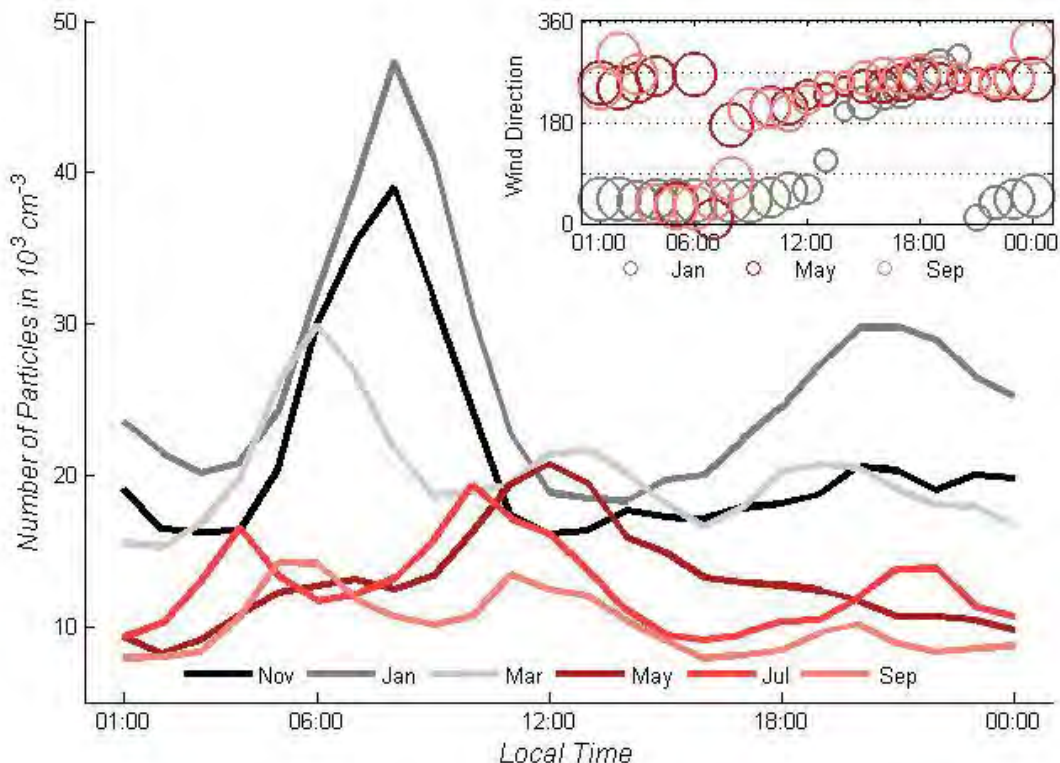


Figure 20: Hourly average particle number concentration at USC plotted for hours of the day in Pacific Standard Time (PST). The relative standard error for the hourly averages reported above was less than 2%. The inset is a plot of vector averaged wind direction (WD) with the bubble area weighed to wind speed plotted for hours of the day in PST.

Figures 21 and 22 compare the average particle size distribution during different time periods of the day at USC during September and December of 2009. As discussed above, the photochemical activity-related peak (observed during the early afternoon period (12:00-14:00), by when previously formed particles grow to a size range that is measurable by SMPS) is very robust in September and weakens progressively through the fall and into December. Insets in Figures 21 & 22 further elucidate this point by comparing the particle size distribution during 10:00-14:00 between September and December, i.e., the warmer and cooler months of our sampling campaign. In September, a simultaneous rise in total particle numbers and the sub-25nm particles can be seen and is attributed to photochemical formation. The possibility of these particles being associated with fresh (traffic) emissions is unlikely because analysis of traffic trends of the neighboring freeway (the major source of fresh emissions at USC) confirms no significant changes either during the hours associated with photochemical activity, or across seasons. Further, the increase in atmospheric mixing height during this time of day would decrease the concentrations of PM of primary origin. Traffic profiles (vehicle count/hr for the month of Sep and Dec) are also shown in the inset figures. The tri-modal diurnal profile observed at USC during warmer months in Figure

20 is limited to sub-50nm particles, while the seasonal variation of the diurnal patterns for particles >100 nm is not clearly evident. This is a distinctly different pattern than that observed at the inland sites, and illustrates a size distribution that is characteristically associated with urban sites in proximity to primary emissions from vehicles (Morawska et al., 1998; Ronkko et al., 2006 & 2007).

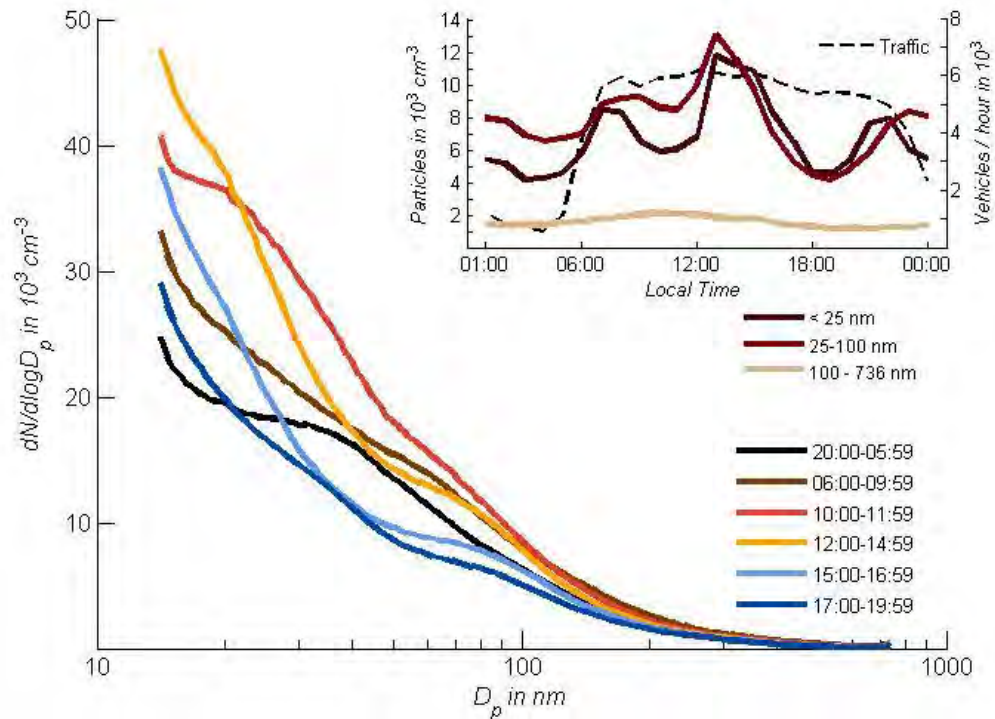


Figure 21: Average size distribution of particles during six time periods of the day at USC during September 2009.

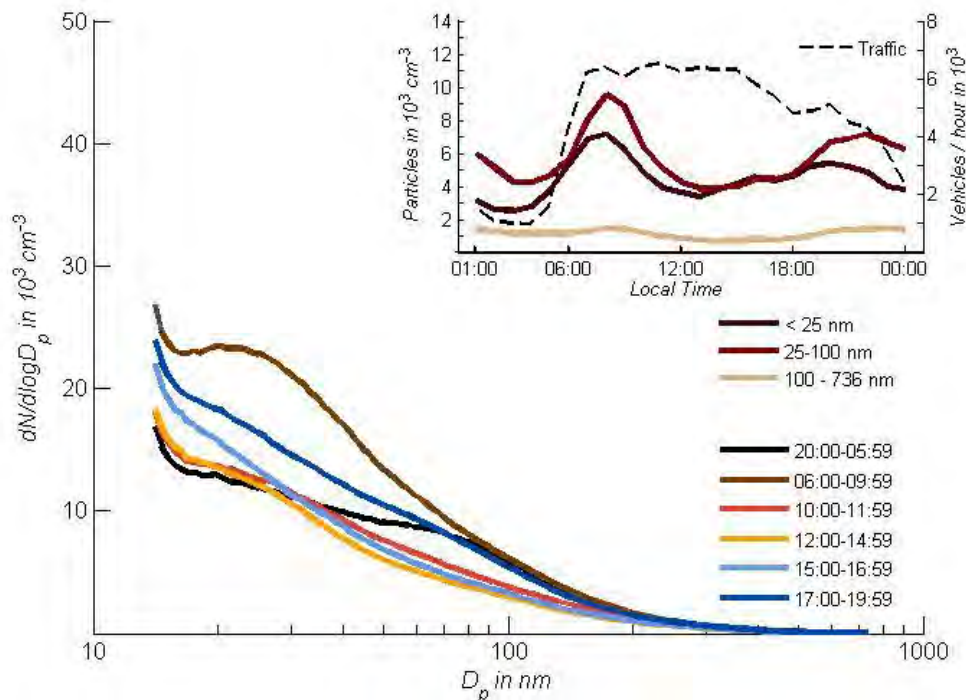


Figure 22: Average size distribution of particles during six time periods of the day at USC during December 2009.

Figure 23 shows monthly average diurnal particle number data across six months of the year at UPL (i.e., Nov, Jan, Feb, May, Aug & Sep). A bi-modal diurnal distribution is observed at this site, with a morning time peak, similar to USC, corresponding to morning commute during 6:00-10:00 hours in winter months that is not as robust during summer. This winter peak is a compound effect of greater vehicular emissions and lower atmospheric mixing heights on winter mornings. A gradual increase in concentrations is observed as winter progresses. The formation of strong surface-based temperature inversions that can lead to almost no vertical mixing (during winters) of the transported PM load, coupled with condensational growth of particles, is responsible for the extended late evening and early night peaks observed at UPL, when PNC plateau overnight. Concentrations as high at $15,000/\text{cm}^3$ can be observed during winter nights compared to only about $10,000/\text{cm}^3$ during summer. The nighttime peak is flatter, broader, and persists longer than the morning traffic peak, and has concentrations that are comparable if not higher than the morning peak, thus producing maximum diurnal concentrations during the night, when local emissions are at their lowest. In comparison, the maximum concentration at USC in the evenings is about half of the morning maximum. Other inland sites exhibit a similar pattern, with nighttime maxima being comparable to morning maxima and the highest PNC being observed during winter months. This concentration pattern may lead to a longer period of exposure to higher PNC in inland areas than in areas with greater local emissions nearer the coast.

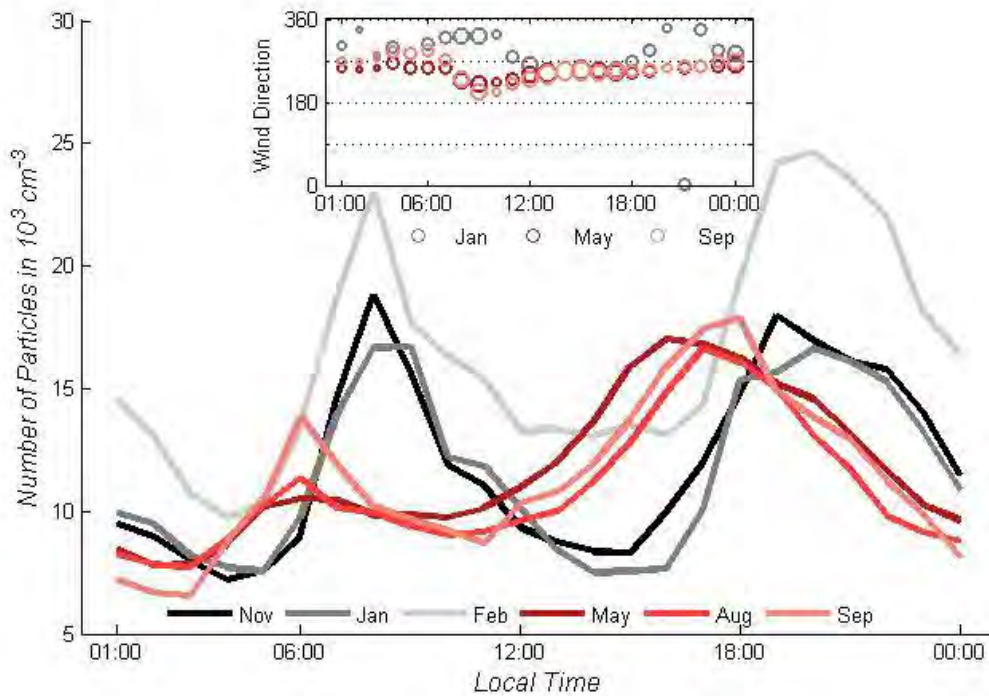


Figure 23: Hourly average particle number concentration at UPL for hours of the day in Pacific Standard Time (PST). The relative standard error for the hourly averages reported above was less than 2%. The inset is a plot of vector averaged wind direction (WD) with the bubble area weighed to wind speed plotted for hours of the day in PST.

Figures 24 and 25 compare the PNC in various size ranges at UPL. Between the warm September and cool December months there is a marked change in the diurnal pattern for different size ranges. The afternoon peak in concentrations associated with photochemical activity, as observed at USC and later at AGO, is not as prominent at UPL. Even though the Particle Number Size Distribution (PNSD) during 10:00-14:00 indicates the presence of particles of sizes that could be attributed to photochemical activity, it is not accompanied by a rise in total PNC, as is observed at USC and AGO. A possible explanation is that the contribution of photochemical activity to the total PNC is obscured (and thus not as distinguishable) by the contribution of the advected aerosols from the upwind urban areas of LAB to the overall PNC. Further, since UPL is distant from major freeways, the concentrations of gaseous and semi-volatile organic vapor precursors that participate in secondary particle formation are lower compared to those at USC (or in general in central LAB), which may decrease the degree of PM formation through this pathway. Analysis of particle concentrations less than 25 nm and total particle concentrations, as reported by the SMPS, during September further corroborate this hypothesis (shown as an inset in Figure 24). No significant differences are observed in PNC < 25nm during 10:00-16:00. The results plotted in Figure 23 show that during 15:00-17:00, when the highest wind speeds of the day are observed, the particle number concentrations in the range of 25-100 nm increase (while the particle number in the 14-25 nm range remains stable). This particle range is typically associated with coagulation and-or growth of preexisting particles via condensation of semi-volatile

organics on pre-existing PM (Rodriguez et al., 2007). The increase in that size range later in the afternoon (during other hours of summer days, the concentrations within this size range remain stable) could be due to the arrival of the polluted air mass from Los Angeles. Similar observations have been made by Kim et al. (2002) and Fine et al. (2004). However, during winters (Figure 25) the distribution is uni-modal and the bi-modal distribution is only observed during evening/night with distinctly higher mode diameter during winter. The size range of 14-25 nm, associated with fresh emissions, shows a sharp increase during morning as well as in evening, as evident in the inset (total PNC increases and the mode particle diameter decreases, shifting the distribution towards freshly emitted PM). This is due to the combined effects of local traffic, coupled with the decreasing temperature (increasing the partitioning of semi-volatile organic emissions towards the particulate phase) and mixing height (which reduces dispersion), all of which lead to a more pronounced effect of local emissions than that observed during summers. These comparisons suggest that there could be significant distinction in the size distribution profiles observed at sites due to seasonal variation.

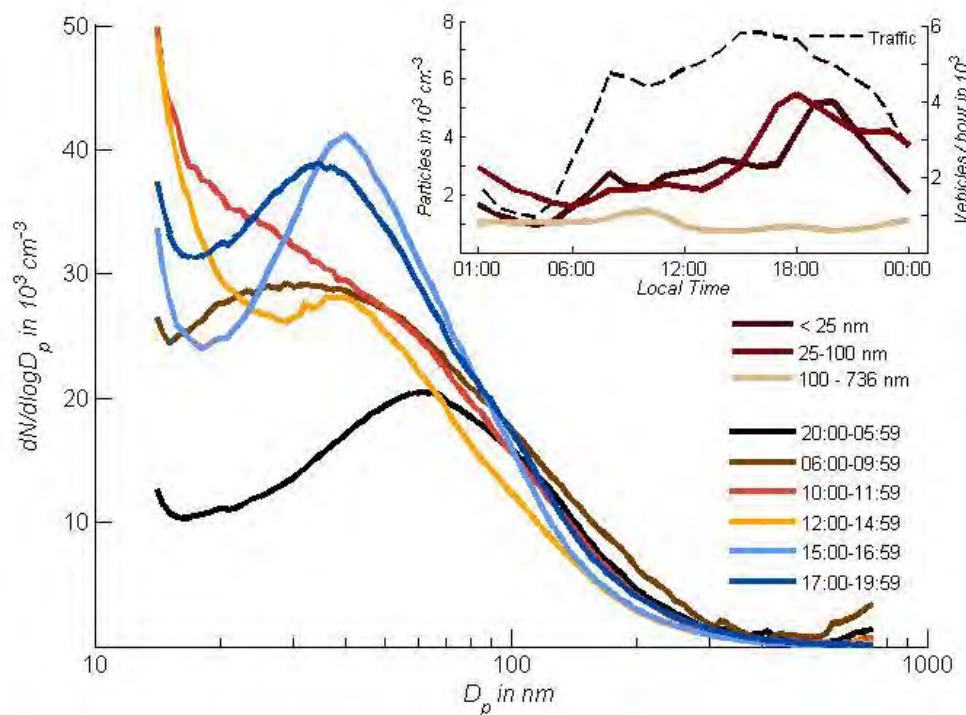


Figure 24: Average size distribution of particles during six time periods (PST) of the day at UPL during September 2009.

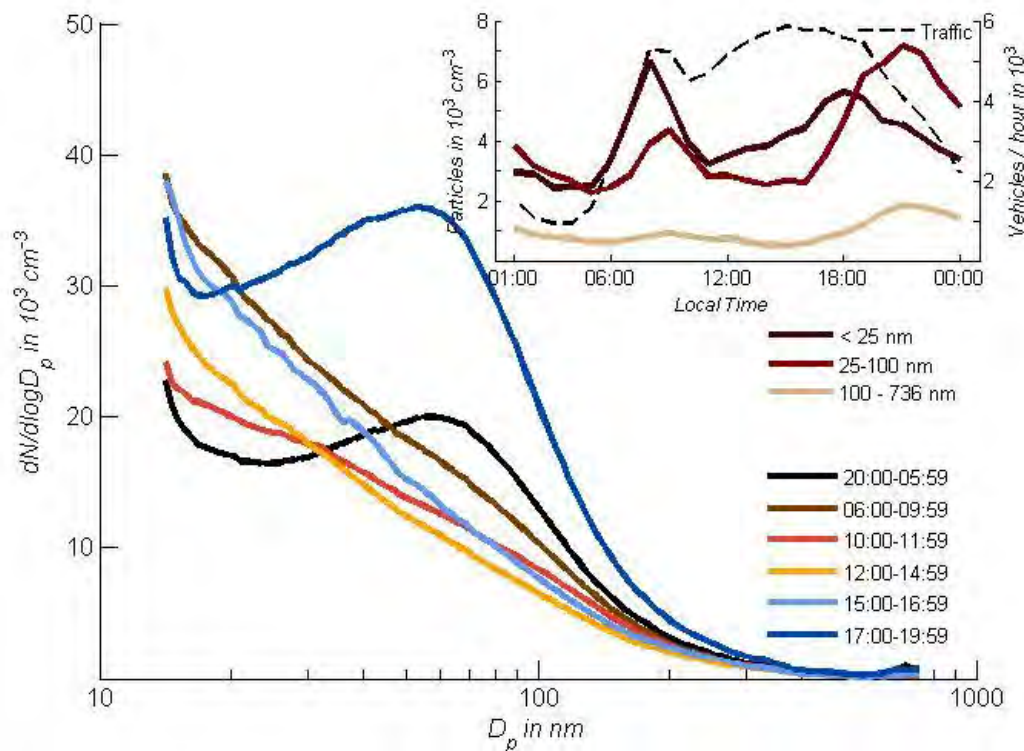


Figure 25: Average Size Distribution of Particles during six time periods (PST) of the day at UPL during December 2009.

Figure 26 shows data for AGO, one of the eastern-most sites of the study. Diurnal averages are shown for late fall (Nov), winter (Jan), spring (Mar) and summer (May, July and September). The morning peak in the plot can be explained by the morning commute (as this site is near a freeway). However, this morning peak subsides as the year progresses into warmer months when there is greater dispersion. Similar to UPL, during colder months, there is an evening and early nighttime rise in concentrations, leading to PNCs comparable to that in mornings. This peak diminishes in the summer and returns in September.

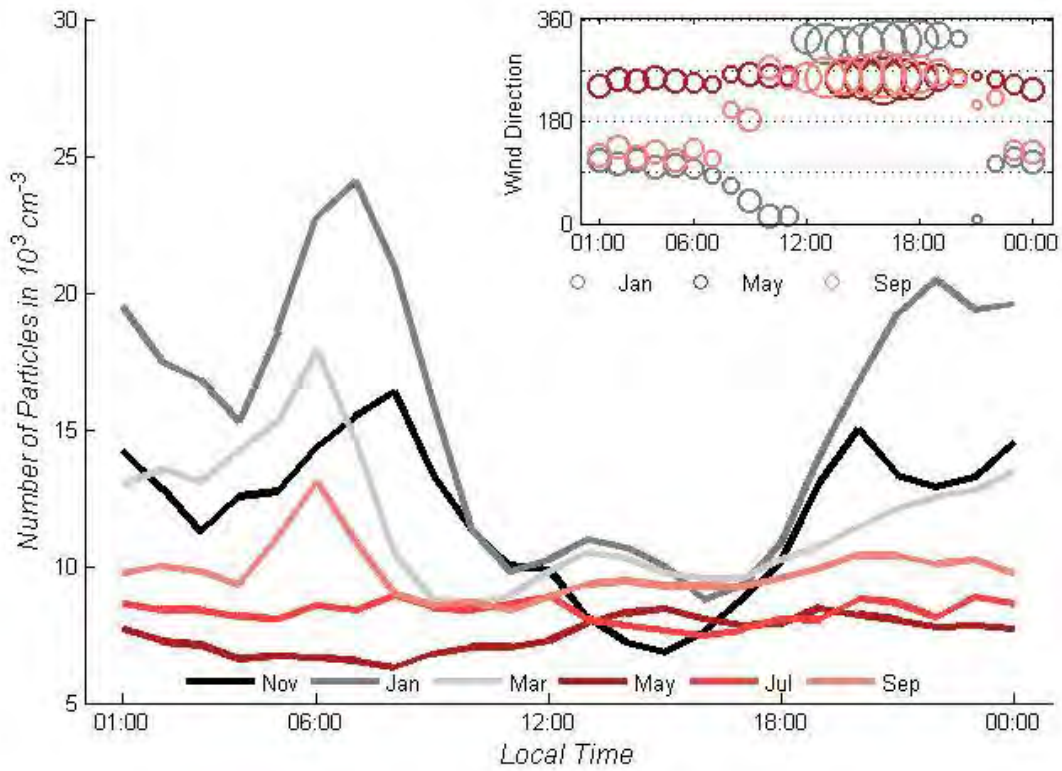


Figure 26: Hourly average particle number concentration at AGO for hours of the day in Pacific Standard Time (PST). The relative standard error for the hourly averages reported above was less than 3%. The inset is a plot of vector averaged wind direction (WD) with the bubble area weighed to wind speed plotted for hours of the day in PST.

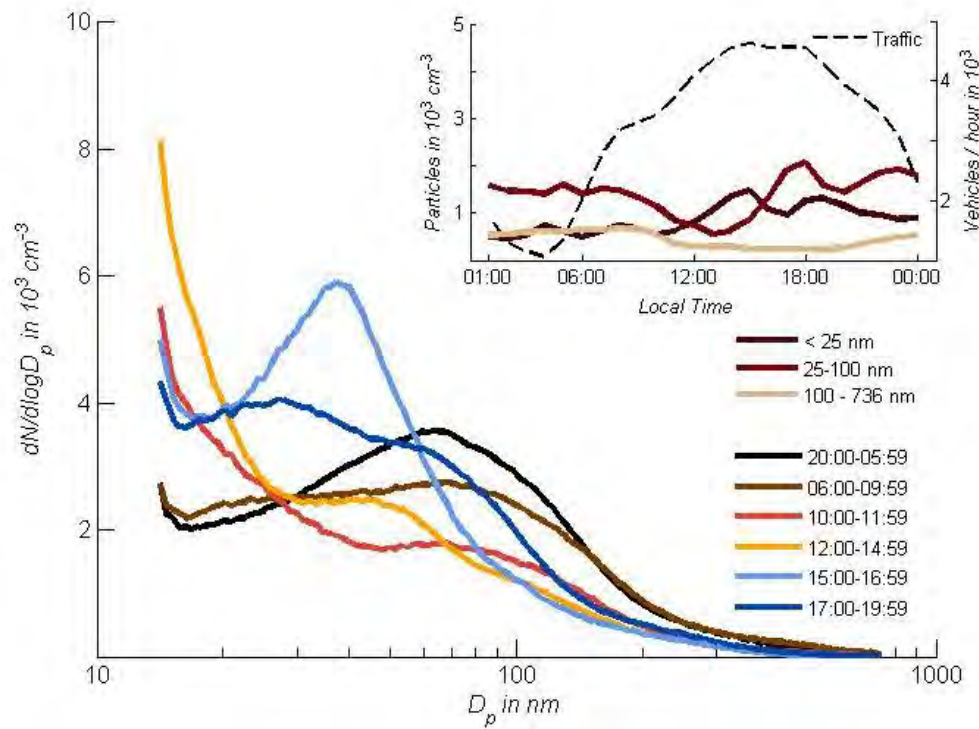


Figure 27: Average size distribution of particles during six time periods (PST) of the day at AGO during September 2009.

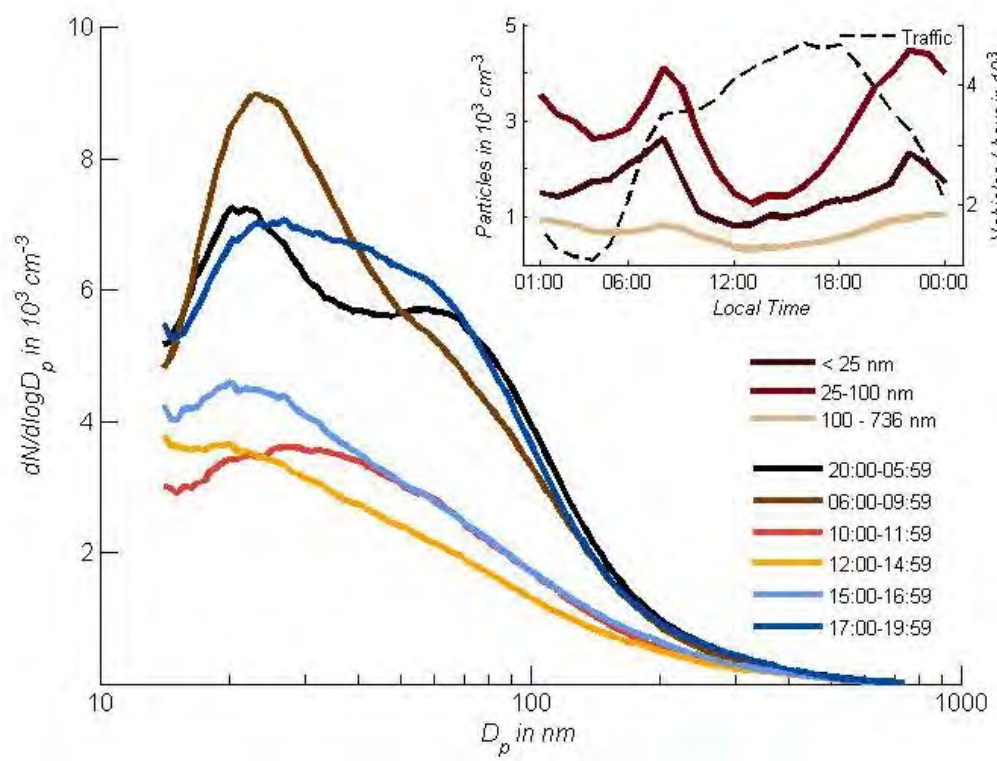


Figure 28: Average size distribution of particles during six time periods (PST) of the day at AGO during December 2009.

Figure 27 and 28 contrast the size distributions during different time periods of the day. During September we observed a rise in the concentrations of smaller particles (<25nm) during the hours coincident with strong solar irradiance and the mode diameter of the distribution decreases from ~30 nm at 11:00 to about 16-17 nm between 11:00 to 14:00. This decrease in mode diameter along with an increase in overall particle numbers, along with the timing, indicates the possibility of new particle formation. Further, this increase is not observed in December, and the peak declines steadily through the fall. Similar observations in that area have been made previously by Fine et al. (2004). An increase in mode diameter along with particle numbers occurs consistently through the months September to December for particles larger than 25 nm in late afternoon.

The diurnal pattern in particle concentrations across these sites, (i.e., USC, AGO and UPL) is dominated by a bi-modal distribution, except for summers at USC. But there is a decrease in overall particle concentrations due to dispersion of the air parcels moving inland (eastwards). The flat peak in nighttime concentrations (at hours when there are limited fresh emissions) at AGO (further inland) are lower than at UPL. PNCs at the RUB and VBR sites, which are further inland than UPL, also are lower than at UPL, but higher than at AGO, which is further east of these sites. A similar pattern is observed in the morning peaks corresponding to commute hours, because the traffic volume decreases as one moves farther inland from downtown Los Angeles.

3.2.2.2 Spatial Distribution of Particle Number Concentrations

Figures 29 and 30 compare all sites across two months to contrast the spatial variation in particle number concentrations across the basin. A representative month from each season was chosen and data have been plotted as the diurnal averages over the span of the month.

Figure 29 shows particle number concentrations and coefficients of divergence across sites in the Los Angeles basin for a winter month (December). The all-hour average December 2008 temperatures across the inland sites ranged from 10.7 to 12.7 degrees Celsius while the relative humidity ranged from 59 to 67%. The wind data in Table 6 and 7 shows the predominant wind direction based on hourly vector averages for different sites. At all inland sites, the morning peak concentrations during winter seem to be comparable to those of the nighttime peak (a mix of local evening commute emissions and the arrival of PM advected from urban Los Angeles) that persist for a far longer period than the morning peak does. This is an important observation since it suggests that, in the receptor areas of the LAB, PM transported from central and west Los Angeles can contribute to higher and more sustained concentration levels even during the hours when local sources have minimum contributions. These results are also consistent with the findings of Zhu et al. (2006) and Hu et al. (2009), both of whom conducted studies of the LAB. The highest morning concentrations were observed at USC and RUB, the two sites closest to freeways. VBR, which is close to RUB, but farther away from any freeways, had lower concentrations during the morning commute. However, VBR and RUB show excellent agreement in PNC during nighttime, when a stable stratification predominates the area, though UPL (which is closer to USC) and AGO (which is farther east) show higher and lower night time concentrations,

respectively, compared to RUB and VBR. The degree of PNC variability was examined using the Coefficient of Divergence. The highest CODs, or the maximum spatial variability, are observed during the hours of morning commute. The overall COD range was 0.17-0.28, indicating that PNC are only moderately heterogeneous.

Figure 30 shows the hourly PNC averages at all sites during August, 2009. USC not only has the highest PNC, but also a very sharp midday peak (related to photochemical particle formation), which is comparable to the morning traffic-related peak, as discussed earlier. Nighttime PNCs become comparable to those at inland sites. The increased PNC pattern during morning commute is observed across all sites even though the numeric values of PNC differ significantly. The morning commute peaks however are not as pronounced as those in winter (December, Figure 5 a) as the primary emissions are quickly dispersed in summer and the higher ambient temperatures may be shifting the partitioning of semi-volatile organics emitted by primary sources to the gas phase (Miracolo et al., 2010, Pinto et al., 2004). Particle number concentrations at all sites were generally lower in summer than in spring or winter. After midday, there is a steady rise in PNCs at all receptor sites, which is due to the combined effects of photochemical activity along with the contribution of PM advected from western Los Angeles. The overall similarity in PNC data at all sites during overnight hours illustrates a well-dispersed regional-scale aerosol during summer nights. The lowest CODs were observed during summer, with the range for August being 0.13-0.23. These data corroborate the effect of dispersion and advection on regional scales as homogenizing factors leading to low variability at the inter-community level. The hourly concentrations observed during this campaign varied across seasons, though the diurnal variations were more consistent. The maximum diurnal change in PNCs across seasons was observed at USC, along with the highest average concentrations. This was expected, as USC is located in the immediate vicinity of a freeway (about 120 m downwind) and in a major source region of the LAB. The higher concentrations observed in the fall/winter months were consistent with the work of Singh et al. (2006). In comparison to our earlier study (Moore et al., 2009), which reported concentrations comparable to USC at several sites in the Wilmington and West Long Beach area of Los Angeles, the receptor sites had lower concentrations due to the lower impact of HDDV emissions in the immediate vicinity.

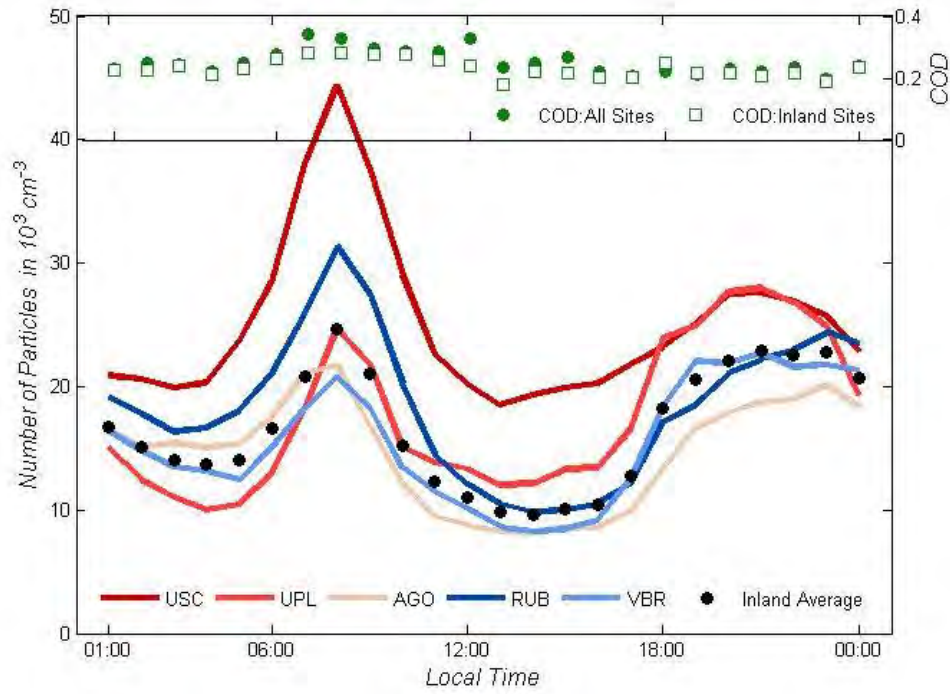


Figure 29: Mean hourly PNC and coefficients of divergence for various sites in the Los Angeles basin during December 2008.

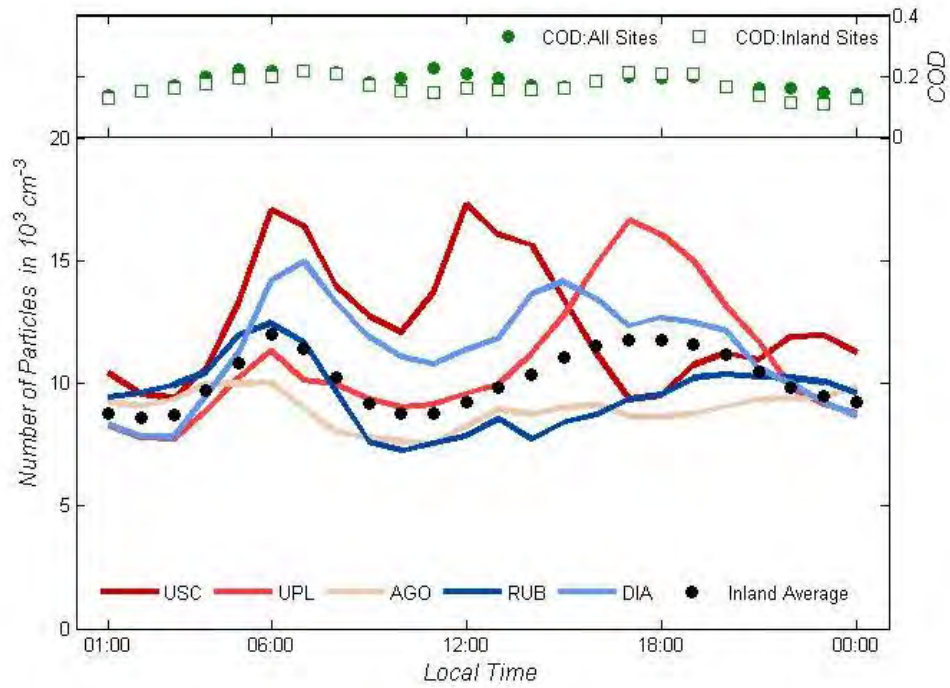


Figure 30: Mean hourly PNCs and coefficients of divergence for various sites in the Los Angeles basin during August 2009.

3.3. SOUNDWALL STUDY

Figures 31 (a and b) show the average particle size distributions at various distances downwind of the I-710 (20, 40, 80, 200 and 450 m) and I-5 (20, 40, 90, 120, 400 m) freeways without roadside noise barriers as measured by FMPS (6-523 nm). The size distributions measured in the immediate proximity of the freeways using the SMPS (10-225 nm) are also included as subplots in the figures for comparison. For all plots, the horizontal axis represents particle size on a log scale while the vertical axis represents normalized particle number concentration.

As shown in the inset plots of Figures 31 a and b, the particle size distributions in the immediate proximity of both freeways displayed a uni-modal shape, with a distinct peak at approximately 10 nm, indicating new particle formation by nucleation of supersaturated semi-volatile organic vapors in the exhaust (Alam et al., 2003). Shortly after, the rapid cooling in the atmosphere causes the highly concentrated vapors (i.e., semi-volatile organic compounds) that are emitted from the tailpipe of vehicles on the freeway to nucleate and form large numbers of nucleation mode particles (Zhang and Wexler, 2004). The peak modal concentrations at approximated 10 nm are 2.7×10^5 and 2.0×10^5 particles/cm³ for I-710 and I-5 freeways, respectively. As particles were transported away from the freeway, the particle size distributions changed markedly, with a dramatic decrease in the number concentrations. In Figure 31a, the particle number concentrations at a particle diameter of 10 nm were 1.7×10^5 , 1.3×10^5 and 7.9×10^4 particles/cm³, at 20 m, 40 m, and 80 m, respectively, which "accounted" for only 63%, 48% and 29% of that measured in the immediate proximity of freeway.

On the other hand, Figure 31b shows the particle size distributions at various distances downwind of the I-5 freeway. In contrast to the observations near I-710, the particle size distributions displayed a consistent bi-modal pattern. The first mode appeared at a particle width of 10 nm, similar to the measurement near I-710 freeway, while a distinct second mode in the larger size range of 30-50 nm was also observed. At 20 m, the modal concentration of 10 nm diameter particles was 8.3×10^4 particles/cm³, nearly half of that measured in the immediate proximity of the freeway, indicating rapid dilution and the associated particle evaporation and diffusion loss. Compared with the corresponding downwind distance of I-710 freeway, the ~10 nm modal concentration is significantly lower at the I-5 site, whereas the second peak, observed at around 35 nm, has similar concentrations at sites near both freeways, resulting in a pronounced dip at ~25 nm in the bimodal distributions at the I-5 sites. The lower nucleation mode particle concentrations indicate a lower strength of fresh traffic emissions at the I-5 freeway, with much lower traffic flow than the I-710 (~8,500 vehicles/hour on I-5 versus ~12,200 vehicles/hour on I-710). As the particles are transported further away from the freeway, particle number concentrations gradually decrease at both modes, and the second mode shifts from 34 nm (at 20 m) to about 40 nm (at 120 m), indicating the possibility of small particle evaporation and vapor condensation onto pre-existing particles (Shi et al., 1999, Zhang et al., 2004) as well as possible coagulation under different dilution conditions (Hinds, 1999, Zhu et al., 2002b). At 120 m, the nucleation mode particles at about 10 nm reached a concentration of 3.6×10^4 particles/cm³, similar to the background level at 450 m; however, the number concentration of particles at the larger

size mode of 39 nm continued to drop after 120 m until it reached background levels at 400 m. Nucleation mode particles have a shorter residence time in the atmosphere, so they decay much faster and reach background levels at a shorter distance than larger particles (Raes et al., 2002).

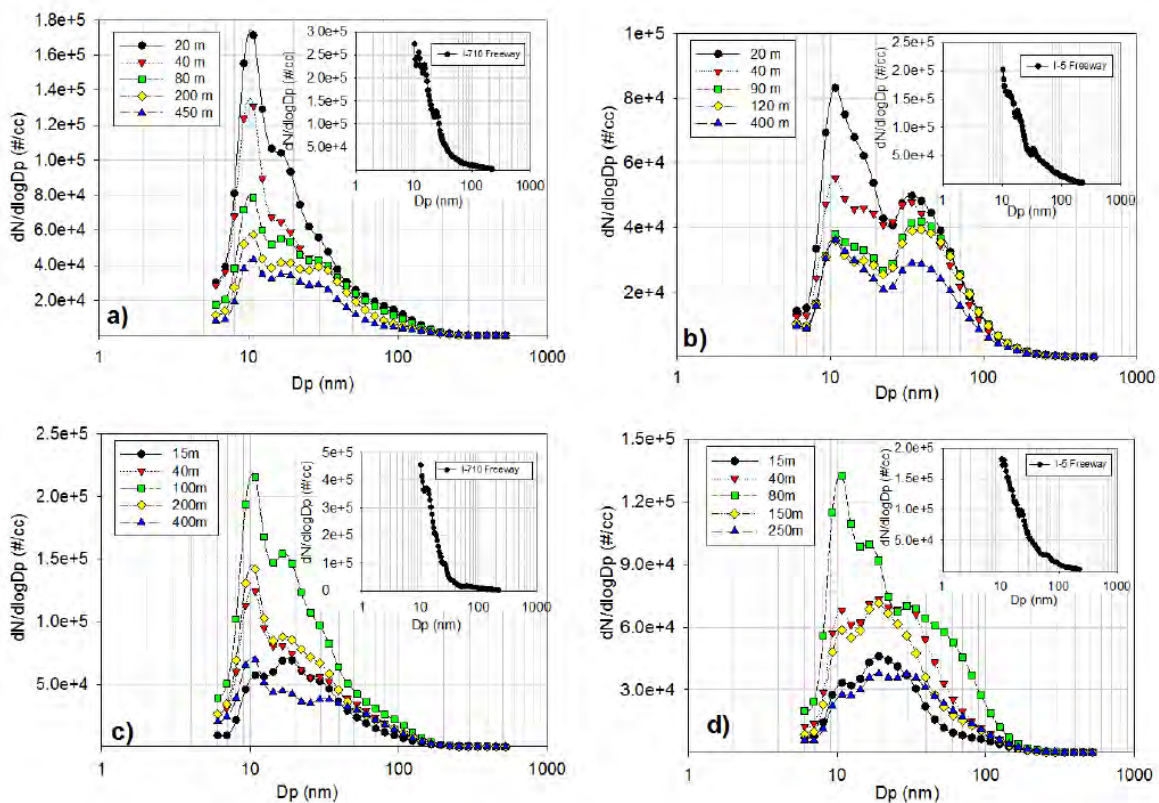


Figure 31: Particle size distributions measured at various distances downwind of freeway using FMPS (6-523nm) and in the immediate proximity of freeway using SMPS (10-225nm) shown as subplot: (a) I-710 without roadside barrier; (b) I-5 without roadside barrier; (c) I-710 with roadside barrier; (d) I-5 with roadside barrier.

Figure 32 shows the concentrations ratios of carbon monoxide (CO), nitrogen dioxide (NO_2) and black carbon (BC) at various distances downwind of the freeways with no roadside noise barrier (a: I-710; b: I-5) and with barrier (c: I-710; d: I-5). The concentration ratios were calculated by dividing the average concentrations measured at different downwind distances by the average concentrations in the immediate proximity of the freeways ($x = 0$). Error bars represent one standard deviation of the average ratios.

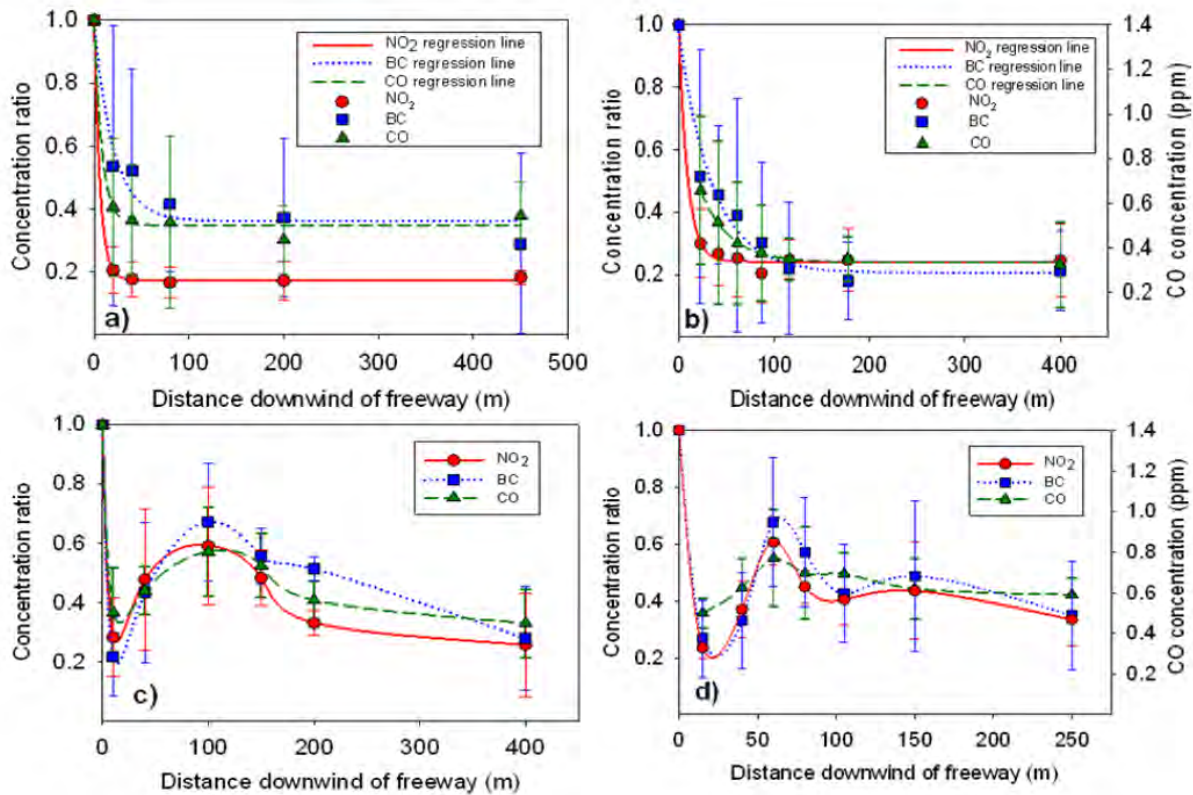


Figure 32: Normalized concentrations of BC and gaseous pollutants at various distances downwind of the freeway: (a) I-710 no noise barrier (b) I-5 no noise barrier; (c) I-710 with noise barrier; and (d) I-5 with noise barrier.

CO and NO₂ were selected because their concentrations in urban environments are closely related to traffic emissions. For the concentration ratios in Figures 32a and b, exponential decay curves were used to fit the decreasing ratios with increasing downwind distances. The best fitting decay equations and their corresponding R² values are listed below.

Table 8: NO₂, BC, and CO concentration decay curves with distance from freeway section without a sound wall barrier.

	NO ₂	BC	CO
I-710	$y = 0.17 + 0.83 e^{(-0.16x)}$ $R^2 = 0.99$	$y = 0.36 + 0.63 e^{(-0.05x)}$ $R^2 = 0.97$	$y = 0.35 + 0.65 e^{(-0.12x)}$ $R^2 = 0.99$
I-5	$y = 0.24 + 0.76 e^{(-0.11x)}$ $R^2 = 0.99$	$y = 0.21 + 0.77 e^{(-0.03x)}$ $R^2 = 0.98$	—

As shown in Figures 32 a and b, all pollutants concentration ratios decreased exponentially with increasing downwind distances of the freeway. For the gaseous

species of CO and NO₂, their concentrations decreased by 70-80% within the first 100 m of each freeway. Particle-bound BC concentration dropped by 60% and 80% in the first 100 m for I-710 and I-5, respectively. Within 150 m, all pollutants concentrations reach asymptotically background levels.

As shown in Table 8 above, the decay coefficients of NO₂ and BC for I-710 were consistently higher than that for I-5, suggesting a faster decay of their concentrations near the I-710 freeway. This may be explained by the higher initial concentrations of these pollutants at the I-710 freeway, which has a roughly 50% higher traffic volume than the I-5 freeway. Other meteorological conditions and the local topography may also contribute to the decay curves of air pollutants from the freeway (Zhu et al., 2002 a & b), but given the overall similarity in both of these sets of parameters between the two freeways, we attribute the faster decrease at the I-710 to the higher traffic volume on that freeway.

In contrast, the concentration ratios downwind of the freeway sections with roadside noise barriers displayed a different trend, as shown in Figures 32 c and d. At downwind distance of 15 m, the closest location downwind of the I-710, the pollutants concentration ratios were 0.36, 0.28 and 0.22 for CO, NO₂ and BC, respectively, comparable to the background levels measured at 400 m (0.33, 0.26, and 0.28 for CO, NO₂ and BC, respectively). The low concentration ratios are consistent with the observations of particle number and mass concentrations, due to the strong turbulence that exists in the recirculation cavity of the roadside noise barrier (Finn et al., 2010).

At 80-100 m, where the concentrations have dropped to background levels for the non-barrier sites (Figure 32a), the pollutants displayed a peak ratio of 0.57, 0.59, and 0.67 for CO, NO₂, and BC, respectively, as shown in Figure 32c for the I-710 with barrier. *The dramatic difference of the pollutant concentration profiles downwind of the freeway underscores the impact of a roadside noise barrier on pollutant dispersion.* As the pollutants are transported further away from freeways, their concentrations gradually decrease and reach background concentrations at 400m and 250m for I-710 and I-5, respectively. The results suggest that the freeway roadside features, such as noise barriers, should also be taken into consideration in assessing public exposure to ambient pollutants from traffic emissions in communities near busy freeways.

4. DISCUSSION

Details of the PNC measurements were presented in the results section. This section of the report discusses the variability among sites during the two study phases using a similar matrix for comparison, i.e., Coefficients of Divergence.

4.1. SOURCE AREA STUDY

Figure 33 shows the overall hourly CODs and correlation coefficients calculated across all site pairs in the source study data. Additional correlation coefficient and COD data for all site pairs with each site are shown in Table 9 below.

Table 9: COD and correlation coefficient for PNC data collected in the source area study (Phase I) and presented by study site.

Site	Correlation coefficient, <i>r</i>				Coefficient of Divergence, COD			
	median	1st quartile	3rd quartile	range	median	1st quartile	3rd quartile	range
LA1	0.34	0.08	0.58	-0.70 - 0.96	0.29	0.24	0.38	0.09 - 0.76
SP1	0.28	0.03	0.49	0.74 - 0.98	0.54	0.45	0.63	0.09 - 0.88
W1	0.46	0.23	0.68	-0.90 - 1.00	0.31	0.25	0.40	0.07 - 0.68
W2	0.26	0.00	0.51	-0.76 - 0.98	0.33	0.27	0.40	0.07 - 0.81
W3	0.50	0.26	0.69	-0.68 - 0.99	0.29	0.23	0.36	0.08 - 0.75
LB1	0.41	0.18	0.62	-0.87 - 0.98	0.45	0.34	0.55	0.09 - 0.88
LB2	0.47	0.24	0.68	-1.00 - 1.00	0.30	0.23	0.39	0.05 - 0.79
LB3	0.68	0.43	0.81	-1.00 - 1.00	0.26	0.20	0.36	0.05 - 0.81
LB4	0.41	0.16	0.62	-0.70 - 0.95	0.29	0.23	0.38	0.04 - 0.85
LB5	0.40	0.18	0.60	-0.87 - 0.98	0.37	0.28	0.48	0.07 - 0.84
LB6	0.51	0.25	0.70	-0.89 - 0.99	0.28	0.21	0.36	0.04 - 0.79
LB7	0.51	0.28	0.69	-0.66 - 0.97	0.28	0.22	0.36	0.04 - 0.85
LB8	0.53	0.28	0.73	-0.56 - 0.99	0.28	0.22	0.37	0.05 - 0.82
LB9	0.43	0.20	0.63	-0.97 - 1.00	0.32	0.25	0.42	0.05 - 0.88

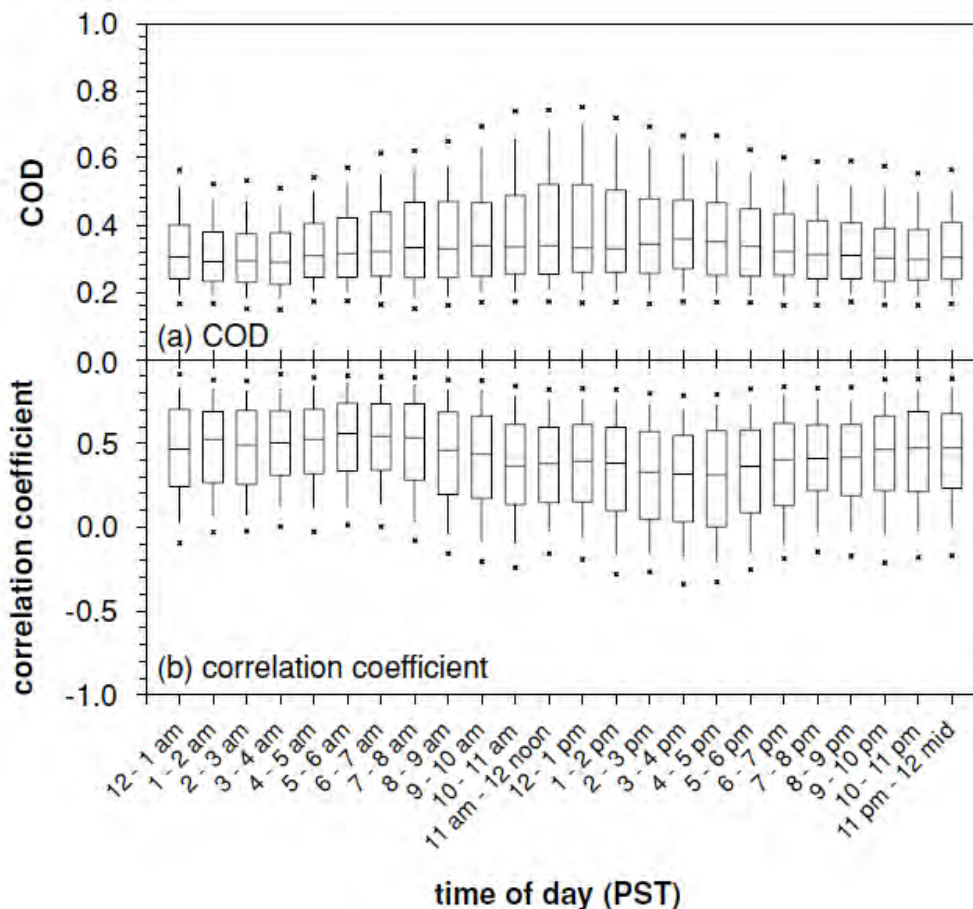


Figure 33: Coefficients of Divergence (CODs, (a)) and the correlation coefficient (r , (b)) calculated for the entire study based upon all hourly mean particle number concentration data and using all site pairs in Phase I study. In both (a) and (b), the 1st quartile, median, and 3rd quartile are represented by the box. The whisker/cross symbols represent the 10%/5% and 90%/95% values.

The hourly CODs for the entire source area study are shown together (Figure 33a) because the month-to-month variations were small. The median COD was approximately 0.30–0.35 for the entire study, and the range between the 1st and 3rd quartiles was mostly on the order of 0.20 units (mean CODs of approximately 0.05 were calculated from the December 2007 side-by-side testing for context). This suggests that overall the total particle number concentrations are moderately heterogeneous for the sites chosen. The correlation coefficients (Figure 33b), in contrast to the COD data, exhibit somewhat more seasonal variability with correlations somewhat better during the summer than in the spring or fall. As shown in Table 9, the median correlation coefficient varied from 0.30 to 0.68 and there is considerable scatter in the data for every hour with values spanning the entire range. The correlation between site pairs is modest, particularly considering the close proximity of these sites to each other. The diurnal patterns in the correlation coefficient and COD data vary (Figure 33). They do not exactly mirror each other, although overall relatively higher correlation coefficients tend to be associated with relatively lower CODs. No fixed numerical relationship,

however, between COD and r values is observed, in general, from site pair-to-site pair. Figure 33 indicates that meaningful variability occurs over the limited geographical area investigated (the LA1 site pairs are included in Figure 33, and do not yield appreciably different results when separated out (Figure 34), although the specific UFP sources/sinks were different than those in the Harbor Communities).

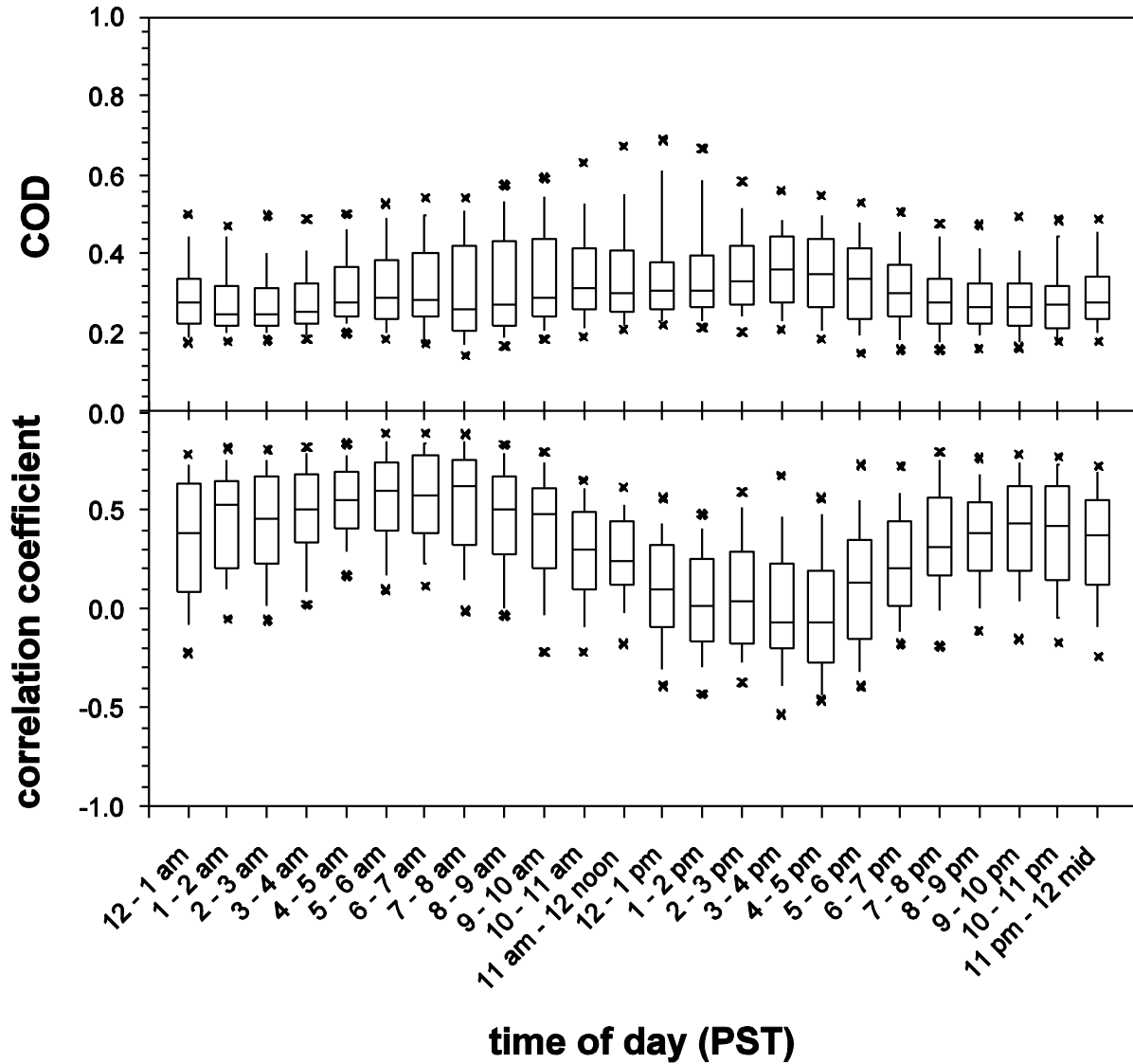


Figure 34: Site LA1 – COD (top) and correlation coefficients (bottom) calculated for PNCs across all site pairs for the entire Phase I study.

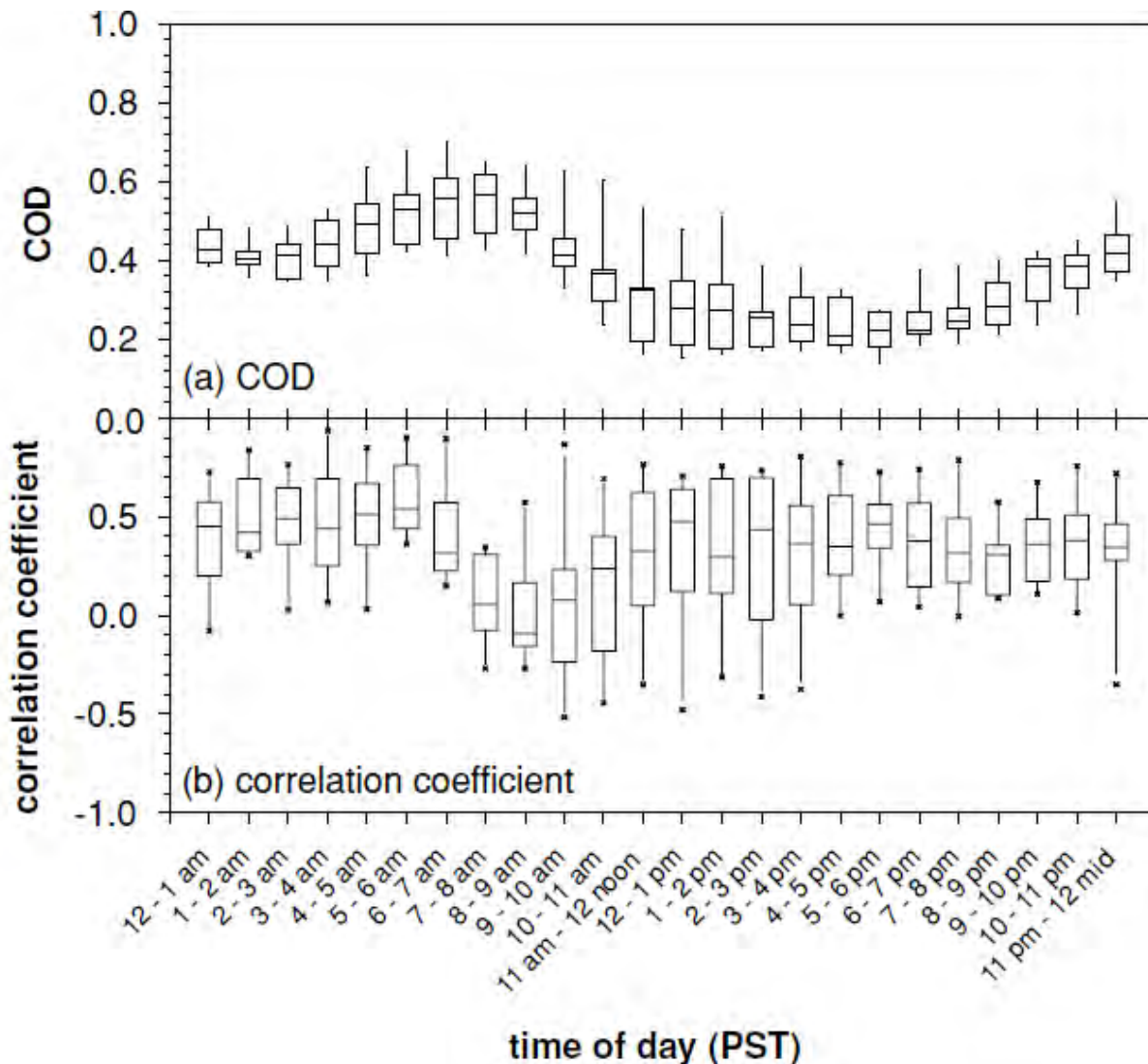


Figure 35: Coefficients of Divergence (CODs, (a)) and correlation coefficient (r, (b)) calculated from all PNC data for only the LB5-LB8 site pair. In both (a) and (b), the 1st quartile, median, and 3rd quartile are represented by the box. The whisker/cross symbols represent the 10%/5% and 90%/95% values.

A representative sample of the diurnal variation for an individual site pair (LB5–LB8) provides COD results that vary from a median value of approximately 0.25–0.55 during the study in a consistent diurnal pattern, but the variability observed for any specific hour was relatively limited (Figure 35a). The consistent diurnal pattern in COD values for specific site pairs reflect the influence of particular sources (e.g., HDDV activity) and their relative persistence throughout the study. The correlation coefficients for this site pair (Figure 35b) exhibit more scatter than the COD values and vary from –0.10 to 0.56. The relatively low/near homogeneous CODs calculated in the later afternoon for this site pair are associated with relatively high correlation coefficients. However, correlation coefficients of similar value (>0.4) are associated with median COD values that are clearly heterogeneous (approximately 0.4) in the late evening. In general, the maximum

COD values (up to 0.88) were associated with site pairs including one of the harbor background locations (either LB1 or SP1, not shown) where the paired number concentration data exhibit the largest difference as has been noted by others (Pinto et al., 2004). Minimum COD values (<0.1) implying spatial homogeneity were associated with pairs located close together or with similar sources (the LB2–LB3 pair, Figure 36). The LB2–LB3 site pair yields the lowest overall CODs and highest correlation coefficients and they are the two sites in closest proximity to each other (approximately 200 m) and are impacted to a similar degree by nearby UFP sources. The uniformly higher correlation coefficients and low CODs shown in Figure 36 were the exception in this data set, however. Only for this site pair with virtually identical sources could the correlation coefficient or the COD alone express the variability between sites.

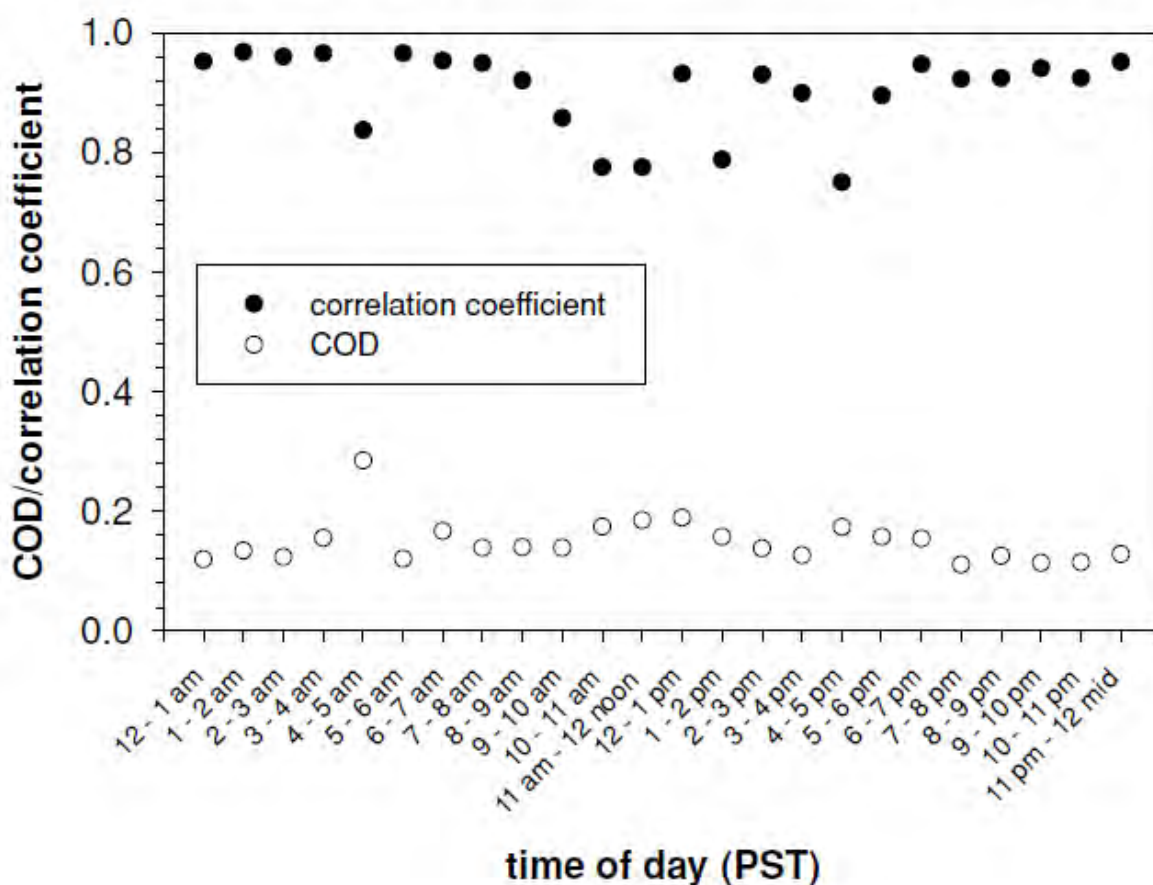


Figure 36: Median coefficients of divergence (CODs) and correlation coefficient (r) calculated for PNCs at the LB2–LB3 site pair (March–May data).

4.2. RECEPTOR AREA STUDY

Figures 37 and 38 compare the CODs for particle number concentrations across summer and winter periods, respectively. Summer seems to be the season with lowest spatial variability in PNCs; in fact, for the majority of the day, COD values were below 0.2, indicating remarkable spatial homogeneity for a metropolitan area of this size and complexity in PM sources. The COD values are generally higher in winter, but still below 0.3, indicating only moderate heterogeneity. The deviation in CODs for all site pairs was highest for the hours in which primary local sources are predominant, implying that one or more sites with a heavy local influence (which in most cases would be traffic) is increasing the COD. This was further ascertained by inspecting individual site pair values. During both summer and winter, homogeneity is observed in late night and early morning concentrations, indicating the presence of a regional aerosol. In comparison to our previous study (Moore et al., 2009 and Krudysz et al., 2009) that reports median COD values of about 0.3-0.5 in source regions of the LAB (the range between first and third quartiles was on the order of 0.2 units), the values reported in this receptor area study are lower. This implies that the *inter-community* variability in PNC across the Los Angeles basin is lower than the *intra-community* variability of areas like the Harbor Communities which are impacted by a multitude of traffic, ship and industrial emissions in a much shorter spatial scale. The relative homogeneity at the inter-community level among receptor sites in LAB can be attributed to the effects of photochemistry and regional transport (both are influenced by meteorology) that override the contributions of local (primary) emissions. The effects of local traffic sources were also observed at the sites in this study, but were restricted to morning and (only during winter) evening commute hours.

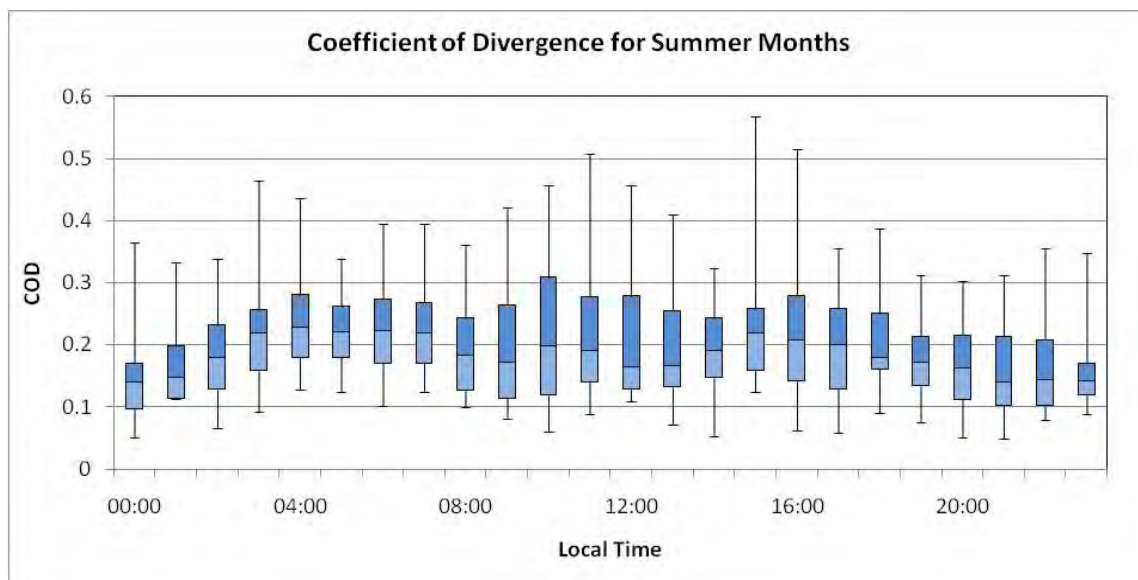


Figure 37: Diurnal variation in the coefficients of divergence for PNCs in the receptor area (Phase II) study during the summer months of May-August, 2009.

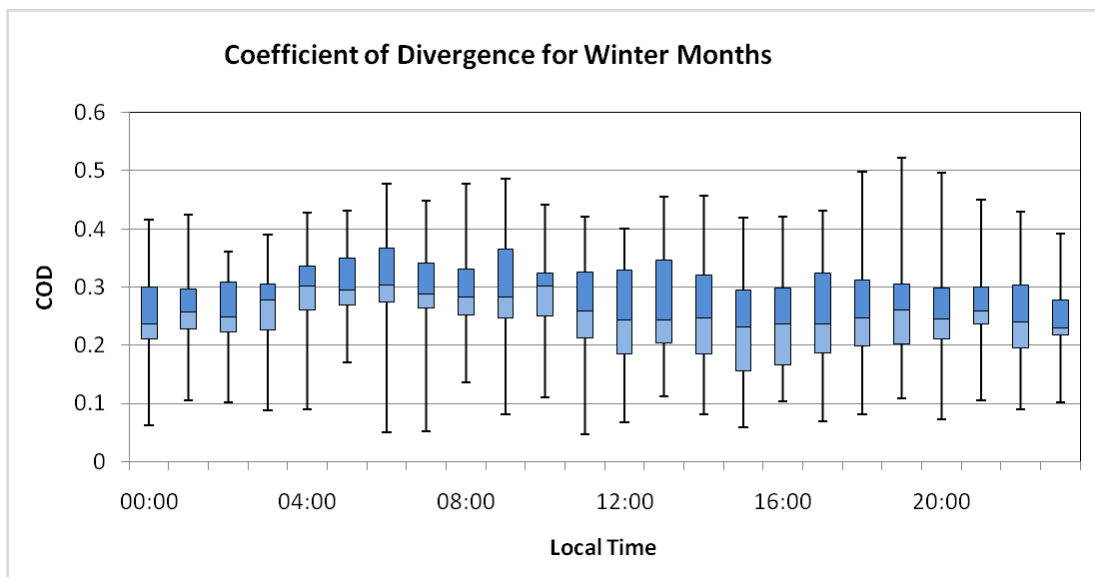


Figure 38: Diurnal variations in coefficients of divergence for PNCs in the receptor area (Phase II) study during the winter months of December 2008 - February 2009.

The spatial complexity of the PNC was further investigated with the size distribution data. Synergistic effects of multiple factors can lead to similar particle number concentrations at two sites; however, the shape in size distributions may be distinctly different at the two locations due to particle source composition. Wongphatarakul et al. (1998) showed that only moderately heterogeneous COD values can be observed for chemical composition of particles even when the sources are different. Since particle size distribution is as important for exposure classification, the spatial variability was assessed for different PM sizes (Figure 39). Overall CODs varied from 0.40-0.67, and exhibited a roughly inverse relationship with particle size. This can in part be accounted for by the difference in sources and their magnitude between USC and the inland sites as well as the PM size range. This observation is further supported by the lower COD values between the inland sites of AGO-UPL 0.35 (range 0.34-0.36) compared to 0.55 (range 0.53-0.57) for USC-AGO (source and inland site). Even though the degree of spatial heterogeneity is moderate for particles in bigger size ranges, this is the size range with minimal divergence in COD values observed for different site pairs. The data in Figures 37 and 38 reinforce the observation that sites appear to be more homogeneous when the local sources (which contribute to the smaller size spectrum of the particle size distribution more than the bigger size) are not dominant. Similar observations were made by Turner et al. (2008) and Costabile et al. (2009).

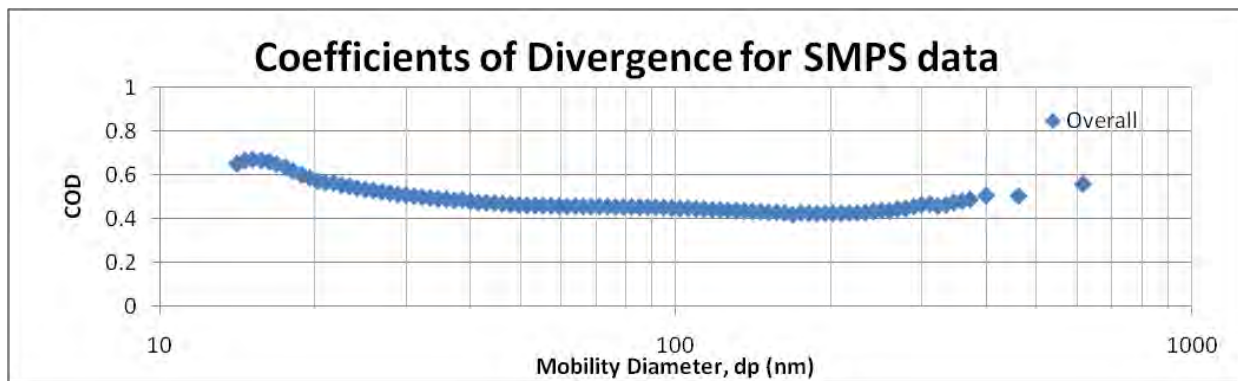


Figure 39: Coefficients of Divergence for different size (mobility diameter) of particles during Sep.-Dec. 2009 at select sites: USC, UPL & AGO.

4.3. COMPARISON WITH CHILDREN'S HEALTH STUDY AND IMPLICATIONS

Monthly mean particle number concentration data (Figure 40) mute profound variations in hourly concentrations (Figures 13–15). Diurnal concentration patterns vary widely due to changes in emissions, wind speed and direction, and other factors. These patterns affect the hourly variability expressed by the COD and correlation coefficient calculations between specific site pairs, although averaging over all site pairs yields moderate heterogeneity and modest correlation both near the Ports and at the regional site 32 km inland subject to different UFP sources, with limited exception. There is no fixed relationship observed between site pairs for calculated COD and r values, although both methods are useful tools in assessing observed differences between sites. The correlation coefficients may well be modest due to the multiplicity of factors affecting concentrations even in this limited area. The predominant UFP source is motor vehicles and similar (e.g., rail) emission sources. Different motor vehicle types (e.g., HDDV and LDGV) and traffic patterns strongly influence the observations. Without detailed knowledge of all of these factors a priori, it is difficult to estimate either inter-urban (as in the CHS) or intra-community (as in this study) variability in total particle number concentrations. Site selection is critical and a sufficient number of sites located in proximity to strong sources are required to capture their effect on total particle number concentrations, observed intra-community variability, and, ultimately, exposure assessments. These results suggest that considering distance between sites alone without also considering the proximity of nearby UFP sources and sinks as well as wind patterns is inadequate. Figure 41 further compares the concentrations observed during Phase II of the study with earlier observations made by Singh et al. (2006), who reported PNC data 6-7 years earlier, using identical instrumentation at similar sites. The sites AGO and UPL are referred to as Riverside and Upland by Singh et al. (2006). The Mira Loma site is about 8 km west of RUB. In general, the observed concentrations in the present study are somewhat lower, which could be interpreted (with some caution) as an encouraging outcome of the implementation of effective emission control technologies and the replacement of older heavy and light duty vehicles by newer

vehicles in the LAB. The seasonal patterns identified in this study are consistent with the earlier observations by Singh et al. (2004).

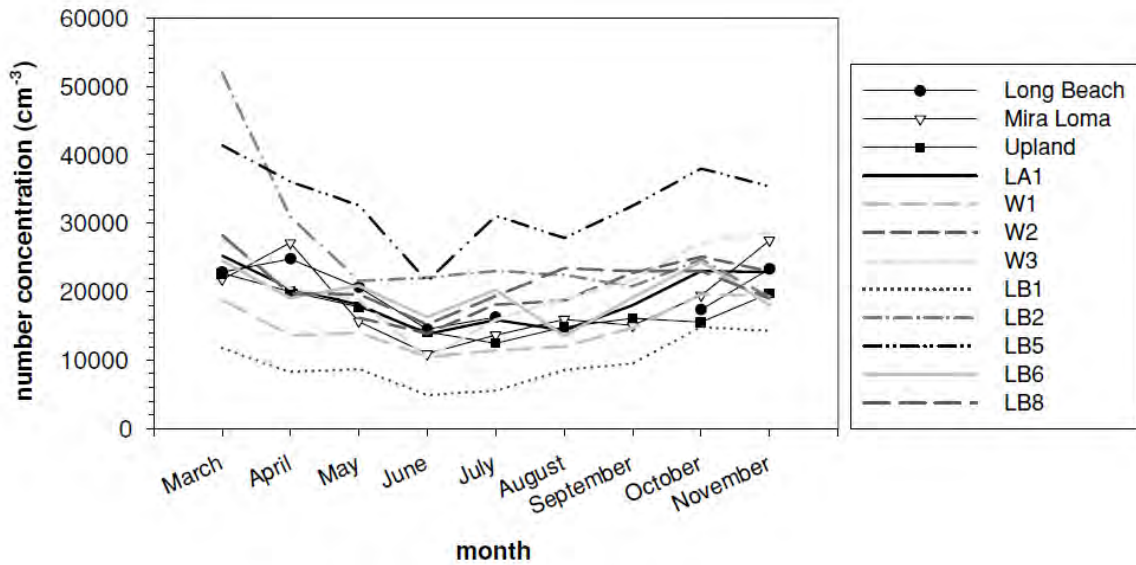


Figure 40: Monthly mean particle number concentrations by month and selected sites including data from the 2002–2003 Children’s Health Study in California (named locations, data from Singh et al., 2006).

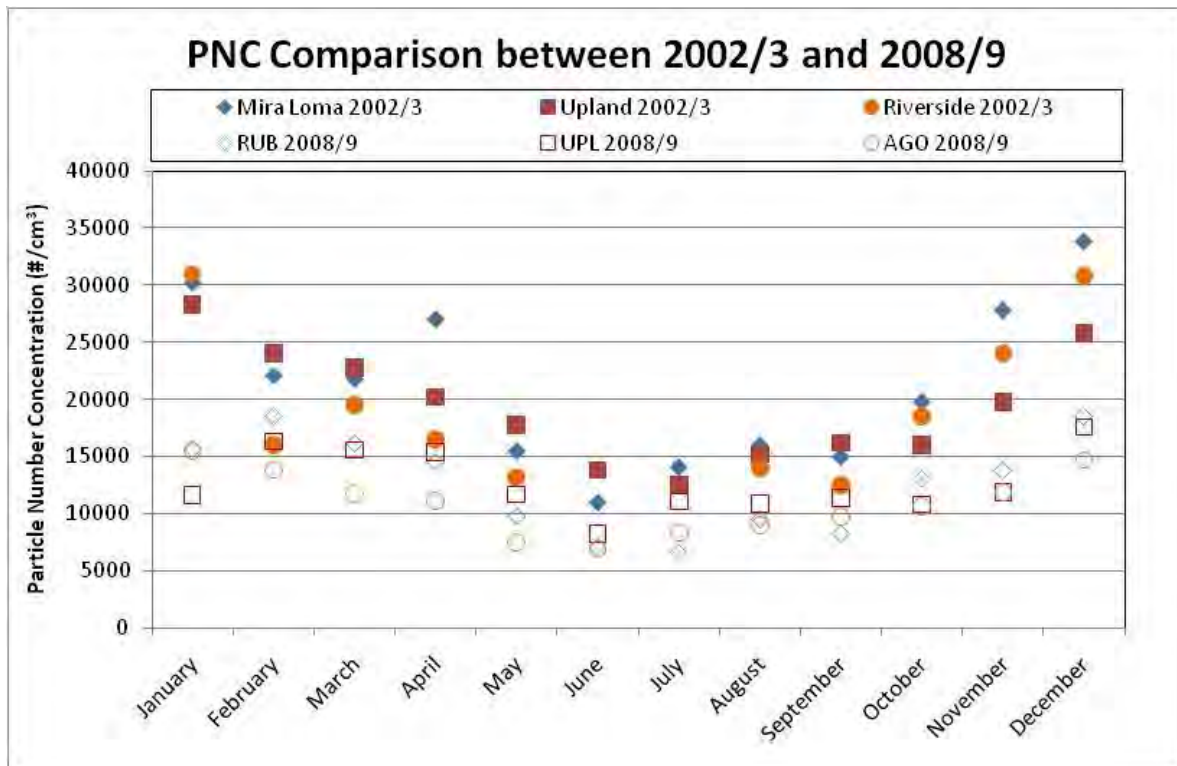


Figure 41: Comparison of PNC at select sites measured during 2008/09 with Singh et al. (2006) measured during 2002/03.

5. SUMMARY AND CONCLUSIONS

5.1 SOURCE AREA STUDY

In order to better understand and quantify intra-community variability in UFP concentrations, a dense network of 14 monitoring sites was set-up in Los Angeles in two clusters—San Pedro/Wilmington and West Long Beach—in communities neighboring the Ports of Los Angeles and Long Beach. The network measured total particle number concentrations greater than 7 nm in diameter. In this range, UFP comprise approximately 90% of the total. Port-related activities, particularly goods movement associated with high volumes of heavy-duty diesel vehicle (HDDV) traffic, represent significant UFP sources. The field study was conducted from mid- February through mid-December 2007 to assess diurnal, seasonal, and spatial patterns and intra-community variability in total particle number concentrations. For sites within a few kilometers of each other, simultaneous particle number concentrations can vary up to a factor of 10 ($<10,000 \text{ cm}^{-3}$ up to $90,000 \text{ cm}^{-3}$ for monthly mean hourly concentrations). The median hourly correlation coefficient (r) across all sites was modest and varied from 0.30 to 0.56. Site locations, particularly proximity to roadways used for goods movement, strongly affect observations. Clear diurnal and seasonal patterns are evident in the data. A diurnal pattern associated with high HDDV volumes and goods movement was identified. Coefficients of Divergence calculated for the site pairs suggest moderate heterogeneity overall (median study COD was about 0.35). The intra-urban variability observed in this study is comparable to and exceeds the inter-urban variability observed in a previous study in Los Angeles. UFP concentrations can vary considerably on short spatial scales in source-rich environments and thus strongly influencing the accuracy of exposure assessments based on one or even a few sites.

Significant intra-community variability in total particle number concentrations was observed near the San Pedro Harbor. Extreme spatial heterogeneity, as characterized by the CODs, was driven by the inclusion of two harbor background sites with relatively low ambient concentrations of UFPs. Correlation between most site pairs was weak. Considerable differences in concentration were observed between sites in close proximity to each other due to multiple factors including proximity to sources, source strength, and traffic patterns. Diurnal patterns varied between sites, and a pattern associated with high HDDV fractions/goods movement was observed at several of the sites.

The intra-community variability observed in this study was on the order of the inter-community variability observed during the Children's Health Study conducted earlier in Los Angeles basin. In view of these observations, the documented concern regarding the applicability of centrally located PM_{2.5} mass concentration measurements in estimating exposure to UFPs is warranted.

5.2. RECEPTOR AREA STUDY

Large spatial variations in the concentrations of air pollutants have been reported at regional scales of tens of kilometers for areas affected by primary emissions. Spatial variability in particle number concentrations (PNC) and size distributions needed to be investigated further, as the representativeness of a single particulate monitoring station in a region is premised on the assumption of homogeneity in both of these metrics. This study was conducted at six sites, one in downtown Los Angeles and five located about 40 - 115 km east in the region of the Los Angeles basin typically downwind of the more urban and industrial emissions source areas of the basin. PNC and size distribution were measured using Condensation Particle Counters (CPC) and Scanning Mobility Particle Sizer (SMPS). The seasonal and diurnal variations of PNC implied that particulate matter might vary significantly with meteorological conditions, even though the general patterns at the sites remain similar across the year due to the consistency of sources and activities around them. Regionally transported particulate matter (PM) from upwind urban areas of the Los Angeles basin decreased spatial variation by acting as a “homogenizing” factor during favorable meteorological conditions. Spatial variability also increased during hours of the day during which the effects of local sources predominate. The spatial variability associated with PNC (quantified using coefficients of divergence, CODs), averaged 0.3, which was generally lower than that based on specific size ranges. Results showed an inverse relationship of COD with particles size, with fairly uniform values in the particle range which is associated with regional transport. Our results suggest that spatial variability, even in the receptor regions of Los Angeles Basin, should be evaluated further for both PNC and size distributions, and should be interpreted in context of seasonal and diurnal influences.

Moderate inter-community variability in total particle number concentrations was observed across the sites of the eastern Los Angeles basin. The extreme Coefficient of Divergence (COD) values were often driven by a specific site pair, (site pair varied by hour and season), but the range of upper and lower quartile of COD values was mostly within 0.1 units, implying that Particle Number Concentration (PNC) in these sites were homogeneous-to-moderately heterogeneous. Although, there were differences in the spatial variability through different seasons, the temporal patterns were consistent, and exhibited least variability in hours when local sources were not dominant. Comparable PNC can be observed in sites separated by several tens of kilometers overnight when local emissions are less and the atmosphere is stable. The variability in size distributions (reflection of the source composition) was higher than that of total particle number concentrations. Overall the spatial variability in PNC was lower than the values reported by Moore et al. (2009) for intra-community variability in urban “source” areas of the LAB. The spatial variability based on particle size distributions support the notion of relative homogeneity in receptor areas in the LAB, where concentrations are dominated by aged aerosols, advected eastwards from the source regions of urban Los Angeles. This interpretation is supported by the observation that particle number concentrations in the size range of 40-100 nm (associated with aged transport) had lower variability compared to sub-30 nm particles (associated with fresh emissions or new particle formation events). The largest differences in PNCs were observed between receptor sites and the urban source site at USC, while PNC were relatively homogeneous among

the receptor sites. Further, the data suggest that meteorological conditions can contribute to spatial homogeneity, when phenomena that are regional in nature (i.e., photochemical processes, transport, and atmospheric mixing) are more active.

5.3. SOUNDWALL STUDY

Increasing epidemiological evidence has established an association between a host of adverse health effects and exposure to ambient particulate matter (PM) and co-pollutants, especially those emitted from motor vehicles. Although dispersion profiles of PM and their co-pollutants near the open freeway have been extensively characterized by means of both experimental measurements and numerical simulations in recent years, such investigations near freeways with roadside barriers have not been well documented in the literature. A few previous studies (Bowker et al., 2007; Baldauf et al., 2008b) suggested that the presence of roadside structures, such as noise barriers and vegetation, may impact the decay of pollutant concentrations downwind of the freeway (e.g., by limiting the initial dispersion of traffic emissions and increasing their vertical mixing due to the upward deflection of airflow, by providing additional surfaces for deposition). Since noise barriers are now common roadside features of the freeways, particularly those running through populated urban areas, it is pertinent to investigate the impact of their presence on concentrations of particulate and gaseous pollutants in areas adjacent to busy roadways.

This study investigated two highly trafficked freeways (I-710 and I-5) in Southern California, with two sampling sites for each freeway, one with and the other without the roadside noise barriers. Particle size distributions and concentrations of air pollutants were measured in the immediate proximity of freeways and at distances downwind of the freeways. The results showed the formation of a “concentration deficit” zone in the immediate vicinity of the freeway with the presence of roadside noise barrier, followed by increased pollutant concentrations further downwind at 80-100 m away from freeway. The particle numbers and gaseous pollutant concentrations reached background levels at further distances of 250 - 400 m compared to 150 - 200 m in areas without roadside noise barriers.

With the presence of a roadside barrier, the dynamics of the particulate and gaseous pollutant dispersion changed dramatically. A recirculation cavity is formed in the close vicinity downwind of the barrier, as observed at 15 m in the present study, resulting in a concentration deficit zone in the lee of the barrier, where the particle number concentrations are 45-50% of those measured at similar downwind distances of freeways without roadside barrier. The particle size distributions and co-pollutants concentrations in the lee of the barrier were comparable to background levels. With increasing downwind distance, particles and gaseous pollutant concentrations increased and peaked at 80-100 m, where the plume of traffic emissions descended back down to ground level. The particle size distribution displayed a sharp nucleation mode peak, with total number concentrations 1.9-2.2 times those observed at similar distances near freeways without barriers. Particle mass, CO, NO₂ and BC also reached maximum concentrations ratios. Background concentrations of particles and gaseous

pollutants were reached at distances of 250-450 m, or about three times further downwind than near non-barrier freeways.

The much longer downwind distance needed to reach background concentrations indicates a larger impact zone of traffic emission sources near the freeways with roadside noise barriers. Our results suggest that freeway roadside features, such as noise barriers, should also be taken into consideration in assessing population exposure to ambient particles and co-pollutants from traffic emissions.

6. RECOMMENDATIONS

Significant intra-community variability in total particle number concentrations was observed near the San Pedro Harbor. In view of these observations, the documented concern regarding the applicability of using centrally located PM_{2.5} mass concentration measurements to estimate exposure to UFPs is warranted.

Even though our results suggest that PNC are moderately heterogeneous in the polluted receptor areas of the LAB, concerns related to population exposure assessment based on monitoring from a central station are still valid, especially in relation to urban areas impacted by a multitude of local and highly variable sources. Moreover, despite the moderate heterogeneity in total PNC at the inter-community level of receptor sites in LAB, particle size distributions may be significantly variable, resulting in differences in the overall inhaled dose of PM mass. Additional efforts should be made to characterize the seasonal variability in both size distributions and number concentrations, because meteorological factors can influence both, even when PM sources are similar.

Some basic recommendations from each of the study phases for this contract are listed below:

Phase I (source area) Study – Conduct additional contemporaneous monitoring of PNCs and size distributions to better characterize not only horizontal gradients but also vertical gradients under various meteorological conditions to inform particulate number modeling and assessments of public exposure.

Phase II (receptor area) Study – Conduct additional contemporaneous monitoring of PNCs and size distributions to characterize vertical gradients and temporal variations under various meteorological conditions to inform particle number modeling.

Phase III (sound wall) Study – Conduct additional contemporaneous monitoring of PNCs and size distributions to better characterize horizontal and vertical gradients under various meteorological conditions (especially wind speeds and directions) to inform particle number modeling and assessments of public exposure. In addition, a similar program should be initiated to investigate the various effects of vegetation (e.g., conifers and deciduous) on PNCs and size distributions.

7. REFERENCES

Adler, K.B., Fischer, B.M., Wright, D.T., Cohn, L.A., and Becker, S. Interactions between Respiratory Epithelial-Cells and Cytokines - Relationships to Lung Inflammation, *Cells and Cytokines in Lung Inflammation*, 1994, 725, 128-145.

Alam, A., J.P. Shi and R.M. Harrison Observations of new particle formation in urban air. *Journal of Geophysical Research-Atmospheres*, 2003, 108, 4093-4108.

Arhami M., Sillanpää M., Hu S., Geller M.D., Schauer J.J. and Sioutas C. Size-segregated Inorganic and Organic Components of PM In the Communities of the Long Angeles Harbor Across Southern Los Angeles Basin, California.” *Aerosol Science and Technology*, 2009, 43,145-160.

Baldauf, R., E. Thoma, M. Hays, R. Shores, J. Kinsey, B. Gullett, S. Kimbrough, V. Isakov, T. Long, R. Snow, A. Khlystov, J. Weinstein, F.L. Chen, R. Seila, D. Olson, I. Gilmour, S.H. Cho, N. Watkins, P. Rowley and J. Bang, Traffic and meteorological impacts on near-road air quality: Summary of methods and trends from the Raleigh near-road study. *Journal of the Air & Waste Management Association*, 2008a, 58,865-878.

Baldauf, R., E. Thoma, A. Khlystov, V. Isakov, G. Bowker, T. Long and R. Snow, Impacts of noise barriers on near-road air quality. *Atmospheric Environment*, 2008b, 42, 7502-7507.

Biswas, S., Ntziachristos, L., Moore, K. F., and Sioutas, C.: Particle volatility in the vicinity of a freeway with heavy-duty diesel traffic, *Atmos. Environ.*, 41, 3479–3493, 2007.

Bowker, G. E., R. Baldauf, V. Isakov, A. Khlystov and W. Petersen, The effects of roadside structures on the transport and dispersion of ultrafine particles from highways. *Atmospheric Environment*, 2007, 41, 8128-8139.

Costabile, F., Birmili, W., Klose, S., Tuch, T., Wehner, B., Wiedensohler, A., Franck, U., König, K., and Sonntag, A. Spatio-temporal variability and principal components of the particle number size distribution in an urban atmosphere, *Atmos. Chem. Phys.*, 2009, 9, 3163-3195.

Cyrys, J., Stolzel, M., Heinrich, J., Kreyling, W.G., Menzel, N., Wittmaack, K., Tuch, T., Wichmann, H.E. Elemental composition and sources of fine and ultrafine ambient particles in Erfurt, Germany, *Science of the Total Environment*, 2003, 305, 143-156.

Dockery, D.W., Pope, C.A., Xu, X.P., Spengler, J.D., Ware, J.H., Fay, M.E., Ferris, B.G., Speizer, F.E. An Association between Air-Pollution and Mortality in 6 United-States Cities, *New England Journal of Medicine*, 1993, 329, 1753-1759.

Donaldson, K., Li, X.Y., MacNee, W. Ultrafine (nanometer) particle mediated lung injury, *Journal of Aerosol Science*, 1998, 29, 553-560.

Fine, P. M., Shen, S., Sioutas, C. Inferring the Sources of Fine and Ultrafine Particulate Matter at Downwind Receptor Sites in the Los Angeles Basin Using Multiple Continuous Measurements. *Aerosol Science and Technology*, 2004, 38, 182-195.

Finn, D., Clawson, K.L., Carter, R.G., Rich, J.D., Eckman, R.M., Perry, S.G., Isakov, V., Heist, D.K., 2010. Tracer studies to characterize the effects of roadside noise barriers on near-road pollutant dispersion under varying atmospheric stability conditions. *Atmospheric Environment*, 44, 204-214.

Heist, D.K., S.G. Perry and L.A. Brixey, A wind tunnel study of the effect of roadway configurations on the dispersion of traffic-related pollution. *Atmospheric Environment*, 2009, 43, 5101-5111.

Hinds, W.C., *Aerosol technology: properties, behavior, and measurement of airborne particles* (2nd Edition). 1999, New York, J. Wiley.

Holscher, N., R. Hoffer, H.J. Niemann, W. Brilon and E. Romberg, Wind-Tunnel Experiments on Microscale Dispersion of Exhausts from Motorways. *Science of the Total Environment*, 1993, 134, 71-79.

Hu, S., Fruin, S., Kozawa, K., Mara, S., Paulson, S. E., and Winer, A. M.: A wide area of air pollutant impact downwind of a freeway during pre-sunrise hours, *Atmos. Environ.*, 43, 2541–2549, 2009.

Kim, S., Shen, S., Sioutas, C., Zhu, Y.F., Hinds, W.C. Size distribution and diurnal and seasonal trends of ultrafine particles in source and receptor sites of the Los Angeles basin, *Journal of the Air & Waste Management Association*, 2002, 52, 297-307.

Kleeman, M.J., Hughes, L.S., Allen, J.O., Cass, G.R. Source contributions to the size and composition distribution of atmospheric particles: Southern California in September 1996, *Environmental Science & Technology*, 1999, 33, 4331-4341.

Krudysz, M.A., Froines, J.R., Moore, K.F., Geller, M.D., and Sioutas, C. Intra-community spatial variability in particle size distributions in the Los Angeles Harbor-area, *Atmos. Chem. Phys.*, 2009, 9, 1061–1075.

Kulmala, M., Vehkamäki, H., Petäjä, T., Dal Maso, M., Lauri, A., Kerminen, V.M., Birmili, W., McMurry, P.H. Formation and growth rates of ultrafine atmospheric particles: a review of observations, *Journal of Aerosol Science*, 2004, 35, 143-176.

Lianou, M., Chalbot, M.C., Kotronarou, A., Kavouras, I.G., Karakatsani, A., Katsouyanni, K., Puustinen, A., Hameri, K., Vallius, M., Pekkanen, J., Medings, C., Harrison, R.M.,

Thomas, S., Ayres, J.G., ten Brink, H., Kos, G., Meliefste, K., de Hartog, J.J., and Hoek, G. Dependence of home outdoor particulate mass and number concentrations on residential and traffic features in urban areas, *J. Air Waste Manage.*, 2007, 57, 1507–1517.

Li, N., Sioutas, C., Cho, A., Schmitz, D., Misra, C., Sempf, J., Wang, M.Y., Oberley, T., Froines, J., Nel, A. Ultrafine particulate pollutants induce oxidative stress and mitochondrial damage, *Environmental Health Perspectives*, 2003, 111, 455-460.

Miracolo, M.A., Presto, A.A., Lambe, A.T., Hennigan, C.J., Donahue, N.M., Kroll, J. H., Worsnop, D.R., and Robinson, A.L. Photo-Oxidation of Low-Volatility Organics Found in Motor Vehicle Emissions: Production and Chemical Evolution of Organic Aerosol Mass, *Environ. Sci. Technol.*, 2010, 44, 1638-1643.

Minguillón M.C., Arhami M., Schauer J.J., Olson M.R., and Sioutas C. Seasonal and spatial variations of sources of fine and quasi-ultrafine particulate matter in neighborhoods near the Los Angeles-Long Beach Harbor. *Atmospheric Environment*, 42, 2008, 7317-7328.

Moore, K. F., Ning, Z., Ntziachristos, L., and Sioutas, C: Daily variation in summer urban ultrafine particle properties – physical characterization and volatility, *Atmos. Environ.*, 41, 8633–8646, 2007.

Moore, K. F., Krudysz, M., Pakbin, P., Hudda, N., and Sioutas, C. Intra-Community Variability in Total Particle Number Concentrations in the San Pedro Harbor Area (Los Angeles, California), *Aerosol Sci. Tech.*, 2009, 43, 587-603.

Morawska, L., Bofinger, N.D., Kocis, L., Nwankwoala, A. Submicrometer and supermicrometer particles from diesel vehicle emissions, *Environmental Science & Technology*, 1998, 32, 2033-2042.

Ning, Z., Geller, M., Moore, K. F., Sheesley, R., Schauer, J. J., and Sioutas, C.: Daily variation in summer urban ultrafine aerosols and inference of their sources, *Environ. Sci. Technol.*, 41, 6000–6006, 2007.

Oberdörster, G. Significance of particle parameters in the evaluation of exposure-dose-response relationships of inhaled particles, *Particulate Science and Technology*, 1996, 14, 135-151.

Oberdörster, G. Pulmonary effects of inhaled ultrafine particles, *International Archives of Occupational and Environmental Health*, 2001, 74,1-8.

Penttinen, P., Timonen, K.L., Tiittanen, P., Mirme, A., Ruuskanen, J., Pekkanen, J. Ultrafine particles in urban air and respiratory health among adult asthmatics; *European Respiratory Journal*, 2001, 17, 428-435.

Peters, A.; Wichmann, H.E.; Tuch, T.; Heinrich, J.; Heyder, J. Respiratory effects are associated with the number of ultrafine particles; *American Journal of Respiratory and Critical Care Medicine*, 1997, 155, 1376-1383.

Pinto, J. P., Lefohn, A. S., and Shadwick, D. S. Spatial Variability of PM_{2.5} in Urban Areas in the United States, *J. Air & Waste Manage. Assoc.*, 2004, 54, 440–449.

Raes, F., R. Van Dingenen, E. Vignati, J. Wilson, J. P. Putaud, J. H. Seinfeld and P. Adams. Formation and cycling of aerosols in the global troposphere. *Atmospheric Environment* 34, 2002, 4215-4240.

Ronkko, T., Virtanen, A., Vaaraslahti, K., Keskinen, J., Pirjola, L., and Lappi, M.: Effect of dilution conditions and driving parameters on nucleation mode particles in diesel exhaust: Laboratory and on-road study, *Atmos. Environ.*, 40, 2893–2901, 2006.

Ronkko, T., Virtanen, A., Kannosto, J., Keskinen, J., Lappi, M., and Pirjola, L.: Nucleation mode particles with a nonvolatile core in the exhaust of a heavy duty diesel vehicle, *Environ. Sci. Technol.*, 41, 6384–6389, 2007.

Sardar, S.B., Fine, P. M., Hoon, A., Sioutas, C. Associations Between Particle Number and Gaseous Co-Pollutant Concentrations in the Los Angeles Basin. *The Journal of the Air and Waste Management Association*, 2004, 54, 992-1005.

Shi, J.P., Khan, A.A., Harrison, R.M. Measurements of ultrafine particle concentration and size distribution in the urban atmosphere, *Science of the Total Environment*, 1999, 235, 51-64.

Singh, M., Phuleria, H., Bowers, K.L., and Sioutas, C. Seasonal and Spatial Trends in Particle Number Concentrations and Size Distributions at the Children’s Health Study Sites in Southern California”. *Journal of Exposure Analysis and Environmental Epidemiology*, 2004, 16, 3–18.

Turner, J.R., and Allen, D.T. Transport of atmospheric fine particulate matter: part 2 – findings from recent field programs on the intraurban variability in fine particulate matter, *J. Air Waste Manage.*, 2008, 58, 196–215.

Verma, V., Ning, Z., Cho, A. K., Schauer, J. J., Shafer, M. M., and Sioutas, C.: Redox activity of urban quasi-ultrafine particles from primary and secondary sources, *Atmos. Environ.*, 43, 6360–6368, 2009.

Watson, J.G., Chow J.C. Estimating middle-, neighborhood-, and urban-scale contributions to elemental carbon in Mexico City with a rapid response Aethalometer, *Journal of the Air & Waste Management Association*, 2001, 51, 1522-1528.

Wilson, J. G., Kingham, S., Pearce, J., and Sturman, A. A Review of Intraurban Variations in Particulate Air Pollution: Implications for Epidemiological Research, *Atmos. Environ.*, 2005, 39, 6444–6462.

Wilson, J. G., and Zawar-Reza, P. Intraurban-Scale Dispersion Modeling of Particulate Matter Concentrations: Applications for Exposure Estimates in Cohort Studies, *Atmos. Environ.*, 2006, 40, 1053–1063.

Wongphatarakul, V., Friedlander, S.K., and Pinto, J.P. A comparative study of PM_{2.5} ambient aerosol chemical databases, *Environ. Sci. Technol.*, 1998, 32, 3926–3934.

Yu, K.N., Cheung, Y.P., Cheung, T., Henry R.C. Identifying the impact of large urban airports on local air quality by nonparametric regression, *Atmospheric Environment*, 2004, 38, 4501-4507.

Zhang, K.M., Wexler, A.S, A hypothesis for growth of fresh atmospheric nuclei, *Journal of Geophysical Research-Atmospheres*, 2002, 107.

Zhang, K.M., Wexler, A.S., Evolution of particle number distribution near roadways - Part I: Analysis of aerosol dynamics and its implications for engine emission measurement. *Atmospheric Environment*, 2004, 38, 6643-6653.

Zhu, Y.F.; Hinds, W.C.; Kim, S.; Shen, S.; Sioutas, C. Study of ultrafine particles near a major highway with heavy-duty diesel traffic; *Atmospheric Environment*, 2002a, 36, 4323-4335.

Zhu, Y.F.; Hinds, W.C.; Kim, S.; Sioutas, C. Concentration and size distribution of ultrafine particles near a major highway; *Journal of the Air & Waste Management Association*, 2002b, 52, 1032-1042.

Zhu, Y., Kuhn, T., Mayo, P., and Hinds, W. C.: Comparison of daytime and nighttime concentration profiles and size distributions of ultrafine particles near a major highway, *Environ. Sci. Technol.*, 40, 2531–2536, 2006.

8. LIST OF INVENTIONS REPORTED AND COPYRIGHTED MATERIALS PRODUCED

1. Krudysz, M.A, Froines, J.R., Fine, P.M. and Sioutas, C. —~~Intra~~-community spatial variation of size-fractionated PM mass, OC, EC and trace elements in Long Beach, CA". *Atmospheric Environment*, 42 (21):5374-5389, 2008
2. Minguillón M.C., Arhami M., Schauer J.J. and Sioutas C. —~~Seasonal~~ and spatial variations of sources of fine and quasi-ultrafine particulate matter in neighborhoods near the Los Angeles-Long Beach Harbor". *Atmospheric Environment*, 42(32):7317-7328, 2008
3. Hu S., Polidori A., Arhami M., Schafer M., Cho A., Schauer J.J., Cho A. and Sioutas C. —~~Redox~~ Activity and Chemical Speciation of Size Fractioned PM in the Communities of the Los Angeles - Long Beach Harbor". *Atmospheric Chemistry and Physics*, 8:6439-6451, 2008
4. Arhami M., Sillanpää M., Hu S., Olson M.R., Schauer J.J. and Sioutas C. —~~Size~~-segregated Inorganic and Organic Components of PM In the Communities of the Long Angeles Harbor Across Southern Los Angeles Basin, California." *Aerosol Science and Technology*, 43(2):145-160, 2009
5. Krudysz M.A., Moore K.F., Geller M.D., Sioutas C. and Froines, J.R. —~~Intra~~-community Spatial Variability of Particulate Matter Size Distributions". *Atmospheric Chemistry and Physics*, 9:1061-1075, 2009
6. Krudysz M.A., Dutton S.J., Brinkman G.L., Hannigan M.P., Fine P.M., Sioutas C. and Froines J.R." Intra-community spatial variation of size-fractionated organic compounds in Long Beach, CA". *Air Quality, Atmosphere and Health*, 2:69–88, 2009

9. GLOSSARY OF TERMS, ABBREVIATIONS, AND SYMBOLS

AQMD	South Coast Air Quality Monitoring District
ARB	Air Resources Board
C	Degrees Centigrade
CHS	Children's Health Study
cm ³	cubic centimeter
COD	Coefficient of Divergence
CPC	Condensation Particle Counter
HCMS	Harbor Communities Monitoring Study
HDDV	Heavy Duty Diesel Vehicle
ICTF	Intermodal Container Transfer Facility
LAB	Los Angeles Air Basin
LDGV	Light Duty Gasoline Vehicle
ms ⁻¹	meters per second
PM	Particulate Matter
PNC	Particle Number Concentration
PNSD	Particle Number Size Distribution
RH	Relative Humidity
SMPS	Scanning Mobility Particle Sizer
UFP	Ultrafine Particle
USC	University of Southern California

APPENDIX A: RELATED PUBLICATIONS

A1.1 Intra-community spatial variation of size-fractionated PM mass, OC, EC and trace elements in Long Beach, CA.

Margaret A. Krudysz^{a, b}, John R. Froines^{a, b}, Philip M. Fine^c and Constantinos Sioutas^c

^aCenter for Occupational and Environmental Health, University of California, Los Angeles, 650 Young Drive South, Los Angeles, CA 90095, USA

^bDepartment of Environmental Health Sciences, School of Public Health, University of California, Box 951772, 56-195 CHS, 650 Young Drive South, Los Angeles, CA 90095, USA

^cDepartment of Civil and Environmental Engineering, University of Southern California, 3620 South Vermont Avenue, Los Angeles, CA 90089, USA

Abstract

Local traffic patterns and proximity to pollution sources are important in assessing particulate matter (PM) exposure in urban communities. This study investigated the intra-community spatial variation of PM in an urban area impacted by numerous local and regional sources. Weekly size-segregated (<0.25, 0.25–2.5, and >2.5 μm) PM samples were collected in the winter of 2005. During each 1-week sampling cycle, data were collected concurrently at four sites within four miles of one another in the Long Beach, CA area. Coefficients of divergence analyses for size-fractionated PM mass, organic and elemental carbon, sulfur, and 18 other metals and trace elements suggest a wide range of spatial divergence. High spatial variability was observed in the <0.25 μm and 0.25–2.5 μm PM fractions for many elements associated with motor vehicle emissions. Relatively lower spatial divergence was observed in the coarse fraction, although road dust components were spatially diverse but highly correlated with each other. Mass and OC concentrations were homogeneously distributed over the sampling sites. Possible oil combustion sources were identified using previously documented markers such as vanadium and nickel and by distinguishing between primary sulfur and secondary sulfate contributions. This study shows that, although PM mass in different size fractions is spatially homogeneous within a community, the spatial distribution of some elemental components can be heterogeneous. This is evidence for the argument that epidemiological studies using only PM mass concentrations from central sites may not accurately assess exposure to toxicologically relevant PM components.

Conclusions

- The results presented in this paper indicate that spatial heterogeneity in size-fractionated PM chemical components can exist on a community scale.
- High spatial variability was observed in the quasi-UF and quasi- Acc PM fractions for many elements associated with motor vehicle emissions, for example elemental carbon, Mg, Al, and Ba.
- This study shows that, although PM mass in different size fractions is spatially homogeneous within a community, the spatial distribution of some elemental components can be heterogeneous.

A1.2 Seasonal and spatial variations of sources of fine and quasi-ultrafine particulate matter in neighborhoods near the Los Angeles-Long Beach Harbor.

María Cruz Minguillón^a, Mohammad Arhami^a, James J. Schauer^b and Constantinos Sioutas^a

^aUniversity of Southern California, Department of Civil and Environmental Engineering, 3620 South Vermont Avenue, Los Angeles, CA 90089, USA

^bUniversity of Wisconsin-Madison, Environmental Chemistry and Technology Program, 660 North Park Street, Madison, WI 53706, USA

Abstract

The Los Angeles–Long Beach harbor is the busiest port in the US. Levels of particulate matter (PM) are relatively high in this area, since it is affected by multiple PM sources. A Chemical Mass Balance (CMB) model was applied to speciated chemical measurements of quasi-ultrafine and fine particulate matter from seven different sites. Winter measurements were obtained during a 7-week period between March and May 2007, and summer measurements corresponded to a 6-week period between July and September 2007. Four of the sites were located within the communities of Wilmington and Long Beach, two sites were located at a background area in the harbor of Los Angeles and Long Beach, and one more site was located further downwind, near downtown Los Angeles, representing urban downtown LA, influenced by mostly traffic sources. The samples were analyzed for organic (OC) and elemental (EC) carbon content, organic species, inorganic ions, water soluble and total elements. The sources included in the CMB model were light duty vehicles (LDV), heavy-duty vehicles (HDV), road dust (RD), biomass burning and ship emissions. The model predictions of the LDV and HDV source contributions accounted, on average, for 83% of total fine OC in winter and for 70% in summer, whereas ship emissions' contribution was lower than 5% of total OC at all sites. In the quasi-ultrafine mode, the vehicular sources accounted for 118% in winter and 103% in summer. Spatial variation of source contributions was not very pronounced with the exception of some specific sites. In terms of total fine PM, vehicular sources together with road dust explain up to 54% of the mass, whereas ship contribution is lower than 5% of total fine PM mass. Our results clearly indicate that, although ship emissions can be significant, PM emissions in the area of the largest US harbor are dominated by vehicular sources.

Conclusions

- The source contribution to OC is dominated by the vehicular sources (42–120% of total fine OC).

- The source contribution to total PM is also dominated by the vehicular sources, hence heavy and light duty vehicles together with road dust account for 24–54% of total fine PM and for 24–100% of total quasi-ultrafine PM.
- The contribution of sea spray accounts for 3.6–16% of total fine PM, with higher values at the background harbor sites (8–18% of ambient fine PM) due to their proximity to the ocean.
- Ship emissions' contributions, although low, are similar in the quasi-ultrafine (0.12–0.33 mg/m³) and fine (0.18–0.42 mg/m³) fractions, indicating that these emissions are mainly in the quasi-ultrafine fraction.

A1.3 Redox Activity and Chemical Speciation of Size Fractioned PM in the Communities of the Los Angeles - Long Beach Harbor.

S. Hu¹, A. Polidori¹, M. Arhami¹, M. M. Shafer², J. J. Schauer², A. Cho³, and C. Sioutas¹

¹University of Southern California, Department of Civil and Environmental Engineering, 3620 South Vermont Avenue, Los Angeles, CA 90089, USA

²University of Wisconsin-Madison, Environmental Chemistry and Technology Program, 660 North Park Street, Madison, WI 53706, USA

³University of California, Los Angeles, School of Medicine, Los Angeles, CA 90095, USA

Abstract

In this study, two different types of assays were used to quantitatively measure the redox activity of PM and to examine its intrinsic toxicity: 1) in vitro exposure to rat alveolar macrophage (AM) cells using dichlorofluorescein diacetate (DCFH-DA) as the fluorescent probe (macrophage ROS assay), and: 2) consumption of dithiothreitol (DTT) in a cell-free system (DTT assay). Coarse (PM_{10?2.5}), accumulation (PM_{2.5?0.25}), and quasi-ultrafine (quasi-UF, PM_{0.25}) mode particles were collected weekly at five sampling sites in the Los Angeles-Long Beach Harbor and at one site near the University of Southern California campus (urban site). All PM samples were analyzed for organic (total and water-soluble) and elemental carbon, organic species, inorganic ions, and total and water-soluble elements. Quasi-UF mode particles showed the highest redox activity at all Long Beach sites (on both a per-mass and per-air volume basis). A significant association ($R^2=0.61$) was observed between the two assays, indicating that macrophage ROS and DTT levels are affected at least partially by similar PM species. Relatively small variation was observed for the DTT measurements across all size fractions and sites, whereas macrophage ROS levels showed more significant ranges across the three different particle size modes and throughout the sites (coefficients of variation, or CVs, were 0.35, 0.24 and 0.53 for quasi-UF, accumulation, and coarse mode particles, respectively). Association between the PM constituents and the redox activity was further investigated using multiple linear regression models. The results showed that OC was the most important component influencing the DTT activity of PM samples. The variability of macrophage ROS was explained by changes in OC concentrations and water-soluble vanadium (probably originating from ship emissions (bunker oil combustion)). The multiple regression models were used to predict the average diurnal macrophage ROS and DTT levels as a function of the OC concentration at one of the sampling sites.

Conclusions

- Quasi-UF mode particles showed the highest redox activities at all sites, on both a per-mass and per-air volume basis.
- A multiple linear regression model showed that OC (emitted from vehicle exhaust and port activities) was the single most important component influencing the DTT levels.

- The predicted DTT and ROS activity rates and measured OC concentrations at one of the port sites were ~3–4 times higher between 9 and 11 a.m. than at 17–18 p.m., confirming that traffic emissions can increase the redox potential of airborne PM substantially and induce oxidative stress on human cells.

A1.4 Size -segregated Inorganic and Organic Components of PM In the Communities of the Long Angeles Harbor Across Southern Los Angeles Basin, California.

Mohammad Arhami^a; Markus Sillanpää^a; Shaohua Hu^a; Michael R. Olson^b; James J. Schauer^b; Constantinos Sioutas^a

^a Department of Civil and Environmental Engineering, University of Southern California, Los Angeles, California, USA

^b Environmental Chemistry and Technology Program, University of Wisconsin—Madison, Wisconsin, USA

Abstract

The Los Angeles Ports complex consists of the port of Long Beach and the port of Los Angeles. Due to the high levels of particulate matter (PM) emitted from many sources in the vicinity of these ports and to their projected massive expansion, the Harbor area will be the focus of future governmental regulations. This study aims to characterize the physicochemical properties of PM at locations influenced by port-affiliated sources. PM samples were collected concurrently at six sites in the southern Los Angeles basin for a 7 week period between March and May 2007. Four sites were set-up within the communities of Wilmington and Long Beach; one site was located at a background location near the harbors of the Los Angeles port; the sixth site, near downtown Los Angeles, was chosen to represent a typical urban area. Coarse (PM_{2.5-10}), accumulation (PM_{0.25-2.5}), and quasi-ultrafine (PM_{0.25}) mode particles were collected at each site. Samples were analyzed for organic and elemental carbon content (OC and EC, respectively), organic species, inorganic ions, water soluble and total elements. The carbon preference index (CPI) for quasi-UF and accumulation mode particles varied from 0.65 to 1.84 among sites, which is in the range of previous findings in areas with high influence of anthropogenic sources. The ratio of hopanes to EC and hopanes to OC over all the sites were in the range of previous roadside measurements near freeways with variable volumes of diesel truck traffic. High overall correlation of vanadium with nickel (R = 0.9) and a considerable gradient of vanadium concentrations with distance to the port, suggest marine vessels as the major sources of these elements.

Conclusions

- The major mass contributions in the quasi-UF fraction were particulate organic matter (POM), nss-sulfate and EC; in the accumulation mode fraction were nss-sulfate, sea salt, POM, and nitrate; and in the coarse fraction were sea salt and insoluble soil.
- In general, PM and its components in accumulation mode showed relatively lower spatial variability compare to the quasi-UF and the coarse modes.
- The carbon preference index (CPI) for quasi-UF and accumulation mode particles varied from 0.65 to 1.84 among sites, which is in the range of previous findings in areas with high influence of anthropogenic sources.

- In sites located close to harbor, the average n-Alkanes and PAHs levels were respectively about 3 and 5 times higher than their corresponding levels at a site located in vicinity of harbor, but upwind of most of local sources.
- The ratio of hopanes to EC and hopanes to OC over all the sites were in the range of previous roadside measurements near freeways with variable volume of diesel truck traffic.
- High overall correlations of vanadium with nickel ($R = 0.9$), as well as a considerable gradient of vanadium concentrations with distance from the coast, suggests marine vessels as the major sources of these elements.

A1.6 Intra-community Spatial Variability of Particulate Matter Size Distributions

M. Krudysz¹, K. Moore², M. Geller², C. Sioutas², and J. Froines¹

¹Center for Occupational and Environmental Health and the Department of Environmental Health Sciences, University of California, Los Angeles, CA 90095, USA

²Department of Civil and Environmental Engineering, University of Southern California, 3620 South Vermont Avenue, Los Angeles, CA 90089, USA

Abstract

Ultrafine particle (UFP) number concentrations vary significantly on small spatial and temporal scales due to their short atmospheric lifetimes and multiplicity of sources. To determine UFP exposure gradients within a community, simultaneous particle number concentration measurements at a network of sites are necessary. Concurrent particle number size distribution measurements aid in identifying UFP sources, while providing data to investigate local scale effects of both photochemical and physical processes on UFP. From April to December 2007, we monitored particle number size distributions at 13 sites within 350 m–11 km of each other in the vicinity of the Ports of Los Angeles and Long Beach using Scanning Mobility Particle Sizers (SMPS). Typically, three SMPS units were simultaneously deployed and rotated among sites at 1–2 week intervals. Total particle number concentration measurements were conducted continuously at all sites. Seasonal and diurnal number size distribution patterns are complex, highly dependent on local meteorology, nearby PM sources, and times of day, and cannot be generalized over the study area nor inferred from one or two sampling locations. Spatial variation in particle number size distributions was assessed by calculating the coefficient of divergence (COD) and correlation coefficients (r) between site pairs. Results show an overall inverse relationship between particle size and CODs, implying that number concentrations of smaller particles (<40 nm) differ from site to site, whereas larger particles tend to have similar concentrations at various sampling locations. In addition, variations in r values as a function of particle size are not necessarily consistent with corresponding COD values, indicating that using results from correlation analysis alone may not accurately assess spatial variability.

Conclusions

- Comparison of the number size distributions measured during different seasons showed that higher concentrations of particles >20 nm and overall higher total PN concentrations are observed more often during the winter season than during the spring/summer season.
- The spatial variability analysis showed concentrations of smaller particles are different at each sampling site, but larger particles tend to be more uniform, in general, which may be a signal of regional aerosol.
- Correlation analysis provides information on the overall trend in association between two sites throughout the sampling period, while COD

analysis shows differences in absolute concentrations among concurrently sampled sites.

- Results presented here show that particle size distributions vary significantly on a community scale, and can differ depending on the season and time of day. Epidemiological studies assessing health effects related to PM exposure should not rely on only one monitoring site, but ought to use data collected from a large number of monitors located close to important UFP sources and operating during different seasons.

A1.7 Intra-community spatial variation of size-fractionated organic compounds in Long Beach, CA

Margaret A. Krudysz¹, Steven J. Dutton², Gregory L. Brinkman³, Michael P. Hannigan³, Philip M. Fine⁴, Constantinos Sioutas⁴ and John R. Froines¹

¹Center for Occupational and Environmental Health and the Department of Environmental Health Sciences, University of California, Los Angeles, CA 90095, USA

²Department of Civil, Environmental and Architectural Engineering, University of Colorado, Boulder, CO 80309, USA

³Department of Mechanical Engineering, College of Engineering and Applied Science, University of Colorado, Boulder, CO 80309, USA

⁴Department of Civil and Environmental Engineering, University of Southern California, 3620 South Vermont Avenue, Los Angeles, CA 90089, USA

Abstract

Quantification of the size distributions of organic molecular markers can provide information about the origin of the carbonaceous particulate matter (PM). Organic molecular marker spatial variability studies provide data that are vital to an accurate determination of a population's exposure to PM from various sources. We have investigated the intra-community spatial variation of size-segregated PM [0–0.25 μm (ultrafine), 0.25–2.5 μm (accumulation), and 2.5–10 μm (coarse)] in a southern California community. The highest concentrations of individual organic compounds were found in the ultrafine fraction, followed by the accumulation and coarse size fractions. Correlations between the three size fractions were weak between compounds in the coarse and corresponding ultrafine and accumulation particles, implying that the coarse PM organic compounds were emitted by different sources than those that emit ultrafine and accumulation mode PM. Evidence of the incomplete combustion of gasoline was found in the ultrafine and accumulation size fractions, while possible diesel emissions were traced to ultrafine particles. Coefficients of divergence and coefficients of variation were investigated to determine the spatial and temporal variability of individual organic compounds. Spatial divergence in organic compounds was comparatively high, but it did not differ appreciably between size fractions or between compound classes. Elemental carbon and tracer compounds, which originate from a few sources, showed higher spatial divergence than organic carbon whose numerous sources can be local and regional. Spatial and temporal variability were not different from each other for this data set and, therefore, it is not possible to determine whether variability in concentrations between sampling sites or the length of the sampling campaign is more important for health effects studies.

Conclusions

- Results show clear differences between size fractions, with stronger correlations within the UF and Acc size fractions compared to those within the coarse fraction.

- Strong correlations across all sites were observed between steranes in the UF and the ACC size fractions, and these were attributed to motor vehicle emissions.
- The large variation in spatial distribution of organic compounds and particle sizes presented here (COD=0.0–0.7) suggests that it may be difficult to characterize a community-average concentration for the molecular marker compounds with only one monitoring station or a single particle size.

APPENDIX B: RELEVANT DETAILS ON CPC 3022A USED

B1 Known recalibration of CPCs used in the study

Table B-1: Known recalibration of CPCs used in the study

Original Site before USC	CARB equipment number	Instrument serial number	Any known previous calibration
Ernst	20017129	483	4/2005, 11/2006
Richland	20017284	505	11/2006, 06/2009
West Tarmac	20017127	481	4/2005
East Tarmac	20017130	484	11/2006
Marine Park	20017285	500	11/2006
Indio	no sticker	360	11/2006
	20017188	498	10/2006
ARB	20017191	494	10/2006
ARB	20017189	499	11/2006
ARB	20017286	502	11/2006
ARB	20022744	596	11/2006
USC	20022743	595	
Upland	20017288	504	11/2006
Alpine	20017128	480	11/2006

B2 Operation Schedule of CPCs at Sites

Table B-2a: Operation Schedule of CPCs at Sites in Phase-I

Site	CPC Number	Operation period	CPC Number	Operation period	CPC Number	Operation period
LB4	CPC # 360	Aug 3,2007-Dec 11,2007				
SP1	CPC # 504	Jun 4, 2007-Dec 12,2007				
LB7	CPC # 360	Feb 23, 2007-Apr 17, 2007	CPC # 483	Apr 20, 2007-Dec 11, 2007		
LB5	CPC # 505	Feb 12, 2007 - Dec 11, 2007				
LB8	CPC # 500	Feb 12, 2007 - Dec 11, 2007				
LB6	CPC # 596	Feb 13, 2007 - Nov 12, 2007				
W1	CPC # 498	Feb 22, 2007- Dec 11, 2007				
LB3	CPC # 504	Mar 7, 2007- May 29, 2007	CPC # 596	Dec 5, 2007 - Dec 11, 2007		
LB1	CPC # 480	Mar 12, 2007 - Apr 30, 2007	CPC # 497	Apr 30, 2007 - Dec 12, 2007		
LB9	CPC # 481	Mar 13, 2007 - May 11, 2007	CPC # 480	May 11 , 2007 - Jun 19, 2007	CPC # 484	Jun 19, 2007 - Dec 12, 2007
W3	CPC # 595	Feb 24, 2007- Dec 12, 2007				
LA1	CPC # 502	Feb 15, 2007- Dec 11, 2007				
W2	CPC # 499	May 7, 2007 - Dec 12, 2007				
LB2	CPC # 483	Feb 15, 2007- Apr 6, 2007	CPC # 497	Apr 6, 2007 - Apr 24, 2007	CPC # 481	May 7, 2007- Dec 11, 2007

Table B-2b: Operation Schedule of CPCs at Sites in Phase-II

Site	CPC Number	Operation period
AGO	CPC # 484	Aug 3,2007-Dec 11,2007
DIA	CPC # 483	Jun 4, 2007-Dec 12,2007
RUB	CPC # 494	Feb 23, 2007-Apr 17, 2007
UPL	CPC # 595	Feb 12, 2007 - Dec 11, 2007
USC	CPC # 497	Feb 12, 2007 - Dec 11, 2007
VBR	CPC # 504	Feb 13, 2007 - Nov 12, 2007

B3 Adjustment Factors for CPCs at Sites in Phase-II and concentrations

Table B-3: Adjustment Factors for CPCs at Sites in Phase-II

Adjustments were made to the CPC data from three sites: AGO, DIA and RUB. The adjustment factor assumed a linear deterioration over the operation period (hours) and was applied to the hourly average concentration number reported.

Mathematically it was expressed as Adjusted Conc. = (1 + Factor * Hours of Operation) * Reported Hourly Average Concentration

Site	CPC Number	Operation period
AGO	CPC # 484	0.0000383499170812604 hr ⁻¹
DIA	CPC # 483	0.0000419463087248322 hr ⁻¹
RUB	CPC # 494	0.0000383499170812604 hr ⁻¹
UPL	CPC # 595	No adjustment
USC	CPC # 497	No adjustment
VBR	CPC # 504	CPC had optic failure in May 2009 and data until that period are as reported.

AGO – UC Riverside Agricultural Office

DIA – Diamond Bar

RUB – Rubidoux

UPL – Upland

USC – University of Southern California (Particle Instrument Unit)

VBR – VanBuren

Table B-4: Average hourly total particle number concentrations at Phase-II sites

Site	Hour	NOV'08	DEC'08	JAN'09	FEB'09	MAR'09	APR'09	MAY'09	JUN'09	JUL'09	AUG'09	SEP'09	DEC'09
AGO	1	14208	16423	19486	17079	13444	10310	7689	7178	8636	9851	9745	11885
AGO	2	12844	15132	17485	16771	13020	10373	7686	6813	8668	9228	9736	11217
AGO	3	11252	15416	16816	14681	13533	10702	7243	6467	8404	9082	10022	10956
AGO	4	12548	15053	15287	14555	13080	11893	7117	6207	8397	9357	9808	13386
AGO	5	12725	15382	18551	16024	14219	12261	6612	6393	8155	9973	9319	12864
AGO	6	14326	17518	22746	18257	15294	15100	6700	6398	8059	9989	11067	12269
AGO	7	15454	21080	24068	18845	17921	14252	6664	6349	8550	10026	13079	14494
AGO	8	16375	21737	20924	18070	14586	10333	6549	6050	8371	8996	10911	12693
AGO	9	13328	16742	15914	14697	10459	7678	6299	6100	8937	8026	8960	9771
AGO	10	11311	12210	11316	10801	8754	7953	6792	6331	8468	7754	8562	9004
AGO	11	10006	9454	9763	9750	8612	8515	7064	6188	8402	7646	8697	8444
AGO	12	9868	8793	10227	9332	8912	10780	7053	6374	8659	7510	8386	8070
AGO	13	8117	8289	10976	9262	9794	12820	7303	6952	8915	8257	8859	8789
AGO	14	7201	8195	10704	9032	10464	12533	7902	7207	8027	8924	9323	9247
AGO	15	6843	8545	9984	9370	10295	11850	8293	7664	7828	8766	9473	8951
AGO	16	7603	8582	8767	9266	9729	11999	8455	7558	7626	9010	9282	8783
AGO	17	8823	9860	9297	9618	9542	11559	8073	7617	7447	9113	9278	8511
AGO	18	10148	13354	10829	10691	9555	10476	7817	7395	7671	8654	9244	8740
AGO	19	13068	16684	14034	14204	10228	10121	7910	7297	8077	8654	9559	9747
AGO	20	14994	17843	16698	16083	10738	9941	8474	7201	8052	8772	9927	10189
AGO	21	13332	18728	19211	15827	11447	10690	8231	7552	8796	9059	10393	11198
AGO	22	12857	18945	20467	16559	12083	11963	8035	7536	8658	9331	10391	12355
AGO	23	13249	20153	19371	16885	12511	11569	7759	7388	8116	9384	10074	11125
AGO	24	14528	18345	19598	16271	12795	11778	7815	7442	8870	9441	10217	11547

Table B-4 (continued)

Site	Hour	NOV'08	DEC'08	JAN'09	FEB'09	MAR'09	APR'09	MAY'09	JUN'09	JUL'09	AUG'09	SEP'09	DEC'09
DIA	1				8425	8816	9272	7773	7316	8969	8707	9115	9119
DIA	2				7749	9534	8729	6907	7418	8692	8293	8969	10198
DIA	3				7999	9448	9322	6698	6537	8543	7859	9122	10128
DIA	4				8263	9531	11941	6804	6608	9114	7817	9122	10674
DIA	5				7710	9234	10511	7152	6577	9671	9500	9244	11269
DIA	6				10866	12464	11976	8696	8321	11203	11216	10042	11905
DIA	7				9115	15882	17317	11948	9562	17528	14197	13149	13278
DIA	8				15756	17437	12580	11043	8016	19347	14960	19621	14939
DIA	9				9193	17910	10595	10365	9360	14910	13285	18847	16098
DIA	10				8663	12157	10883	10295	9221	11875	11912	16069	17706
DIA	11				11806	10800	11193	9897	9117	10037	11088	14475	15948
DIA	12				10726	11812	14159	10229	9300	9371	10787	13492	14669
DIA	13				11056	12390	16954	10587	9678	10854	11350	12394	13326
DIA	14				9915	11313	18476	12582	11453	13138	11848	13607	13457
DIA	15				8837	12302	19685	14041	14031	13938	13655	14889	14292
DIA	16				9340	12387	18982	14854	14193	13462	14156	14998	14121
DIA	17				9407	13137	17019	13645	13371	12565	13441	14465	13614
DIA	18				8477	13093	14353	12023	11528	10996	12351	13520	14076
DIA	19				8573	12607	12800	10988	10044	10128	12682	13418	14566
DIA	20				10254	12262	12350	10162	9280	10415	12476	13120	13790
DIA	21				10847	10953	11620	9803	8843	9435	12096	12494	13023
DIA	22				9177	10547	10777	9540	8273	8971	10621	11354	12084
DIA	23				8325	9568	9935	8890	8167	8986	9993	10196	11332
DIA	24				9675	8490	8893	7913	8033	8546	9215	9655	10383

Table B-4 (continued)

Site	Hour	NOV'08	DEC'08	JAN'09	FEB'09	MAR'09	APR'09	MAY'09	JUN'09	JUL'09	AUG'09	SEP'09	DEC'09
RUB	1	14128	19083	16866	20002	16277	14146	9230	6786	5601	9601	7696	13117
RUB	2	13778	17822	16727	19323	17485	14537	8760	6627	5812	9421	7734	13458
RUB	3	13424	16329	16709	18735	16357	14994	8677	6552	5783	9614	7305	13851
RUB	4	13751	16642	15417	19114	16720	16980	9226	6344	5936	9932	8562	14590
RUB	5	15260	18092	16308	19971	20990	17781	9484	6451	6109	10458	9108	16226
RUB	6	18595	20998	19231	22528	24603	21068	11511	7123	7102	11963	10003	19935
RUB	7	20505	25830	25793	26270	30639	22345	10260	6716	6931	12457	11364	22622
RUB	8	25032	31355	28492	31250	27826	16074	8075	6751	6444	11675	10387	21429
RUB	9	22134	27458	26575	27196	18106	10746	7342	6138	6534	9616	7729	15726
RUB	10	15551	20235	18992	19988	12554	8952	7315	5735	6415	7625	6464	10548
RUB	11	11812	14499	12305	15351	9963	8855	7363	5594	5687	7234	6307	8156
RUB	12	8618	12048	10263	12733	9879	11707	8114	6425	6344	7567	6588	7943
RUB	13	6940	10490	10194	11566	11329	14758	9298	7188	6844	7853	7394	9225
RUB	14	6969	9831	9710	11919	12208	15611	10390	7257	6736	8563	7960	9870
RUB	15	7670	10018	9832	12063	12373	15921	11416	8045	6716	7713	8282	9879
RUB	16	7503	10524	9355	11910	12575	15606	11954	8927	7244	8419	8731	9986
RUB	17	9331	12144	9850	12489	12972	15114	12539	9021	7507	8734	8849	9520
RUB	18	11630	17157	11290	14170	12419	13492	11902	8516	7302	9359	8375	9719
RUB	19	13033	18532	11572	17979	13526	12529	11180	8029	7598	9575	8168	10947
RUB	20	14828	21039	13548	18672	14577	12111	10706	7821	7279	10216	8356	11858
RUB	21	15438	22176	14635	19263	15179	13090	10149	7559	7163	10373	8478	13455
RUB	22	14912	22936	16196	19617	15559	13821	10030	7215	7017	10251	8491	14300
RUB	23	14867	24390	17740	20990	16017	14039	9948	7036	6668	10234	8456	13486
RUB	24	14642	23540	17216	20429	16338	13626	9710	6999	6374	10057	8176	13470

Table B-4 (continued)

Site	Hour	NOV'08	DEC'08	JAN'09	FEB'09	MAR'09	APR'09	MAY'09	JUN'09	JUL'09	AUG'09	SEP'09	DEC'09
UPL	1	9485	15049	9902	14549	11854	10285	9645	7177	8860	8788	8133	7190
UPL	2	8954	12496	9442	13017	14388	15085	8440	6439	8484	8238	7214	6302
UPL	3	7956	11007	8172	10711	17391	17624	7798	6109	8577	7800	6670	5727
UPL	4	7187	9993	7686	9749	21036	21197	7804	6003	8286	7718	6559	6127
UPL	5	7574	10477	7543	10355	16569	15277	8661	6718	9641	8867	8760	7981
UPL	6	8976	13010	9764	13427	14924	15621	10162	7588	13384	10236	10533	11715
UPL	7	14540	18208	13991	18677	15189	11984	10526	7058	11380	11333	13876	15812
UPL	8	18771	24674	16673	22994	14379	12907	10442	6833	11243	10133	11837	14416
UPL	9	15593	21815	16704	17679	12150	16341	9839	6759	11332	9948	10183	9850
UPL	10	11897	15082	12199	16355	11387	20855	9858	6220	9338	9383	9676	9397
UPL	11	11021	13868	11835	15372	11753	22763	9729	6297	8699	9019	9218	9126
UPL	12	9312	13320	10086	13285	12672	21913	10101	6431	9448	9148	8704	8175
UPL	13	8722	12008	8421	13344	13294	21353	10970	6860	9784	9567	10333	8832
UPL	14	8335	12132	7484	13062	15093	21407	11972	7361	10381	9954	10736	8752
UPL	15	8304	13324	7542	13526	16354	22176	13628	8014	12043	11209	11929	10169
UPL	16	9987	13415	7666	13103	17440	21483	15895	10276	14070	12771	13718	11135
UPL	17	12014	16517	10073	14377	18104	20697	17025	11961	15516	14830	15937	12696
UPL	18	14769	24001	15345	19431	19408	17843	16813	12383	15741	16639	17414	15232
UPL	19	17967	24863	15661	24150	20561	16736	16270	11999	13834	16071	17863	15804
UPL	20	16978	27643	16646	24617	19616	13990	15197	11804	13311	14971	14910	16122
UPL	21	16110	27980	16116	23544	18235	12710	14591	11081	13053	13088	13833	15215
UPL	22	15783	26817	15264	22043	16307	12645	13157	10362	10455	11700	12901	13416
UPL	23	14025	24925	13199	18090	14058	10526	11671	8894	9850	9815	11255	11268
UPL	24	11500	19298	10902	16513	11985	9714	10260	7840	8808	9149	9834	9385

Table B-4 (continued)

Site	Hour	NOV'08	DEC'08	JAN'09	FEB'09	MAR'09	APR'09	MAY'09	JUN'09	JUL'09	AUG'09	SEP'09	DEC'09
USC	1	19036	20880	23505	14456	16656	14150	9733	8848	10657	10445	10882	17778
USC	2	16419	20601	21493	13011	15487	13985	9339	7667	9267	9564	9886	17575
USC	3	16199	19923	20147	12632	15252	15449	8231	7369	10225	9412	9976	17552
USC	4	16321	20284	20815	12890	16787	17713	9082	9188	12966	10624	10444	18272
USC	5	20447	23710	24184	14309	19703	22944	10796	10732	16556	13285	13310	21765
USC	6	29909	28468	32073	19531	26053	27967	12233	12149	13340	17084	17796	25751
USC	7	35396	38003	39321	26311	29917	26636	12668	10862	11699	16405	17688	25320
USC	8	39027	44373	47296	26270	26750	20047	13083	9711	12080	13964	14778	22295
USC	9	31702	37509	41053	20529	21715	17135	12397	10487	13167	12752	13322	20246
USC	10	24482	29018	30776	16857	18607	16392	13349	11130	15668	12082	12694	19955
USC	11	17318	22633	22693	14845	18886	18615	16203	13129	19360	13698	13286	19545
USC	12	16111	20194	18831	14279	19416	21055	19390	15680	17147	17299	16804	19209
USC	13	16349	18449	18476	14263	21320	22913	20759	16396	16117	16028	15530	20155
USC	14	17733	19303	18296	16181	21693	22282	19470	15590	13698	15611	15009	19995
USC	15	17236	19906	19691	15464	20079	18197	15875	12777	11066	13426	12964	18745
USC	16	17042	20297	19998	15253	18081	16076	14887	11709	9429	11253	11429	17948
USC	17	17845	21753	22343	15382	16567	14516	13237	9675	9113	9358	9910	17749
USC	18	18121	23220	24477	15619	17870	15545	12876	9167	9495	9513	10093	17965
USC	19	18723	25090	27337	16916	20243	18129	12718	10396	10316	10756	10504	18651
USC	20	20578	27466	29734	17961	20688	20644	12355	9698	10437	11238	11976	20782
USC	21	20304	27615	29781	18967	20526	21995	11695	9400	11911	10987	12661	20544
USC	22	19044	26843	28906	17918	19065	19443	10653	9915	13747	11892	11057	19795
USC	23	19998	25726	26522	16371	18011	17312	10654	9786	13854	11950	10385	19333
USC	24	19790	22862	25249	15812	17960	16282	10406	9334	11335	11269	10653	18569

Table B-4 (continued)

Site	Hour	NOV'08	DEC'08	JAN'09	FEB'09	MAR'09	APR'09	MAY'09	JUN'09	JUL'09	AUG'09	SEP'09	DEC'09
VBR	1	11479	16396	10552	13452	10144	7377						
VBR	2	10129	14744	10152	13291	9853	7445						
VBR	3	9436	13563	9606	12037	9336	7495						
VBR	4	9426	13129	8562	11085	9556	7814						
VBR	5	9303	12392	8985	11307	11613	8468						
VBR	6	10954	15059	10758	13812	13156	9839						
VBR	7	14331	18241	12712	16161	15396	9468						
VBR	8	15679	20811	14568	18643	12743	7181						
VBR	9	11578	18258	13005	15236	8914	6199						
VBR	10	9296	13448	9657	11433	7357	6008						
VBR	11	8067	11475	7073	8965	7033	6261						
VBR	12	7636	10089	5907	8361	7444	6940						
VBR	13	7584	8664	5666	8303	7970	7476						
VBR	14	7740	8231	5204	8944	8633	7614						
VBR	15	7448	8406	5302	8626	8136	7644						
VBR	16	7923	9201	5597	9150	8110	7457						
VBR	17	8744	12538	6210	9555	8241	7717						
VBR	18	10010	18392	8217	11661	8935	7546						
VBR	19	13081	22062	9206	14706	9486	7417						
VBR	20	13340	21861	10620	15285	9920	7992						
VBR	21	13262	22679	9838	15882	10076	8279						
VBR	22	13158	21602	10530	16071	9728	7835						
VBR	23	12454	21779	10033	15128	10062	7747						
VBR	24	12549	21350	9759	13860	9790	7582						

THIS PAGE BLANK INTENTIONALLY